New Biocatalytic Approaches for Alcohol Oxidations and Ketone Reductions Using (Deaza)Flavoenzymes

Martin, Caterina

DOI:
10.33612/diss.145245371

NEW BIOCATALYTIC APPROACHES FOR ALCOHOL OXIDATIONS AND KETONE REDUCTIONS USING (DEAZA)FLAVOENZYMES

CATERINA MARTIN

university of groningen

New Biocatalytic Approaches for Alcohol Oxidations and Ketone Reductions Using (Deaza)Flavoenzymes

PhD thesis

to obtain the degree of PhD at the
University of Groningen
on the authority of the
Rector Magnificus Prof. C. Wijmenga
and in accordance with
the decision by the College of Deans.

This thesis will be defended in public on

Friday 4 December 2020 at 14.30 hours

by

Caterina Martin

born on 20 October 1991
in Motta Di Livenza, Italy

The research described in this thesis was carried out at the GBB Institute of the University of Groningen and was financially supported by the Dutch Research Council (NWO).

Cover design: C. Martin & Lovebird design.

Layout design: Lovebird design
www.lovebird-design.com

Supervisors
Prof. M.W. Fraaije
Prof. D.B. Janssen

Assessment Committee
Prof. G. Maglia
Prof. G.J. Poelarends
Prof. F. Hollmann

Ai miei genitori, la mia più grande fortuna

TABLE OF CONTENTS

Aim and outline of the thesis

AIM AND OUTLINE OF THE THESIS

Biocatalysis is increasing in popularity compared to chemical approaches to produce the most diverse chemical components. This popularity is often the consequence of the lower environmental impact and/or of the selectivity of biocatalysts. Despite this, to compete with chemical processes, biocatalysts must fulfill many requirements. Therefore, there is a strong demand for stable, fast, and easy to produce biocatalysts. The research described in this thesis focused on the exploration of new or engineered redox enzymes that can be used for selective alcohol oxidations or ketone reductions.

In **Chapter 1** an important oxidative biocatalysts family is described, the flavin-dependent oxidases. Flavoprotein oxidases represent a relevant group of biocatalysts that are already used in many different applications. Based on structural features, different subclasses of FAD- or FMN-containing oxidases can be identified. The chapter discusses the use of these oxidases in biotechnological applications. Particular attention is given to glucose oxidase, cholesterol oxidase, (hydroxymethyl)-furfural oxidase (HMFO) and methanol oxidase.

In **Chapter 2** the protagonist is HMFO. This flavoprotein oxidase is a key enzyme in the quest for a new process to produce a bio-based plastic, an eco-friendly alternative to petrol-based plastic. In this chapter it is shown that an engineered HMFO can be used to efficiently produce furandicarboxylic acid (FDCA). The work performed in this chapter involved the use of the computational FRESCO method to predict stabilizing mutations. By combining a number of identified beneficial mutations, a highly stable HMFO variant was engineered which displays an improved thermostability and high catalytic performance. It brings this flavoprotein oxidase closer to industrial applications.

Chapter 3 follows the trend of optimizing HMFO for industrial application. The two goals of this study were to improve the yield of heterologous expression and to explore a non-traditional immobilization of HMFO. Secretion of the expressed enzyme using *P. pastoris* and immobilization of the biocatalyst on the spore surface of *B. subtilis* represent two ways to try to improve HMFO production and application. These two methods aimed at facilitating downstream processing of enzyme production (purification of secreted or immobilized enzyme) and its ease of use in conversions (conversion performed in media containing secreted enzyme or recycling of the immobilized enzyme).

In **Chapter 4** the attention is turned to a newly characterized alcohol oxidase. An alcohol oxidase (AOX) from a white-rot fungus was studied for its substrate tolerance. This revealed that the oxidase can be used for a large number of alcohols. Perhaps the most intriguing finding was its ability to oxidize diols into hydroxyacids. The ability to convert alcohols into acids renders AOX an attractive biocatalyst for selective alcohol oxidations.

Finally, **Chapter 5** represents an explorative study on the use of deazaflavoenzymes as biocatalysts. Knowledge regarding F_{420}-dependent enzymes and their biocatalytic potential is limited mainly due to the low commercial availability of the cofactor. The research described in this chapter pursued two main goals. First, it was explored whether a F_{420}-dependent alcohol dehydrogenase can be used for the enantioselective reduction of prochiral ketones. Gratifyingly, the studied alcohol dehydrogenase was found to perform such enantioselective reductions. The second target was to provide a cost-effective cofactor regeneration system which was achieved by varying the utilized cofactor, the cosubstrate and the cofactor regeneration enzyme.

1

The Multipurpose Family of Flavoprotein Oxidases

Caterina Martin, Claudia Binda, Marco W. Fraaije*, Andrea Mattevi

Molecular Enzymology Group, University of Groningen, Nijenborgh 4, 9747AG, Groningen, The Netherlands

*Corresponding author

Published in:
The Enzymes, (2020) (In Press)

ABSTRACT

This chapter represents a journey through flavoprotein oxidases. The purpose is to excite the reader curiosity regarding this class of enzymes by showing their diverse applications. We start with a brief overview on oxidases to then introduce flavoprotein oxidases and elaborate on the flavin cofactors, their redox and spectroscopic characteristics, and their role in the catalytic mechanism. The six major flavoprotein oxidase families will be described, giving examples of their importance in biology and their biotechnological uses. Specific attention will be given to a few selected flavoprotein oxidases that are not extensively discussed in other chapters of this book. Glucose oxidase, cholesterol oxidase, 5-(hydroxymethyl)furfural (HMF) oxidase and methanol oxidase are four examples of oxidases belonging to the GMC-like flavoprotein oxidase family and that have been shown to be valuable biocatalysts. Their structural and mechanistic features and recent enzyme engineering will be discussed in details. Finally, we give a look at the current trend in research and conclude with a future outlook.

INTRODUCTION

Biocatalytic oxidations have attracted the interest of academic and industrial research since many decades [1]. The ability to carry out oxidations with high enantioselectivity together with the broad substrate scope and mild reaction conditions render enzymes attractive, environmentally sustainable catalysts [2]. Redox reactions are performed by peroxidases, oxidases, oxygenases, reductases and dehydrogenases. Such enzymes can be used to produce for example: alcohols, aldehydes, ketones and carboxylic acids that may be problematic to obtain in a single step via traditional chemical approaches. Oxidative biocatalysts employ various mechanisms that involve a variety of different electron acceptors, electron donors and/or redox cofactors. Common redox cofactors are metals (e.g. iron or copper), heme cofactors, nicotinamide cofactors (NADH and NADPH), and flavin cofactors (FAD and FMN). Typical electron acceptors/donors are small redox-active proteins (such as cytochrome C), nicotinamide coenzymes, cosubstrates, molecular oxygen and hydrogen peroxide [3].

An oxidase is defined as an oxidoreductase that utilizes molecular oxygen (O_2) as electron acceptor [4]. In contrast to oxygenases, reductases, and dehydrogenases, oxidases are of major interest because they do not depend on coenzymes (such as nicotinamide cofactors or quinones) that need to be regenerated, but rely only on molecular oxygen as electron acceptor. Their ability to work without any coenzyme regeneration make them cost-effective and less complicated, and therefore more suitable for industrial applications [5]. In contrast to other redox enzymes, such as dehydrogenases, oxidases are not very abundant in nature [6]. This is probably due to the fact that in most cases oxidases catalyze the reduction of dioxygen into hydrogen peroxide. This means that the electrons generated through the oxidation of an organic substrate are irreversibly lost and cannot be used in metabolic route. Moreover, the typical byproduct of the reaction, hydrogen peroxide, is a reactive and toxic molecule. In some cases, reduction of dioxygen can even lead to more damaging reactive oxygen species, such as superoxide. Only in a few oxidases, such as some reported NADH oxidases, reduction of dioxygen into harmless water is accomplished. Oxidases can be subdivided in two major groups based on the employed cofactor: copper- and flavin-containing oxidases [6].

In this chapter we focus on the flavin-containing oxidases. Many members of the flavoprotein oxidase family are regarded as valuable tools for biotechnological applications. Flavoprotein oxidases often are highly selective (for a particular substrate or exhibiting high enantio- or chemoselectivity), display a high activity, do not rely on any metals,

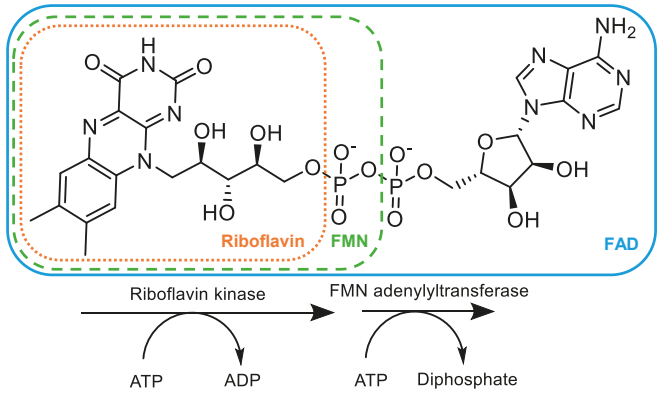

Figure 1 Structures of riboflavin, FMN and FAD. The enzymes involved in the synthesis of FMN and FAD are also indicated.

and require no expensive coenzymes or cosubstrates. These features make them good candidates for various biotechnological applications, for synthesis of high value compounds[7] or biosensors [8].

FLAVIN COFACTORS

Flavin-containing oxidases contain flavin mononucleotide (FMN) or flavin adenine dinucleotide (FAD) as redox cofactor (Figure 1). In only a few cases, flavoprotein oxidases contain one or more additional cofactors [9]. FAD and FMN are synthetized starting from riboflavin (vitamin B_2). Phosphorylation of riboflavin by action of riboflavin kinase results in FMN. Adenylation of FMN yields FAD, the most common flavin cofactor in flavoenzymes [10].

The majority of flavin-containing enzymes, using either FAD or FMN, contain a tightly non-covalently bound flavin. In a relatively small number of flavoproteins, the flavin cofactor is covalently bound. In most cases, this involves a covalent tethering of the protein to the benzyl moiety of a FAD cofactor. For some covalent flavoproteins, the role of such covalent linkage has been shown to be essential to increase the redox potential of the flavin cofactor, to allow oxidations of compounds that are difficult to oxidize. In other cases, the covalent attachment may serve other purposes such as allowing enzymes to adopt a relatively open active site, increase the stability or protecting the protein from proteolysis [11] [12].

The spectroscopic characteristics of riboflavin, FAD and FMN are comparable. This is mainly due to the shared isoalloxazine core structure [13]. The variability in the UV/Vis absorption spectra depend largely on the oxidation state of the flavin (quinone, semiquinone or hydroquinone) [13]. The flavin absorption spectra in the oxidized state in water exhibit four distinct peaks at around 445, 375, 265, and 220 nm, with extinction coefficients above $10^4\ M^{-1}\ cm^{-1}$ [14]. The absorbance spectra of 1- and 2-electron reduced flavins are totally different, with the fully reduced flavins exhibiting very little absorbance in the visible range. While the direct protein environment around a protein-bound flavin can affect UV/Vis absorbance features to a small extent, the fluorescence of flavin cofactors in proteins is typically influenced to a large extent. The neutral forms of oxidized flavins exhibit an intense yellow-green fluorescence at around 520 nm [14]. The polypeptide chain and especially certain amino acids (tryptophan and tyrosine) are potent quenchers of flavin fluorescence [13] [15]. The effect of the protein on flavin fluorescence is often exploited for biochemical studies of flavoenzymes. For example, the ThermoFAD assay has been developed that allows an easy way of determining the apparent melting temperature (thermostability) of flavoproteins. It relies on detecting the difference in flavin fluorescence upon unfolding a (purified) flavoprotein using a temperature gradient, which is typically performed by using a real-time PCR machine [16]. The protein amount and assay time required for this assay are minimal and it can be used in a high-throughput fashion [16]. It is the ideal system to evaluate libraries of variants in thermostability studies. The assay is so sensitive that, if the flavoenzyme is well expressed, it can be performed using cell-free extracts [17].

The redox potentials for the two-electron reductions of FAD and FMN free in solution at pH 7.0 are respectively -219 mV and -205 mV [18] [19]. In aqueous solution the flavin cofactor can be found in three different redox states: the oxidized redox state, the flavin semiquinone (one-electron reduced), or the fully reduced state (two-electron reduced) (Scheme 1).

The catalytic cycle of flavoenzymes typically comprises of two half-reactions. In the reductive half-reaction the oxidized flavin is reduced by its first substrate. In the second half-reaction, the reduced flavin is reoxidized. In the case of flavoprotein oxidases, molecular oxygen is able to act as efficient electron acceptor in the latter oxidative half-reaction (Scheme 2). The ability to swiftly react with molecular oxygen, to reduce it to hydrogen peroxide, sets flavoprotein oxidases apart from other flavoproteins [20]. The exact details on how molecular oxygen is converted into hydrogen peroxide, with the concomitant reoxidation of the flavin cofactor, are still not well understood. It is thought that the first step of the reaction involves the generation of a superoxide anion and flavin semiquinone [21]. In a second electron transfer process, hydrogen peroxide is generated along with fully oxidized flavin. The

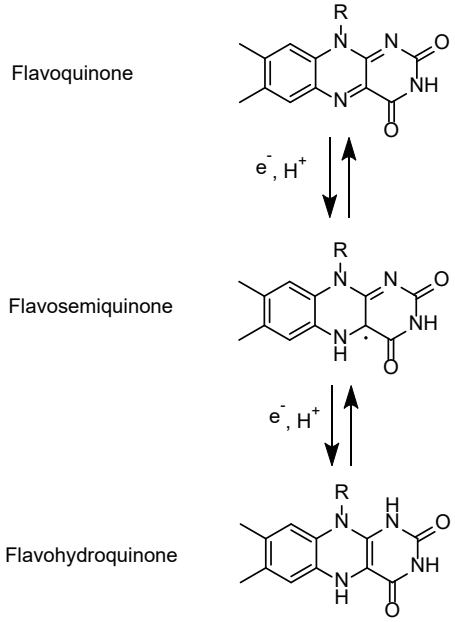

Scheme 1 Flavin cofactor redox states

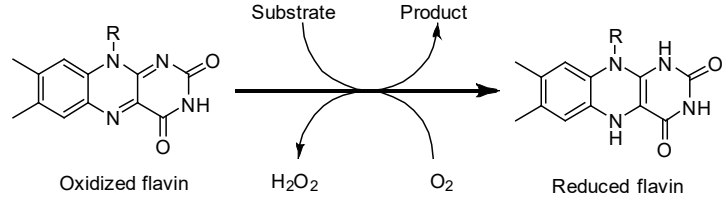

Scheme 2 Catalytic cycle of the flavin cofactor in flavoprotein oxidases.

rate-limiting step is thought to be the first electron transfer (from the fully reduced flavin to O_2) [22].

FLAVOPROTEIN OXIDASES FAMILY

Based on sequence and structure similarity, the majority of flavoprotein oxidases have been classified in six distinct flavoprotein families [6]. The structural diversity is illustrated in Figure 2 which shows the structures of representative oxidases from all six flavoprotein families. Here, we provide an overview for each class focusing on the biotechnological applications of these enzymes. This includes a more detailed description of recent findings and engineering efforts concerning two representatives of the GMC-family: methanol oxidase and HMF oxidase.

Vanillyl alcohol oxidase from *Penicillium simplicissimum*
PDB:1VAO

D-Amino Acid Oxidase from *Homo sapiens*
PDB:2E49

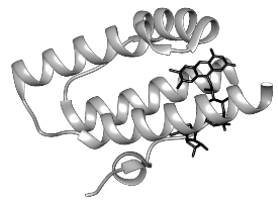

Sulfhydryl oxidase ERV2 from *Saccharomyces cerevisiae*
PDB:1JR8

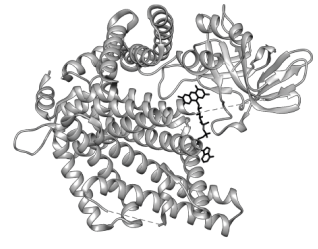

Acyl-CoA oxidase from *Rattus norvegicus*
PDB:2DDH

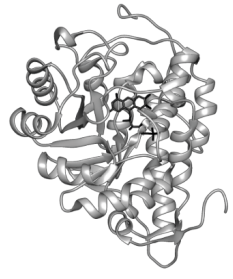

L-Lactate oxidase from *Aerococcus viridans*
PDB:2DU2

Alcohol oxidase from *Phanerochaete chrysosporium*
PDB:6H3O

Figure 2 Structures of several flavoprotein oxidases. The flavin cofactor is shown in black sticks.

THE VAO-TYPE OXIDASE FAMILY

The vanillyl alcohol oxidase from the fungi *Penicillium simplicissimum* (EC 1.1.3.38) (VAO) could be regarded as the founder of the VAO-type oxidase family [23]. This enzyme has been extensively characterized from a biochemistry point of view [24] [25]. Several studies report on the engineering of VAO to clarify the amino acids involved in catalysis and their role in (covalent) FAD binding [26] [27]. A relatively large number of VAO-type oxidases contain a covalently bound FAD, usually tethered to a histidine residue, in a conserved FAD-binding domain (FAD_binding_4 domain, Pfam01565) [28]. Members of this family have been found to be able to produce a variety of high-value aromatic compounds [29]. As the name suggests, VAO can oxidize vanillyl alcohol (4-hydroxy-3-methoxybenzyl alcohol) to vanillin (4-hydroxy-3-methoxy benzaldehyde), but it is also active on plant-derived allylic phenols such as chavicol and eugenol. Remarkably it is also able to stereoselectively convert catecholamines to hydroxylate alkylphenols [24] [30]. More recently another member of the VAO family was discovered and characterized: eugenol oxidase from the bacterium *Rhodococcus sp.* strain RHA1 [31]. This oxidase is also active towards vanillyl alcohol, but displays a higher efficiency for eugenol, converting it into coniferyl alcohol. The high levels of heterologous expression of eugenol oxidase and the robustness stimulated further studies related to its structural properties and to explore the biocatalytic scope [32] [33] [34]. In 2005, Huang and coworkers discovered the first VAO-type oxidase that contain a covalent FAD attached by two covalent bonds: via 6-S-cysteinyl- and 8α-N1-histidyl bonds [35]. This oxidase from the fungus *Acremonium strictum* is active on glucooligosaccharides (EC 1.1.99.B3). More recently also other FAD-containing oxidases, presenting the same bicovalent FAD-linkage has been discovered [36]. It has been hypothesized that the FAD cofactor, anchored by two covalent bonds, may allow such enzymes to evolve a moderately open active site. Enzymes that contain bicovalently bound FAD typically act on relatively bulky substrates like oligosaccharides and secondary metabolites [35]. Moreover, the two covalent FAD-linkages increase the flavin redox potential resulting in the highest redox potentials measured for flavoproteins which allows them to catalyze demanding reactions [12].

THE AMINE OXIDASE FAMILY

This family of flavoprotein oxidases includes enzymes able to oxidize primary and secondary amines, as well as polyamines and amino acids [6] [37]. All amine oxidases have a similar N-terminal domain that assures binding of FAD. As observed for the VAO family, some members contain a covalently bound FAD. However, in these cases the linkage typically involves a cysteinyl bond, not a histidyl bond. Amine oxidases can be grouped according to their substrate scope: amino acids, polyamines, monoamines and methylated lysines. D-Amino acid oxidases (DAAO) (EC 1.4.3.3) are flavoenzymes that oxidize with excellent stereoselectivity natural D-amino acids. The oxidation of D-amino acids results in the formation of imino acids that spontaneously hydrolyze into to the corresponding α-keto acids and ammonia [38]. D-amino acid oxidase from *Rhodotorula gracilis* is of great biotechnological interest because it can be employed for the industrial synthesis of cephalosporins. This DAAO oxidizes cephalosporin C to α-keto adipil-7-ACA, which is an important intermediate for the synthesis of semisynthetic cephalosporins [39]. L-Amino acid oxidases (LAAO) (EC 1.4.3.2) catalyze the oxidative deamination of L-amino acids to the corresponding α-keto acids [40]. Snake venom is rich of L-amino acid oxidases that are subject of many studies and attracted biotechnology interest because they participate in apoptosis induction, cytotoxicity, induction and/or inhibition of platelet aggregation, hemolysis, as well as antiparasitic and have anti-HIV activities [41] [42]. Recently, an LAAO with antimicrobial activity was discovered from a marine microorganism which may be a relevant finding in the context of the urgent quest for new antibiotics [43]. DAAOs and LAAOs are employed also in deracemization of α-amino acids and in biosensors [44] [45] [46]. Polyamine oxidases play a role in the catabolism of spermine and spermidine and their acetyl derivatives. They are fundamental for cell growth and a deregulated metabolic pathways of polyamine oxidases can cause cancer [47] [48]. Monoamine oxidase (MAO) A and B are located on the outer mitochondrial membrane and oxidize primary, secondary, and tertiary amines as well as several neurotransmitters, to the corresponding imines [49]. MAO inhibitors have been used for the treatment of depression and neurodegenerative diseases as Parkinson's disease and Alzheimer's disease [50]. A fungal MAO has been developed into a valuable biocatalyst for the preparation of enantiopure amines [51]. The last subgroup of amine oxidases is constituted by the lysine-specific demethylase. An eminent member of this group is the lysine-specific demethylase 1 (LSD1) (EC 1.14.11.B1) which is fundamental in epigenetic regulation of gene expression in cells, modulating cellular activities including growth and differentiation [37]. LSD1 catalyzes the oxidation of the carbon-nitrogen bond between the methyl group and the epsilon amine of the lysine. The result is the demethylation of the lysine residues in the N-terminal of histone H3 and the tumor suppressor protein p53. An uncontrolled expression of LSD1 has been correlated

with various cancers, playing an important role in differentiation and self-renewal of tumor cells, therefore inhibition of LSD1 could be employed as anticancer measure [52] [53].

THE SULFHYDRYL OXIDASE FAMILY

Enzymes belonging to this family catalyze the pairing of cysteine thiols into disulfide bonds [54]**.** These oxidases are characterized by an all-α fold where the isoalloxazine ring is positioned in a helix bundle and the flavin cofactor is never covalently bound [55]. Two main sub-families can be recognized: Erv-like (Pfam04777) and Ero-like (Pfam04137). Erv-like sulfhydryl oxidases are present in different cellular compartments, for example in the mitochondrial intermembrane space and in the endoplasmic reticulum (ER) [56]. They have been also found in viral genomes where they are suspected to be implicated in the oxidative folding of viral proteins and in the assembly of viral particles [57]. Ero-like oxidases are found only in the ER where they form disulfide bonds in newly synthetized proteins [54]. Sulfhydryl oxidases (SOXs) are interesting from a biotechnological viewpoint, and several patents have been filed in very different fields. Many applications concern the food industry ranging from dairy and baked products to flavours control [58] [59] [60]. In the baking industry they might be employed to improve the strength of the dough. This effect is due to the oxidation of low-molecular weight thiols which avoids the formations of thiol-disulfide bonds that depolymerize the gluten proteins, reducing the dough elasticity [61]. There are speculations also on potential use of SOXs in dyes, detergents and in cosmetics for hair treatments [62] [63]. SOXs could also be employed in biosensors, for the detection of glutathione, or determination of sulfhydryl content and amino acids concentration [64] [65] [66]. SOXs also find industrial applications regarding formation of disulfide bonds in recombinant proteins in large scale protein production [67].

THE ACYL-COA OXIDASE-TYPE OXIDASE FAMILY

Acyl-CoA oxidase (ACO) (EC 1.3.3.6) is the representative model of this family [68]**.** This FAD-containing oxidase catalyzes the Cα-Cβ oxidation of fatty acids and is active on CoA derivatives of fatty acids with aliphatic chains from 8 to 18 carbons [69]. Structural studies have revealed that the N-terminal domain is constituted of only α-helices (Pfam02771) and the enzyme has a middle domain formed by a β-barrel (Pfam02770), and a C-terminal domain of α-helices (Pfam00441) [70]. Lately an ACO from *Arabidopsis thaliana* was employed for the synthesis of an atypical polyketide extender unit in a one-pot reaction [71]. ACO was recently expressed in an engineered yeast strain and

employed to produce adipic acid which is a platform chemical for the synthesis of for example nylons and resins [72]. Another example of an acyl-CoA oxidase-type is the fungal nitroalkane oxidase (NAO) (EC 1.7.3.1) isolated from *Fusarium oxysporum* grown in a medium containing nitroethane [73]. NAO catalyzes the oxidation of neutral nitroalkanes to the corresponding aldehydes or ketones, releasing nitrite [74].

THE 2-HYDROXYACID OXIDASE FAMILY

Members of this family have conserved common structural motifs and typically contain FMN as flavin cofactor. Examples of oxidases belonging to the 2-hydroxyacid oxidase (HAO) family are L-lactate monooxygenase[75] and glycolate oxidase [76]. HAOs present a β8/α8 TIM barrel structure and have a conserved arginine in the active site [75]. Plants possess HAOs with different specificities for medium- and long-chain hydroxyacids. These enzymes are involved in fatty acid and protein catabolism as well as in plant photorespiration like the glycolate oxidases (EC 1.1.3.15) [77]. HAO has been found also in mammals. They share a similar structure to the plant HAOs and they are also active on glycolate and 2-hydroxy fatty acids [78]. Glycolate oxidase from spinach has been used for kinetic resolution of racemates to produce different *R*-2-hydroxy acids [79]. L-lactate-oxidase (EC 1.1.3.2) was exploited to obtain D-lactate from racemic lactate which is a valuable starting material for manufacturing chiral compounds [80]. Lately Faber and co-workers designed a biocatalytic oxidative cascade employing a (S)-specific α-hydroxyacid oxidase from *Aerococcus viridans* for the conversion of fatty acids into α-ketoacids [81]. Remarkably, among the members of this family, another nitroalkane oxidase from *Streptomyces ansochromogenes* (EC 1.7.3.1) was identified. Like the above mentioned acyl-CoA oxidase-type NAO, it can oxidize primary nitroalkanes to aldehydes or ketones [82].

THE GMC-TYPE OXIDASE FAMILY

At the beginning of 90s the glucose-methanol-choline oxidoreductase protein family (GMC) was identified [83]. These enzymes can oxidize a broad variety of substrates maintaining an overall conserved N-terminal GMC_oxred_N domain (Pfam 00732) which has a role in FAD binding [84]. The C-terminal region is less conserved because it is involved in substrate binding. Nevertheless, an active site histidine is usually conserved because it is involved in the catalytic mechanism of substrate oxidation and FAD reoxidation [85] [86]. Members of the GMC family typically contain a dissociable FAD cofactor and oxidize a broad range of primary and secondary alcohols, forming

the corresponding aldehydes or ketones. In some rare cases they are also capable to further oxidize the aldehyde moiety into the respective carboxylic acid [87] [88] [89]. Over the years the catalytic mechanism has been debated, but the current consensus is that it involves a hydride transfer mechanism regardless of the type of alcohol [90]. The reaction is likely to start with proton abstraction from the hydroxyl group of the substrate by the conserved active site histidine. GMC oxidoreductases from fungal sources find many applications in biosensors [91] and in the food industry [92]. Some fungal GMC enzymes are employed in biomass valorization, as these oxidases are involved in lignocellulose degradation [93]. GMC-type FAD-containing oxidases, like most other flavoprotein oxidases, produce hydrogen peroxide as a byproduct which can inactivate the oxidase or other biocatalysts. This can be a major drawback of using such oxidases for bulk chemicals production [94]. Catalase (EC 1.11.1.6) can be coupled in oxidation reaction as it has a high activity and can easily decompose H_2O_2 to oxygen and water [95].

Many GMC-type oxidases have been extensively studied, but the most representative member of this family is glucose oxidase (GOX) (EC 1.1.3.4). GOX is considered as the "Ferrari" of oxidases with an astonishing k_{cat}/K_M (O_2) of $1.5X10^6$ M^{-1} s^{-1}. It catalyzes the oxidation of β-D-glucose to D-glucono-δ-lactone producing H_2O_2 [96] [86]. Glucose oxidase is an enzyme produced by fungi and insects, its main natural roles are related to the production of hydrogen peroxide [92]. For example, GOX is secreted by honey bees in honey to act as anti-bacterial [97]. *Penicillium chrysogenum* glucose oxidase has been studied to evaluate its anti-fungal effect and for possible application as antimicrobial for disinfection of medical devices [98]. This extraordinary oxidase has countless applications in the food industry. In the baking industry GOX could be employed to improve bread's texture as alternative to potassium bromate which could be cancerogenic [99]. It can also be used to improve food shelf-life thanks to the ability to oxidize glucose and reduce the effects of Maillard reaction, or as oxygen scavenger [100] [101]. Already 30 years ago GOX was recognized as an "ideal enzyme" for biosensors applications thanks to stability and other factors [102]. Thanks to the high glucose specificity in presence of other sugars, for many years GOX has dominated the field, but now thanks to protein engineering more enzymes are making their way [8].

Another well-known GMC-type flavoprotein oxidase is cholesterol oxidase (CHOX) (EC 1.1.3.6). CHOX is a FAD-containing oxidase able to catalyze the oxidation of cholesterol to its 3-keto-4-ene derivative, cholestenone. Cholesterol oxidases with the FAD cofactor noncovalently bound and are part of the GMC family, while CHOX in which the FAD is covalently linked belongs to the VAO family [103]. CHOX has been found in several microorganisms and has a role in the initial step of cholesterol metabolism or, in pathogens, it helps to alter the physical structure of the cell membrane [104]. As in the case of GOX, also for this oxidase there are numerous applications with great commercial value. Regarding the biosensing field, similarly as GOX, immobilized CHOX can be used in biosensors to detect cholesterol in food samples, blood serum and other clinical samples [105]. This enzyme finds applications also in the production of steroids, such as 4-androstene-3, 17-dione (AD) and 1,4-androstadiene-3,17-dione (ADD) which are important starting chemicals for anabolic drugs and contraceptive hormones synthesis [106] [107]. Due to its original role in pathogens CHOX is also used in biomedical applications to treat bacterial infections because of its ability to damage the cell membrane [108]. It can be used also for agriculture purposes thanks to its insecticidal effect against the larvae *Anthonomus grandis* [109].

HMF OXIDASE

HMF oxidase (HMFO) (EC 1.1.3.47) represents a good example of the multipurpose potential of flavin-dependent oxidases. HMFO was only recently discovered and quickly became popular for its ability of oxidizing HMF. It can accept also many others industrially relevant chemicals such as vanillyl alcohol and furans [88]. The interest in HMFO mainly lays in the fact that the fully oxidized product of HMF, 2,5-furandicarboxylic acid (FDCA), is considered as a versatile bio-based chemical building block. By being able to convert HMF into FDCA, polymers can be made using renewable material as HMF can be prepared from carbohydrates [110] [111] [112]. HMF and 2,5-furandicarboxylic acid (FDCA) are furan compounds, which were listed as the top 10 value-added bio-based products by the US Department of Energy [111]. FDCA has applications with high commercial value especially in the polymer field because it can potentially substitute terephthalic, isophthalic, and adipic acids in the manufacture of polyamides, polyesters, and polyurethanes [113]. Its versatility as building block made it the best candidate for renewable polyester synthesis such as polyethylene furanoate (PEF). PEF is breaking into the petroleum-based PET supremacy as competitive technology thanks to its similar if not superior structural properties. Current chemical methods to synthetize FDCA rely on high temperature and high pressure and expensive or toxic chemicals [114]. Therefore, biocatalytic approaches with their mild operational conditions would represent a greener approach to obtain FDCA. Among the biocatalytic approaches to produce FDCA from HMF it is possible to distinguish four categories: lipase-based, multienzymatic cascades,

whole-cell biocatalysts and single enzyme [115]. The discovery of HMFO (EC 1.1.3.47) from *Methylovorus sp.* strain MP688 in 2014 by the Fraaije group represented a major breakthrough in the quest for a catalyst capable to convert HMF into FDCA [116]. HMFO was the first oxidase shown to be able to convert HMF into FDCA via three oxidative steps. The ability to convert alcohols to the corresponding carboxylic acid is a known feature among the members of the GMC family [117] [118]. The catalytic mechanism starts with the oxidation of the alcohol group of HMF resulting in the formation of furan-2,5-dicarbaldehyde (DFF). The hydrated *gem*-diol form of the aldehyde moiety can be further oxidized yielding 5-formylfuran-2-carboxylic acid (FFCA) and the last oxidation yields to FDCA Scheme 3 [119].

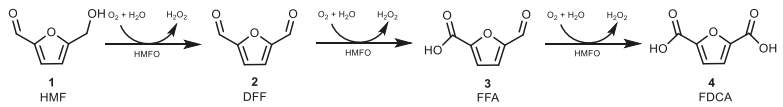

Scheme 3 Oxidation reaction of 5-hydroxymethylfurfural (HMF) to 2,5-furandicarboxylic acid (FDCA) by HMFO.

Despite the outstanding ability of this oxidase to generate FDCA using HMF as starting material, the yield of FDCA was poor and the main product of the conversion was FFCA. Thanks to the elucidation of the crystal structure of HMFO it was possible to tailor the active site to improve the last rate-limiting oxidation step [120].

The elucidated crystal structure revealed that HMFO folds into a globular and compact structure organized in two domains: an FAD-binding domain with the classical Rossmann fold and a smaller cap domain that covers the flavin active site [120]. The enzyme active site can be described as a deep and narrow cleft. A conserved histidine (H467) of the GMC family is located at the bottom of the active site cleft close to the flavin ring. This residue was shown to be essential for catalysis [116]. HMFO is efficient in oxidizing various primary alcohols while it also displayed a low but significant activity on aldehydes. Oxidation of aldehydes was found to be catalyzed by oxidizing the hydrate form of the aldehydes, the *gem*-diols. Yet, *gem*-diols present bulkier substituents on the α-carbon which led to the speculation that an enlarged active site cleft would improve the activity on aldehydes. This led to the preparation of a double mutant (W466F/V367R) which display a 1000-fold improved catalytic efficiency (k_{cat}/K_M) for FFCA compared with the wild type HMFO. The mutation W466F increased the activity towards the aldehyde of FFCA by enlarging the active site cleft, while the V367R boosted the activity on FFCA by promoting proper positioning of the substrate [120]. As a next step in improving the biocatalytic performance of HMFO for FDCA production, engineering was performed to increase its stability. For this, the FRESCO method (Framework for Rapid Enzyme Stabilization by COmputational libraries) was employed. FRESCO is a computational approach that allows to computationally predict, using the crystal structure, mutations that increase the overall enzyme stability [121] [122] [123]. This led to a more robust HMFO variant which allowed a significantly more efficient conversion of HMF into FDCA [17]. The biocatalytic potential of HMFO is definitely not limited to the synthesis of FDCA. Faber and coworkers focused on improving HMFO through enzyme engineering towards production of other carboxylic acids from primary alcohols. By rational engineering they improved the binding of the *gem*-diol form of the aldehyde in the active site to boost aldehyde-oxidase activity. This was achieved by mutating two residues in the active site. The mutant W466H V465T merged high activity and high enantioselectivity, and allowed an improved ratio (37% against the 6% of the wild type) of carboxylic acid to aldehyde formation [124]. HMFO has also been used for the synthesis of enantiopure *sec*-thiols to answer the demand of chiral building blocks for pharmaceuticals [125]. Classical chemical based approaches to obtain nonracemic *sec*-thiols involve complex procedures that involve expensive catalysts [126]. It was shown that HMFO can be used for the kinetic resolution of 1-phenylethane-thiols via enantioselective oxidation [125].

METHANOL OXIDASE

Methylotrophic organisms such as *Pichia pastoris* have evolved to utilize lower primary alcohols as sole source of carbon. A crucial enzyme, present in different isoforms, involved in the metabolism of methanol is the FAD-containing methanol oxidase [127] [128]. Methanol oxidase (EC 1.1.3.13) belongs to the GMC-like family and is also often referred to as alcohol oxidase (AOX). Expression of AOX in the original yeasts is strong and tightly regulated, absent during growth in presence of glucose or ethanol and strongly induced by methanol [129]. This pathway is so well-regulated that quite a number of studies have been carried out for biotechnological applications of the involved promotors such as in recombinant proteins expression in yeast [130] [131] [132]. AOX is localized in peroxisomes where the methanol is oxidized to formaldehyde and H_2O_2, the latter is then broken down into oxygen and water by peroxisomal catalase [133]. Methanol is the natural substrate, but in vitro experiments have revealed that AOXs can also oxidize short aliphatic alcohols such as ethanol and 1-propanol.

Another form of AOX has been found in basidiomycetes. In these fungi it is differently localized. In the wood-degrading fungi *Gloeophyllum trabeum* AOX has been found in the hyphal periplasmic space and in the extracellular matrix. The C-terminus indeed differs from the yeast AOX preventing translocation into peroxisomes. In basidiomycets AOX oxidizes the methanol that becomes available from the degradation of biomass. The generated H_2O_2 has been implicated to assist in the production of destructive radicals essential in lignin degradation [134] . Thanks to their ability of oxidizing various primary alcohols, AOXs have found applications in biosensors, mostly used for ethanol detection. System can employ amperometric electrodes to detect O_2 depletion or H_2O_2, production, or can be coupled bioenzymatic assays with horse radish peroxidase [135] [136]. Crystal structures of AOXs have elucidated only recently. It consists of an oligomeric assembly of eight identical subunits organized, each containing a strongly, but non-covalently, bound FAD [137]. The assembly pathway of AOX is quite complex. After synthesis of the monomeric apo enzyme, FAD binds with the help of cytosolic protein pyruvate carboxylase protein. Then, the FAD-containing AOX is transported to the lumen of the target peroxisome. Inside the organelle the assembly of the mature octamer takes place [129]. Recently, a newly discovered intracellular alcohol oxidase from the white-rot basidiomycete *Phanerochaete chrysosporium* (*Pc*AOX) was reported to be active on glycerol [138]. Glycerol constitutes an abundant by-product of biodiesel manufacture. Over the last years there has been a growing interest in increasing the sustainability of this process through the valorization of glycerol [139] [140]. Therefore, the discovered glycerol oxidase may represent a valuable biocatalyst. Previous attempts to engineer an effective glycerol oxidase was not very successful: a variant of alditol oxidase showed a k_{cat} value for glycerol of only 0.06 s^{-1} [141]. The discovery of the *Pc*AOX prompted further research. First, heterologous expression of *Pc*AOX in *Escherichia coli* was established, which allowed more detailed biochemical studies [142]. It was soon found that *Pc*AOX only showed very poor activity towards glycerol. Fortunately, the crystal structure could be elucidated which revealed a very similar structure when compared with the structure of yeast AOX [142]. It also provided an explanation for the observed preference for small alcohols as substrates (methanol and ethanol). The substrate binding site is rather small and solvent-inaccessible. With these structural insights, mutations were introduced with the aim to enlarge the substrate binding pocket, to allow binding of glycerol. In particular, residues F101 and M103 were targeted because they sterically limit the binding of substrates at the re-site of the flavin cofactor. The best performing mutant *Pc*AOX, when tested for glycerol oxidation, proved to be F101S. Thanks to an enlarged cavity, this variant was able to convert glycerol to glyceraldehyde with a k_{cat} value of 3 s^{-1} [142]. As previously mentioned only a few oxidases are able to perform a double oxidation of alcohols into the corresponding carboxylic acids (e.g. HMFO). It was found that the variant F101S of *Pc*AOX was also able to catalyze double oxidations of alcohols. This led to the interesting finding that, when offered diols, this oxidase can produce hydroxy acids by selectively oxidizing only one hydroxyl group [89]. Among all the substrate tested, some of the corresponding lactones or hydroxy acids find application as building block for biodegradable polymers [143].

CONCLUSIONS

Flavin cofactors represent crucial molecules in nature. Remarkably, about 1-3% of the genes in prokaryotic and eukaryotic organisms are predicted to encode for FAD- and FMN-containing proteins [21]. Nature evolved a palette of different flavin-containing enzymes for the oxidation of alcohols and amines. Flavoprotein oxidases in particular are particularly suited for such reactions and have been studied in detail to understand (1) what their role is in nature, (2) how they function at molecular level, and (3) whether they can be used for biotechnological applications. Genome mining has been efficient in the last 20 years bringing to light new remarkable oxidases such as HMF oxidase, eugenol oxidase [31], sulfhydryl oxidases [144] and chitooligosaccharide oxidase [145]. The last five years are experiencing an expansion of the toolbox for protein engineers: directed evolution and advanced molecular biology techniques and computational tools are becoming every day cheaper, faster and/or more reliable. This will help in discovery and engineering of flavoprotein oxidases with pre-defined properties, suitable for industrial applications.

REFERENCES

[1] F. Hollmann, I.W.C.E. Arends, K. Buehler, A. Schallmey, B. Bühler, Enzyme-mediated oxidations for the chemist, Green Chem. 13 (2011) 226–265.

[2] N.J. Turner, Enantioselective oxidation of C-O and C-N bonds using oxidases, Chem. Rev. 111 (2011) 4073–4087.

[3] D. Monti, G. Ottolina, G. Carrea, S. Riva, Redox reactions catalyzed by isolated enzymes, Chem. Rev. 111 (2011) 4111–4140.

[4] H.J. Bright, D.J.T. Porter, Flavoprotein Oxidases, Academic Press, 1975.

[5] P.N.R. Vennestrøm, C.H. Christensen, S. Pedersen, J. Grunwaldt, J.M. Woodley, Next-generation catalysis for renewables : Combining enzymatic with inorganic heterogeneous catalysis for bulk chemical production, ChemCatChem. 2 (2010) 249–258.

[6] W.P. Dijkman, G. De Gonzalo, A. Mattevi, M.W. Fraaije, Flavoprotein oxidases: Classification and applications, Appl. Microbiol. Biotechnol. 97 (2013) 5177–5188.

[7] W.J.H. Van Berkel, Special issue: Flavoenzymes, Molecules. 23 (2018) 5–8.

[8] S. Ferri, K. Kojima, K. Sode, Review of glucose oxidases and glucose dehydrogenases: A bird's eye view of glucose sensing enzymes, J. Diabetes Sci. Technol. 5 (2011) 1068–1076.

[9] P. MacHeroux, B. Kappes, S.E. Ealick, Flavogenomics - A genomic and structural view of flavin-dependent proteins, FEBS J. 278 (2011) 2625–2634.

[10] A.C. Ludolph, Vitamins and nutrition, Curr. Opin. Neurol. Neurosurg., (1991) 458–461.

[11] M.W. Fraaijet, R.H.H. Van Den Heuvel, W.J.H. Van Berkel, A. Mattevi, Covalent flavinylation is essential for efficient redox catalysis in vanillyl-alcohol oxidase, J. Biol. Chem. 274 (1999) 35514–35520.

[12] D.P.H.M. Heuts, N.S. Scrutton, W.S. McIntire, M.W. Fraaije, What's in a covalent bond?: On the role and formation of covalently bound flavin cofactors, FEBS J. 276 (2009) 3405–3427.

[13] J. Galbán, I. Sanz-Vicente, J. Navarro, S. De Marcos, The intrinsic fluorescence of FAD and its application in analytical chemistry: A review, Methods Appl. Fluoresc. 4 (2016).

[14] S. Weber, E. Schleicher, Flavins and flavoproteins methods and protocols, Flavins Flavoproteins Methods Protoc. 1146 (2014) 1–13.

[15] N. Mataga, H. Chosrowjan, Y. Shibata, F. Tanaka, Ultrafast fluorescence quenching dynamics of flavin chromophores in protein nanospace, J. Phys. Chem. B. 102 (1998) 7081–7084.

[16] F. Forneris, R. Orru, D. Bonivento, L.R. Chiarelli, A. Mattevi, ThermoFAD, a Thermofluor-adapted flavin ad hoc detection system for protein folding and ligand binding, FEBS J. 276 (2009) 2833–2840.

[17] C. Martin, A. Ovalle Maqueo, H.J. Wijma, M.W. Fraaije, Creating a more robust 5-hydroxymethylfurfural oxidase by combining computational predictions with a novel effective library design, Biotechnol. Biofuels. 11 (2018) 56.

[18] H. j. Lowe, W.M. Clark, Studies on oxidation-reduction, J. Biol. Chem. 221 (1956) 983–992.

[19] R.D. Draper, L.L. Ingraham, A potentiometric study of the flavin semiquinone equilibrium, Arch. Biochem. Biophys. 125 (1968) 802–808.

[20] E. Romero, J.R. Gómez Castellanos, G. Gadda, M.W. Fraaije, A. Mattevi, Same substrate, many reactions: oxygen activation in flavoenzymes, Chem. Rev. 118 (2018) 1742–1769.

[21] A. Mattevi, To be or not to be an oxidase: challenging the oxygen reactivity of flavoenzymes, Trends Biochem. Sci. 31 (2006) 276–283.

[22] V. Massey, Activation of molecular oxygen by flavins and flavoprotein, Am. Soc. Biochem. Mol. Biol. 269 (1994) 22459–22462.

[23] E. De Jong, W.J.H. Van Berkel, R.P. Van der Zwan, J.A.M. de Bont, Purification and characterization of vanillyl-alcohol oxidase from *Penicillium simplicissimum:* A novel aromatic alcohol oxidase containing covalently bound FAD, Eur. J. Biochem. 208 (1992) 651–657.

[24] M.W. Fraaije, C. Veeger, W.J.H. Van Berkel, Substrate specificity of flavin-dependent vanillyl-alcohol oxidase from *Penicillium simplicissimum* evidence for the production of 4-hydroxycinnamyl alcohols from 4-allylphenols, Eur. J. Biochem. 234 (1995) 271–277.

[25] A. Mattevi, M.W. Fraaije, A. Coda, W.J.H. Van Berkel, Crystallization and preliminary x-ray analysis of the flavoenzyme vanillyl-alcohol oxidase from *Penicillium simplicissimum*, Proteins Struct. Funct. Genet. 27 (1997) 601–603.

[26] M.W. Fraaije, R.H.H. Van Den Heuvel, W.J.H. Van Berkel, A. Mattevi, Structural analysis of flavinylation in vanillyl-alcohol oxidase, J. Biol. Chem. 275 (2000) 38654–38658.

[27] T.A. Ewing, Q.T. Nguyen, R.C. Allan, G. Gygli, E. Romero, C. Binda, M.W. Fraaije, A. Mattevi, W.J.H. Van Berkel, Two tyrosine residues, Tyr-108 and Tyr-503, are responsible for the deprotonation of phenolic substrates in vanillyl-alcohol oxidase, J. Biol. Chem. 292 (2017) 14668–14679.

[28] M.W. Fraaije, W.J.H. Van Berkel, J.A.E. Benen, J. Visser, A. Mattevi, A novel oxidoreductase family sharing a conserved FAD-binding domain, Trends Biochem. Sci. 23 (1998) 206–207.

[29] G. Gygli, R.P. de Vries, W.J.H. Van Berkel, On the origin of vanillyl alcohol oxidases, Fungal Genet. Biol. 116 (2018) 24–32.

[30] R.H.H. Van Den Heuvel, M.W. Fraaije, A. Mattevi, C. Laane, W.J.H. Van Berkel, Vanillyl-alcohol oxidase, a tasteful biocatalyst, J. Mol. Catal. - B Enzym. 11 (2001) 185–188.

[31] J. Jin, H. Mazon, R.H.H. Van Den Heuvel, D.B. Janssen, M.W. Fraaije, Discovery of a eugenol oxidase from *Rhodococcus sp.* strain RHA1, FEBS J. 274 (2007) 2311–2321.

[32] Q.T. Nguyen, G. de Gonzalo, C. Binda, A. Rioz-Martínez, A. Mattevi, M.W. Fraaije, Biocatalytic properties and structural analysis of eugenol oxidase from *Rhodococcus jostii* RHA1: A versatile oxidative biocatalyst, ChemBioChem. (2016) 1359–1366.

[33] M.H.M. Habib, P.J. Deuss, N. Lončar, M. Trajkovic, M.W. Fraaije, A biocatalytic one-pot approach for the preparation of lignin oligomers using an oxidase/peroxidase cascade enzyme system, Adv. Synth. Catal. 359 (2017) 3354–3361.

[34] M. Habib, M. Trajkovic, M.W. Fraaije, The biocatalytic synthesis of syringaresinol from 2,6-dimethoxy-4-allylphenol in one-pot using a tailored oxidase/peroxidase system, ACS Catal. 8 (2018) 5549–5552.
[35] C.H. Huang, W.L. Lai, M.H. Lee, C.J. Chen, A. Vasella, Y.C. Tsai, S.H. Liaw, Crystal structure of glucooligosaccharide oxidase from *Acremonium strictum*: A novel flavinylation of 6-S-cysteinyl, 8α-N1-histidyl FAD, J. Biol. Chem. 280 (2005) 38831–38838.
[36] A.R. Ferrari, M. Lee, M.W. Fraaije, Expanding the substrate scope of chitooligosaccharide oxidase from *Fusarium graminearum* by structure-inspired mutagenesis, Biotechnol. Bioeng. 112 (2015) 1074–1080.
[37] H. Gaweska, P.F. Fitzpatrick, Structures and mechanism of the monoamine oxidase family, Biomol. Concepts. 2 (2011) 365–377.
[38] L. Pollegioni, S. Sacchi, G. Murtas, Human D-amino acid oxidase: Structure, function, and regulation, Front. Mol. Biosci. 5 (2018) 1–14.
[39] V. Obregón, I. de la Mata, F. Ramón, C. Acebal, M.P. Castillón, Oxidation by hydrogen peroxide of D-amino acid oxidase from *Rhodotorula gracilis*, Stab. Stab. Biocatal. 15 (1998) 89–94.
[40] K. Hahn, Y. Hertle, S. Bloess, T. Kottke, T. Hellweg, G.F. Von Mollard, Activation of recombinantly expressed L-amino acid oxidase from *Rhizoctonia solani* by sodium dodecyl sulfate, Molecules. 22 (2017).
[41] T.R. Costa, S.M. Burin, D.L. Menaldo, F.A. de Castro, S. V. Sampaio, Snake venom L-amino acid oxidases: An overview on their antitumor effects, J. Venom. Anim. Toxins Incl. Trop. Dis. 20 (2014) 1–7.
[42] L.F.M. Izidoro, J.C. Sobrinho, M.M. Mendes, T.R. Costa, A.N. Grabner, V.M. Rodrigues, S.L. Da Silva, F.B. Zanchi, J.P. Zuliani, C.F.C. Fernandes, L.A. Calderon, R.G. Stábeli, A.M. Soares, Snake venom L-amino acid oxidases: Trends in pharmacology and biochemistry, Biomed Res. Int. (2014) .
[43] A. Andreo-Vidal, A. Sanchez-Amat, J.C. Campillo-Brocal, The *Pseudoalteromonas luteoviolacea* L-amino acid oxidase with antimicrobial activity is a flavoenzyme, Mar. Drugs. 16 (2018).
[44] K. Soda, T. Oikawa, K. Yokoigawa, One-pot chemo-enzymatic enantiomerization of racemates, J. Mol. Catal. - B Enzym. 11 (2001) 149–153.
[45] N.J. Turner, Controlling chirality, Curr. Opin. Biotechnol. 14 (2003) 401–406.
[46] M. Trojanowicz, M. Kaniewska, Electrochemical chiral sensors and biosensors, Electroanalysis. 21 (2009) 229–238.
[47] N. Seiler, Chapter 33 Polyamine oxidase, properties and functions, in: P.M. Yu, K.F. Tipton, A.A. Boulton (Eds.), Curr. Neurochem. Pharmacol. Asp. Biog. Amin., (1995)333–344.
[48] N. Minois, D. Carmona-Gutierrez, F. Madeo, Polyamines in aging and disease, Aging 3 (2011) 716–732.
[49] B. Schilling, K. Lerch, Cloning, sequencing and heterologous expression of the monoamine oxidase gene from *Aspergillus niger*, MGG Mol. Gen. Genet. 247 (1995) 430–438.
[50] M.B.H. Youdim, D. Edmondson, K.F. Tipton, The therapeutic potential of monoamine oxidase inhibitors, Nat. Rev. Neurosci. 7 (2006) 295–309.

[51] S. Herter, F. Medina, S. Wagschal, C. Benhaïm, F. Leipold, N.J. Turner, Mapping the substrate scope of monoamine oxidase (MAO-N) as a synthetic tool for the enantioselective synthesis of chiral amines, Bioorganic Med. Chem. 26 (2018) 1338–1346.
[52] P. Vianello, O.A. Botrugno, A. Cappa, R. Dal Zuffo, P. Dessanti, A. Mai, B. Marrocco, A. Mattevi, G. Meroni, S. Minucci, G. Stazi, F. Thaler, P. Trifiró, S. Valente, M. Villa, M. Varasi, C. Mercurio, Discovery of a novel inhibitor of histone lysine-specific demethylase 1A (KDM1A/LSD1) as orally active antitumor agent, J. Med. Chem. 59 (2016) 1501–1517.
[53] A. Hosseini, S. Minucci, A comprehensive review of lysine-specific demethylase 1 and its roles in cancer, Epigenomics. 9 (2017) 1123–1142.
[54] G. Faccio, O. Nivala, K. Kruus, J. Buchert, M. Saloheimo, Sulfhydryl oxidases: Sources, properties, production and applications, Appl. Microbiol. Biotechnol. 91 (2011) 957–966.
[55] D. Fass, The Erv family of sulfhydryl oxidases, Biochim. Biophys. Acta - Mol. Cell Res. 1783 (2008) 557–566.
[56] S.K. Ang, H. Lu, Deciphering structural and functional roles of individual disulfide bonds of the mitochondrial sulfhydryl oxidase Erv1p, J. Biol. Chem. 284 (2009) 28754–28761.
[57] M. Hakim, D. Fass, Dimer Interface migration in a viral sulfhydryl oxidase, J. Mol. Biol. 391 (2009) 758–768.
[58] H.E. Swaisgood, Process of removing the cooked flavor from milk, US 4053644 A, (1977).
[59] H. Sampsa, P. Timo, V. Seppo, T. Ina, Enzyme product and method of improving the properties of dough and the quality of bread, US 4990343 A, (1991).
[60] S.K. Javier, D. Andreas, Increased stability of flavor compounds, US 2010/0015276 A1, (2010).
[61] M.W. Fraaije, W.J.H. van Berkel, Flavin-containing oxidative biocatalysts, Biocatal. Pharm. Biotechnol. Ind. (2006) 181–202.
[62] O. Timothy, M. Karl-heinz, W. Thomas, P. Inken, Compositions comprising perhydrolases and alkylene glycol diacetates, EP 2171048 A1, (2010).
[63] T. Colin, J. Jennifer, Isolation of quiescin-sulfhydryl oxidase from milk, US 7625733 B2, (2009).
[64] S. Timur, D. Odaci, A. Dincer, F. Zihnioglu, A. Telefoncu, Biosensing approach for glutathione detection using glutathione reductase and sulfhydryl oxidase bienzymatic system, Talanta. 74 (2008) 1492–1497.
[65] N. Aoyama, A. Miike, Y. Shimizu, T. Tatano, Method for the determination of mercapto compounds and reagent for use therein, EP 0159870 B1, (1992).
[66] G. Faccio, O. Nivala, K. Kruus, J. Buchert, M. Saloheimo, Sulfhydryl oxidases: Sources, properties, production and applications, Appl. Microbiol. Biotechnol. 91 (2011) 957–966.
[67] V.D. Nguyen, F. Hatahet, K.E.H. Salo, E. Enlund, C. Zhang, L.W. Ruddock, Pre-expression of a sulfhydryl oxidase significantly increases the yields of eukaryotic disulfide bond containing proteins expressed in the cytoplasm of *E.coli*, Microb. Cell Fact. 10 (2011) 1.

[68] A. Kawaguchi, S. Tsubotani, Y. Seyama, T. Yamakawa, T. Osumi, T. Hashimoto, T. Kikuchi, M. Ando, S. Okuda, Stereochemistry of dehydrogenation catalyzed by acyl-CoA oxidase, J. Biochem. 88 (1980) 1481–1486.
[69] F.A.G. Reubsaet, J.H. Veerkamp, S.G.F. Bukkens, J.M.F. Trijbels, L.A.H. Monnens, Acyl-CoA oxidase activity and peroxisomal fatty acid oxidation in rat tissues, Biochim. Biophys. Acta (BBA)/Lipids Lipid Metab. 958 (1988) 434–442.
[70] K. Tokuoka, Y. Nakajima, K. Hirotsu, I. Miyahara, Y. Nishina, K. Shiga, H. Tamaoki, C. Setoyama, H. Tojo, R. Miura, Three-dimensional structure of rat-liver acyl-CoA oxidase in complex with a fatty acid: Insights into substrate-recognition and reactivity toward molecular oxygen, J. Biochem. 139 (2006) 789–795.
[71] B. Vögeli, K. Geyer, P.D. Gerlinger, S. Benkstein, N.S. Cortina, T.J. Erb, Combining promiscuous acyl-CoA oxidase and enoyl-CoA carboxylase/reductases for atypical polyketide extender unit biosynthesis, Cell Chem. Biol. 25 (2018) 833–839.
[72] J.H. Ju, B.R. Oh, S.Y. Heo, Y.U. Lee, J. hoon Shon, C.H. Kim, Y.M. Kim, J.W. Seo, W.K. Hong, Production of adipic acid by short- and long-chain fatty acid acyl-CoA oxidase engineered in yeast *Candida tropicalis*, Bioprocess Biosyst. Eng. 43 (2020) 33–43.
[73] T. Kido, K. Hashizume, K. Soda, Purification and properties of nitroalkane oxidase from *Fusarium oxysporum*, J. Bacteriol. 133 (1978) 53–58.
[74] P.F. Fitzpatrick, Nitroalkane oxidase: Structure and mechanism, Arch. Biochem. Biophys. 632 (2017) 41–46.
[75] Y. Umena, K. Yorita, T. Matsuoka, A. Kita, K. Fukui, Y. Morimoto, The crystal structure of l-lactate oxidase from *Aerococcus viridans* at 2.1 Å resolution reveals the mechanism of strict substrate recognition, Biochem. Biophys. Res. Commun. 350 (2006) 249–256.
[76] Y. Lindqvist, C.I. Branden, F.S. Mathews, F. Lederer, Spinach glycolate oxidase and yeast flavocytochrome b2 are structurally homologous and evolutionarily related enzymes with distinctly different function and flavin mononucleotide binding, J. Biol. Chem. 266 (1991) 3198–3207.
[77] C. Esser, A. Kuhn, G. Groth, M.J. Lercher, V.G. Maurino, Plant and animal glycolate oxidases have a common eukaryotic ancestor and convergently duplicated to evolve long-chain 2-hydroxy acid oxidases, Mol. Biol. Evol. 31 (2014) 1089–1101.
[78] J.M. Jones, J.C. Morrell, S.J. Gould, Three human peroxisomal 2-hydroxy acid oxidases, Biochemistry. 275 (2000) 12590–12597.
[79] W. Adam, M. Lazarus, B. Boss, C.R. Saha-Möller, H.U. Humpf, P. Schreier, Enzymatic resolution of chiral 2-hydroxy carboxylic acids by enantioselective oxidation with molecular oxygen catalyzed by the glycolate oxidase from spinach (Spinacia oleracea), J. Org. Chem. 62 (1997) 7844–7849.
[80] T. Oikawa, S. Mukoyama, K. Soda, Chemo-enzymatic D -enantiomerization of DL -lactate, Biotechnol. Bioeng. 73 (2001) 1–3.
[81] S. Gandomkar, A. Dennig, A. Dordic, L. Hammerer, M. Pickl, T. Haas, M. Hall, K. Faber, Biocatalytic oxidative cascade for the conversion of fatty acids into α-ketoacids via internal H_2O_2 recycling, Angew. Chemie - Int. Ed. 57 (2018) 427–430.

[82] Y. Li, Z. Gao, H. Hou, L. Li, J. Zhang, H. Yang, Y. Dong, H. Tan, Crystal structure and site-directed mutagenesis of a nitroalkane oxidase from *Streptomyces ansochromogenes*, Biochem. Biophys. Res. Commun. 405 (2011) 344–348.
[83] D.R. Cavener, GMC oxidoreductases. A newly defined family of homologous proteins with diverse catalytic activities, J. Mol. Biol. 223 (1992) 811–814.
[84] R.D. Finn, J. Mistry, J. Tate, P. Coggill, A. Heger, J.E. Pollington, O.L. Gavin, P. Gunasekaran, G. Ceric, K. Forslund, L. Holm, E.L.L. Sonnhammer, S.R. Eddy, A. Bateman, The Pfam protein families database, Nucleic Acids Res. 38 (2009) 211–222.
[85] M. Kiess, H.-J. Hecht, H.M. Kalisz, Glucose oxidase from *Penicillum amagaskiense* primary structure and comparison with other glucose-methanol-choline (GMC) oxidoreductases, Eur. J. Biochem. 252 (1998) 90–99.
[86] J.P. Roth, J.P. Klinman, Catalysis of electron transfer during activation of O_2 by the flavoprotein glucose oxidase, Proc. Natl. Acad. Sci. U. S. A. 100 (2003) 62–67.
[87] F. Fan, G. Gadda, On the catalytic mechanism of choline oxidase, J. Am. Chem. Soc. 127 (2005) 2067–2074.
[88] W.P. Dijkman, M.W. Fraaije, Discovery and characterization of a 5-hydroxymethylfurfural oxidase from *Methylovorus sp.* strain MP688, Appl. Environ. Microbiol. 80 (2014) 1082–1090.
[89] C. Martin, M. Trajkovic, M.W. Fraaije, Production of hydroxy acids through selective double oxidation of diols by a flavoprotein alcohol oxidase, Angew. Chemie. 59 (2020) 4869–4872
[90] E. Romero, G. Gadda, Alcohol oxidation by flavoenzymes, Biomol. Concepts. 5 (2014) 299–318.
[91] J.I. Reyes-De-Corcuera, H.E. Olstad, R. García-Torres, Stability and stabilization of enzyme biosensors: the key to successful application and commercialization, Annu. Rev. Food Sci. Technol. 9 (2018) 293–322.
[92] C.M. Wong, K.H. Wong, X.D. Chen, Glucose oxidase: Natural occurrence, function, properties and industrial applications, Appl. Microbiol. Biotechnol. 78 (2008) 927–938.
[93] B. Bissaro, A. Várnai, Å.K. Røhr, V.G.H. Eijsink, Oxidoreductases and reactive oxygen species in conversion of lignocellulosic biomass, Microbiol. Mol. Biol. Rev. 82 (2018) 1–51.
[94] M.R. Gray, Substrate inactivation of enzymes in vitro and in vivo, Biotechnol. Adv. 7 (1989) 527–575.
[95] P. George, Reaction between catalase and hydrogen peroxide, Nature. 160 (1947) 41–43.
[96] K. Kleppe, The effect of hydrogen peroxide on glucose oxidase from *Aspergillus niger*, Biochemistry. 5 (1966) 139–143.
[97] P.C. Molan, Honey as an Antimicrobial Agent, in: A. Mizrahi, Y. Lensky (Eds.), Bee Prod. Prop. Appl. Apitherapy, Springer US, Boston, MA, (1997) 27–37.
[98] É. Leiter, F. Marx, T. Pusztahelyi, H. Haas, I. Pócsi, P*enicillium chrysogenum* glucose oxidase - A study on its antifungal effects, J. Appl. Microbiol. 97 (2004) 1201–1209.

[99] M.M. Moore, T. Chen, Mutagenicity of bromate: Implications for cancer risk assessment, Toxicology. 221 (2006) 190–196.
[100] C. Sisak, Z. Csanádi, E. Rónay, B. Szajáni, Elimination of glucose in egg white using immobilized glucose oxidase, Enzyme Microb. Technol. 39 (2006) 1002–1007.
[101] T.P. Labuza, W.M. Breene, Applications of "active packaging" for improvement of shelf-life and nutritional quality of fresh and extended shelf-life foods, J. Food Process. Preserv. 13 (1989) 1–69.
[102] R. Wilson, A.P.F. Turner, Glucose oxidase: an ideal enzyme, Biosens. e Bioelectron. 7 (1992) 165–185.
[103] A. Vrielink, S. Ghisla, Cholesterol oxidase: Biochemistry and structural features, FEBS J. 276 (2009) 6826–6843.
[104] S. Devi, S.S. Kanwar, Cholesterol oxidase: source, properties and applications., Insights Enzym. Res. 1 (2018) 1–12.
[105] S. Ghosh, R. Ahmad, S.K. Khare, Immobilization of cholesterol oxidase: an overview, Open Biotechnol. J. 12 (2018) 176–188.
[106] L. Pollegioni, L. Piubelli, G. Molla, Cholesterol oxidase: Biotechnological applications, FEBS J. 276 (2009) 6857–6870.
[107] M. Pickl, M. Fuchs, S.M. Glueck, K. Faber, K. Faber, The substrate tolerance of alcohol oxidases, Appl. Microbiol. Biotechnol. 99 (2015) 6617–6642.
[108] L. Kumari, S. S. Kanwar, Cholesterol oxidase and its applications, Adv. Microbiol. 02 (2012) 49–65.
[109] J.P. Purcell, J.T. Greenplate, M.C. Jennings, J.S. Ryerse, J.C. Pershing, S.R. Sims, M.J. Prinsen, D.R. Corbin, M. Tran, R.D. Sammons, R.J. Stonard, Cholesterol oxidase: A potent insecticidal protein active against boll weevil larvae, Biochem. Biophys. Res. Commun. 196 (1993) 1406–1413.
[110] J. Lewkowski, Synthesis, chemistry and applications of 5-hydroxymethyl-furfural and its derivatives, Arkivoc. 2001 (2001) 17–54.
[111] S.P. Teong, G. Yi, Y. Zhang, Hydroxymethylfurfural production from bioresources: past, present and future, Green Chem. 16 (2014) 2015–2026.
[112] F. Menegazzo, E. Ghedini, M. Signoretto, 5-Hydroxymethylfurfural (HMF) production from real biomasses, Molecules. 23 (2018) 2201.
[113] A. Corma Canos, S. Iborra, A. Velty, Chemical routes for the transformation of biomass into chemicals, Chem. Rev. 107 (2007) 2411–2502.
[114] Z. Zhang, K. Deng, Recent Advances in the catalytic synthesis of 2 , 5-furandicarboxylic acid and its derivatives, (2015) 6529–6544.
[115] L. Hu, A. He, X. Liu, J. Xia, J. Xu, S. Zhou, J. Xu, Biocatalytic transformation of 5-hydroxymethylfurfural into high-value derivatives: recent advances and future aspects, ACS Sustain. Chem. Eng. 6 (2018) 15915–15935.
[116] W.P. Dijkman, M.W. Fraaije, Discovery and characterization of a 5-hydroxymethylfurfural oxidase from *Methylovorus sp.* strain MP688, Appl. Environ. Microbiol. 80 (2014) 1082–1090.
[117] A.S. Gandomkar, E. Jost, D. Loidolt, M. Pickl, W. Elaily, B. Daniel, P. Macheroux, W. Kroutil, Biocatalytic enantioselective oxidation of sec-allylic alcohols with flavin-dependent oxidases, Adv. Synth. Catal. 361 (2019) 5264–5271.

[118] S. Ikuta, S. Imamura, H. Misaki, Y. Horiuti, Purification and characterization of choline oxidase from *Arthrobacter globiformis*, J. Biochem. 82 (1977) 1741–1749.
[119] W.P. Dijkman, D.E. Groothuis, M.W. Fraaije, Enzyme-catalyzed oxidation of 5-hydroxymethylfurfural to furan-2,5-dicarboxylic acid, Angew. Chemie - Int. Ed. 53 (2014) 6515–6518.
[120] W.P. Dijkman, C. Binda, M.W. Fraaije, A. Mattevi, Structure-based enzyme tailoring of 5-hydroxymethylfurfural oxidase, ACS Catal. 5 (2015) 1833–1839.
[121] H.J. Wijma, R.J. Floor, P.A. Jekel, D. Baker, S.J. Marrink, D.B. Janssen, Computationally designed libraries for rapid enzyme stabilization, Protein Eng. Des. Sel. 27 (2014) 49–58.
[122] H.J. Wijma, M.J.L.J. Fürst, D.B. Janssen, A Computational Library Design Protocol for Rapid Improvement of Protein Stability: FRESCO, in: U.T. Bornscheuer, M. Höhne (Eds.), Protein Eng. Methods Protoc., 2018: pp. 69–85.
[123] M.J.L.J. Fürst, C. Martin, N. Lončar, M.W. Fraaije, Experimental protocols for generating focused mutant libraries and screening for thermostable proteins, Methods Enzymol. 608 (2018) 151–187.
[124] M. Pickl, E. Jost, S.M. Glueck, K. Faber, Improved biooxidation of benzyl alcohols catalyzed by the flavoprotein (5-Hydroxymethyl)furfural oxidase in organic solvents, Tetrahedron. 73 (2017) 5408–5410.
[125] M. Pickl, A. Swoboda, E. Romero, C. Winkler, C. Binda, A. Mattevi, K. Faber, M. Fraaije, Kinetic resolution of sec-thiols via enantioselective oxidation with rationally engineered 5-(hydroxymethyl)furfural oxidase, Angew. Chemie Int. Ed. 57 (2018) 2864–2868.
[126] B. Xu, S.F. Zhu, Z.C. Zhang, Z.X. Yu, Y. Ma, Q.L. Zhou, Highly enantioselective S-H bond insertion cooperatively catalyzed by dirhodium complexes and chiral spiro phosphoric acids, Chem. Sci. 5 (2014) 1442–1448.
[127] C. Koch, P. Neumann, O. Valerius, I. Feussner, R. Ficner, Crystal structure of alcohol oxidase from *Pichia pastoris*, PLoS One. 11 (2016) 1–17.
[128] P. Goswami, S.S.R. Chinnadayyala, M. Chakraborty, A.K. Kumar, A. Kakoti, An overview on alcohol oxidases and their potential applications, Appl. Microbiol. Biotechnol. 97 (2013) 4259–4275.
[129] P. Ozimek, M. Veenhuis, I.J. Van Der Klei, Alcohol oxidase: A complex peroxisomal, oligomeric flavoprotein, FEMS Yeast Res. 5 (2005) 975–983.
[130] T. Vogl, L. Sturmberger, T. Kickenweiz, R. Wasmayer, C. Schmid, A.M. Hatzl, M.A. Gerstmann, J. Pitzer, M. Wagner, G.G. Thallinger, M. Geier, A. Glieder, A toolbox of diverse promoters related to methanol utilization: functionally verified parts for heterologous pathway expression in *Pichia pastoris*, ACS Synth. Biol. 5 (2016) 172–186.
[131] F.W. Krainer, C. Dietzsch, T. Hajek, C. Herwig, O. Spadiut, A. Glieder, Recombinant protein expression in *Pichia pastoris* strains with an engineered methanol utilization pathway, Microb. Cell Fact. 11 (2012) 22.
[132] J.E. Fischer, A. Glieder, Current advances in engineering tools for *Pichia pastoris*, Curr. Opin. Biotechnol. 59 (2019) 175–181.
[133] F.S. Hartner, A. Glieder, Regulation of methanol utilisation pathway genes in yeasts, Microb. Cell Fact. 5 (2006).

[134] G. Daniel, J. Volc, L. Filonova, O. Plíhal, E. Kubátová, P. Halada, Characteristics of *Gloeophyllum trabeum* alcohol oxidase, an extracellular source of H_2O_2 in brown rot decay of wood, Appl. Environ. Microbiol. 73 (2007) 6241–6253.
[135] A.R. Vijayakumar, E. Csöregi, A. Heller, L. Gorton, Alcohol biosensors based on coupled oxidase-peroxidase systems, Anal. Chim. Acta. 327 (1996) 223–234.
[136] A.M. Azevedo, D.M.F. Prazeres, J.M.S. Cabral, L.P. Fonseca, Ethanol biosensors based on alcohol oxidase, Biosens. Bioelectron. 21 (2005) 235–247.
[137] J. Vonck, E.F.J. van Bruggen, Electron microscopy and image analysis of two-dimensional crystals and single molecules of alcohol oxidase from *Hansenula polymorpha*, Biochim. Biophys. Acta (BBA)/Protein Struct. Mol. 1038 (1990) 74–79.
[138] D. Linke, N. Lehnert, M. Nimtz, R.G. Berger, An alcohol oxidase of *Phanerochaete chrysosporium* with a distinct glycerol oxidase activity, Enzyme Microb. Technol. 61–62 (2014) 7–12.
[139] A.B. Leoneti, V. Aragão-Leoneti, S.V.W.B. de Oliveira, Glycerol as a by-product of biodiesel production in Brazil: Alternatives for the use of unrefined glycerol, Renew. Energy. 45 (2012) 138–145.
[140] M.R. Monteiro, C.L. Kugelmeier, R.S. Pinheiro, M.O. Batalha, A. da Silva César, Glycerol from biodiesel production: Technological paths for sustainability, Renew. Sustain. Energy Rev. 88 (2018) 109–122.
[141] S. Gerstenbruch, H. Wulf, N. Mußmann, T. O'Connell, K.H. Maurer, U.T. Bornscheuer, Asymmetric synthesis of D-glyceric acid by an alditol oxidase and directed evolution for enhanced oxidative activity towards glycerol, Appl. Microbiol. Biotechnol. 96 (2012) 1243–1252.
[142] Q.-T. Nguyen, E. Romero, W. Dijkman, S.P. de Vasconcellos, C. Binda, A. Mattevi, M.W. Fraaije, Structure-based engineering of *Phanerochaete chrysosporium* alcohol oxidase for enhanced oxidative power towards glycerol, Biochemistry. 57 (2018) 6209–6218.
[143] N. Goonoo, R. Jeetah, A. Bhaw-luximon, D. Jhurry, Polydioxanone-based bio-materials for tissue engineering and drug / gene delivery applications, Eur. J. Pharm. Biopharm. 97 (2015) 371–391.
[144] G. Faccio, K. Kruus, J. Buchert, M. Saloheimo, Secreted fungal sulfhydryl oxidases: Sequence analysis and characterisation of a representative flavin-dependent enzyme from *Aspergillus oryzae*, BMC Biochem. 11 (2010).
[145] D.P.H.M. Heuts, D.B. Janssen, M.W. Fraaije, Changing the substrate specificity of a chitooligosaccharide oxidase from *Fusarium graminearum* by model-inspired site-directed mutagenesis, FEBS Lett. 581 (2007) 4905–4909.

Creating a More Robust 5-hydroxymethylfurfural Oxidase by Combining Computational Predictions with a Novel Effective Library Design

Caterina Martin, Amaury Ovalle Maqueo , Hein J. Wijma and Marco W. Fraaije*

Molecular Enzymology Group, University of Groningen, Nijenborgh 4, 9747AG, Groningen, The Netherlands

*Corresponding author

Published in:
Biotechnology for Biofuels, (2018) (11:56)

ABSTRACT

Background HMF oxidase (HMFO) from *Methylovorus sp.* is a recently characterized flavoprotein oxidase. HMFO is a remarkable enzyme as it is able to oxidize 5-(hydroxymethyl)furfural (HMF) into 2,5-furandicarboxylic acid (FDCA): a catalytic cascade of three oxidation steps. Because HMF can be formed from fructose or other sugars and FDCA is a polymer building block, this enzyme has gained interest as an industrially relevant biocatalyst.

Results To increase the robustness of HMFO, a requirement for biotechnological applications, we decided to enhance its thermostability by using the recently developed FRESCO method: a computational approach to identify thermostabilizing mutations in a protein structure. To make this approach even more effective, we now developed a new and facile gene shuffling approach to rapidly combine stabilizing mutations in a one-pot reaction. This allowed the identification of the optimal combination of seven beneficial mutations. The created thermostable HMFO mutant was further studied as a biocatalyst for the production of FDCA from HMF and was shown to perform significantly better than the original HMFO.

Conclusions The described new gene shuffling approach quickly discriminates stable and active multi-site variants. This makes it a very useful addition to FRESCO. The resulting thermostable HMFO variant tolerates the presence of cosolvents and also remained thermotolerant after introduction of additional mutations aimed at improving the catalytic activity. Due to its stability and catalytic efficiency, the final HMFO variant appears to be a promising candidate for industrial scale production of FDCA from HMF

INTRODUCTION

The solution to overcome the increasing demand for polymers, while fossil oil resources are rapidly depleting, could be the use of biomass as a renewable starting material [1]. A promising alternative to the petroleum-based poly(ethylene-terephthalate) (PET) polymer is poly(ethylene-furandicarboxylate) (PEF). Thanks to its similar characteristics, PEF has attracted attention because it is a bio-based polymer obtained from furan-2,5-dicarboxylic acid (FDCA) and this monomer can be synthesized from the most abundant renewable material: carbohydrates [2,3]. For this reason, FDCA production has gained a lot of interest and different methods have been developed to convert carbohydrates or carbohydrate derived products (such as HMF) into FDCA [4]. Chemical methods to obtain FDCA from HMF by homogeneous or supported metal catalysts typically present several disadvantages: high costs, low yields, byproducts and the requirement of organic solvents which are not environmentally sustainable [5,6]. Several biocatalytic routes from HMF to FDCA have recently been described [7,8,9]. Among these approaches, only one was shown to be dependent on merely one biocatalyst, HMF oxidase (HMFO), a highly attractive feature. We identified HMFO in the predicted proteome of *Methylovorus sp.* strain MP688 [8]. The oxidase contains a flavin adenine dinucleotide (FAD) cofactor as prosthetic group and only requires molecular oxygen as electron acceptor to catalyze various oxidation reactions which include alcohol and thiol oxidations [8,10]. HMFO was shown to be capable to convert HMF into FDCA in a three step reaction (Scheme 1) [8,10].

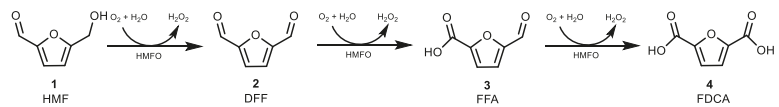

Scheme 1 Oxidation reaction of 5-hydroxymethylfurfural (HMF) to 2,5-furandicarboxylic acid (FDCA) by HMFO

In order to develop HMFO into an industrially applicable biocatalyst, its catalytic and stability properties have to be improved. While the enzyme is efficient in catalyzing the first step in the catalytic cascade, it is rather inefficient in the last step. Furthermore, the enzyme displays only a modest stability. Upon elucidating the crystal structure of HMFO, we successfully identified mutations that improve its performance in oxidation of the hydrated form of 5-formyl-2-furancarboxylic acid (FFA) to FDCA, the last step in the catalytic cascade [11]. The mutant

V367R-W466F HMFO was found to be the best variant for FDCA production with a *k*cat/K_m value for FFA conversion >1000-fold higher than for the wild-type enzyme [11]. Yet, as often observed when engineering enzyme activity, the higher catalytic performance was at the expense of enzyme thermostability.

Since HMFO has the potential to become an important biocatalytic tool, development of a robust variant is essential. An enzyme with a higher thermostability will be more suitable for use under harsh reaction conditions such as elevated temperatures and the presence of organic cosolvents [12]. Moreover a stable enzyme is the ideal template for further enzyme engineering efforts aimed to improve or change its catalytic properties [13]. Several methods have been designed to enhance the (thermo)stability of enzymes [14]. Completely random approaches like directed evolution can be effective but are time consuming and require high-throughput screening methods [15].

Rational design of stabilizing mutations is still challenging due to the fact that it is too complicated to accurately explain the effects of a mutation in terms of ΔΔH and ΔΔS [16]. Yet, state-of-the-art computational methods have evolved to such a level that they have predictive value in selecting putative thermostabilizing mutations. This can be used as input for the design of relatively small mutant libraries for screening *in vitro* [17]. We have recently developed a Framework for Rapid Enzyme Stabilization by Computational libraries (FRESCO) which is a computationally assisted method that includes predicting a large number of independent stabilizing mutations that are *in silico* screened in order to define a relatively small set of mutations that need to be tested experimentally [18,19]. This approach has demonstrated its validity with different enzymes, leading to high T_m^{app} improvements of up to 32 °C [20,21,22]. The initial steps of the FRESCO strategy consist of computational and visual selections based on free energy predictions and molecular dynamic (MD) simulations of single point mutations. This is followed by an *in vitro* phase to identify variants with significantly improved stability and finally the combination of the selected mutations should result in a highly stable enzyme variant. FRESCO is an attractive approach when dealing with a protein for which the crystal structure has been determined and, therefore, HMFO is a suitable candidate. The aim of this work was to obtain a stable HMFO variant which performs well in the conversion of HMF into FDCA.

RESULTS AND DISCUSSION

Computational Screening. The *in silico* phase of the FRESCO strategy was necessary to create an enriched library of single point mutants of HMFO. The crystal structure of the reduced form of the enzyme (PDB:4UDQ) was selected as model as it was solved at a better resolution (1.6 Å) than the oxidized enzyme [11]. Using this structure all possible point mutations were modelled (excluding residues that are within 5 Å from the FAD cofactor) and their respective values in free energy of folding were compared with that of the wild type enzyme ($\Delta\Delta G^{Fold}$). By omitting the residues that are close to the active site, the risk of creating a mutant with lower or no activity is limited. The first *in silico* step consisted of a selection based on free energy prediction: single mutants with a predicted $\Delta\Delta G^{Fold}$ higher than –5 kJ mol^{-1} were discarded. This decreased the number of variants to screen from 9044 to 744. The Dynamic Disulfide Discovery (DDD) algorithm was not included in this FRESCO approach because disulfide bonds may complicate protein expression [20]. The MD simulations of the 744 variants were visually inspected comparing the modelled structure of the wild-type with the mutants ones. The goal was to select variants with putative improvements in their thermostability profile. The screening was based on avoiding features that are normally found to cause a decrease in stability such as an increased flexibility (backbone and sidechain), an increase in hydrophobic surface exposure and diminished hydrogen-bonding interactions [21]. Those 140 mutants that scored well in the free energy of folding and did not show such aberrant structural features upon MD simulation and visual inspection, were selected to be experimentally tested for thermostability.

Screening of single mutants. Using PCR all 140 mutations were introduced in the HMFO-expression plasmid. The 140 mutant proteins and wild-type HMFO were produced in 96-well plates, which allowed efficient testing of all variants. To establish the effect of each mutation on stability the apparent melting temperature (T_m^{app}) was determined for each variant using the ThermoFAD assay [22]. The latter method reports on the temperature at which the flavin cofactor is released from the protein, thereby becoming more fluorescent because flavin fluorescence is typically quenched when it is bound in a protein. This provides a good estimate of the thermostability of the studied flavoprotein as cofactor release is the result of protein unfolding. Because HMFO is well expressed, we did not only determine the T_m^{app} value for each variant after enzyme purification, but the T_m^{app} was also measured using cell extracts. This revealed that the stability of the variants could

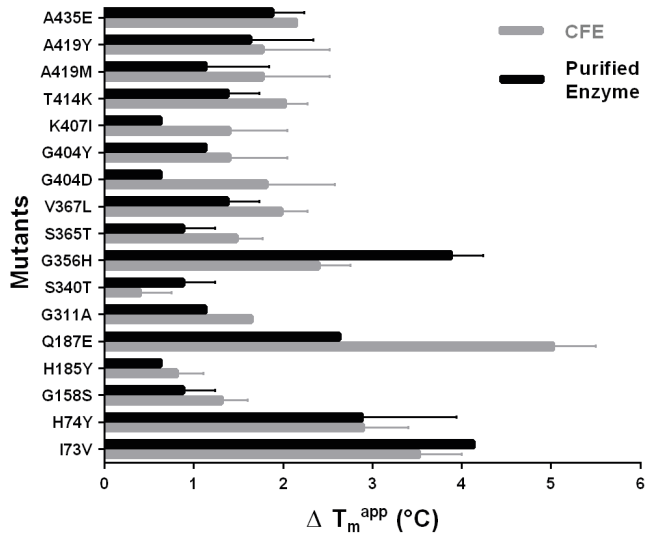

Figure 1. ΔT_m^{app} values of 17 selected mutants. The values correspond to an increase in T_m^{app} when compared with WT HMFO (T_m^{app} = 48.5 °C)

also be measured in cell extracts as the T_m^{app} values obtained with cell free extracts were quite consistent compared with the purified enzymes. It demonstrates that the ThermoFAD method can be a very powerful approach to efficiently screen a large set of flavoprotein variants without the need for enzyme purification. Importantly, the ThermoFAD measurements revealed 17 mutations that led to a significant positive ΔT_m^{app} in comparison with the wild-type enzyme (Figure 1) (Additional file 1: Table S1).

Golden Gate Gene Shuffling. As next step in the FRESCO method, the best combination of beneficial mutations needs to be identified. The addition of several single mutations does not necessarily lead to a more thermostable variant, because beneficial single mutations may not be compatible. So far the strategy to combine the mutations was based on a good analysis of the ΔT_m^{app} together with the mutation position and its predicted effect. Yet, such an approach is time consuming since the mutations need to be combined in a step-wise fashion, one by one or in groups and tested at each step [18,20,21,22]. We set out to develop a more effective method to quickly identify the best combination of mutations that results in a stable and active variant. For this, we aimed at randomly combining mutations through a gene shuffling approach. Various gene shuffling methods have been developed in the field of protein engineering, often with the focus

to merge certain wanted properties of two or more distinct proteins into one[25,26]. We developed a controlled approach that can be applied in cases when it is desired to test all different combinations of several specific gene fragments (with predefined mutations). In our method we take advantage of the fact that gene (fragment) synthesis has become relatively cheap [27]. For the gene shuffling library, we chose the 8 mutations which resulted in the highest T_m^{app} values: I73V, H74Y, Q187E, G356H, V367L, T414K, A419Y, and A435E. To assess if the catalytic properties of the corresponding mutant enzymes were unaffected, we measured HMFO activity towards vanillyl alcohol [8]. The benefit of using this substrate is that it allows direct detection of product formation as the formed vanillin displays light absorbance at 340 nm. Gratifyingly, all mutants showed similar activity when compared with the wild-type enzyme (Additional file 2: Table S2). Before performing gene shuffling, the mutations I73V and H74Y, being neighboring residues, were combined to verify whether they display an additive effect. This was found to be the case as the double mutant presents a T_m^{app} that is 6 °C higher when compared with the wild-type enzyme (the single mutations displayed 3-4 °C higher T_m^{app} values, Figure 1). This double mutation was included in the gene shuffling approach instead of the two individual mutations, reducing the number of mutation sites to 7. The aim of the gene shuffling approach was to create a library of all the possible combinations (128) of the selected 7 sites and subsequently test them for thermostability and activity towards HMF. The gene shuffling protocol described in this work is based on the Golden Gate cloning system [25]. Previously, other approaches used type IIs restriction enzymes to combine gene fragments or plasmid modules; these methods involve cloning of each module flanked by BsaI sites in individual vectors, or add type IIs restriction enzyme sites by separate PCRs for each module [29,30]. The Golden Gate gene shuffling we developed for the FRESCO strategy is a one-pot reaction that involves only three designed vectors and a single restriction-ligation reaction (Figure 2).

The first step was the design of two synthetic genes, one wild-type version and one with the selected 7 mutations, each containing 8 BsaI restriction sites that flank the 7 gene modules that contain the target mutation sites. The positions of the modules were defined identically for the two versions and were designed such that all the desired mutation sites could be introduced in separate modules and that the 4 nucleotide overhangs for the ligation were unique and not palindromic. The innovation of this method is in the design of the BsaI restriction sites. Each module is flanked by two BsaI sites: between two modules there are two mirrored BsaI sites and the 4 overhang nucleotides at the end

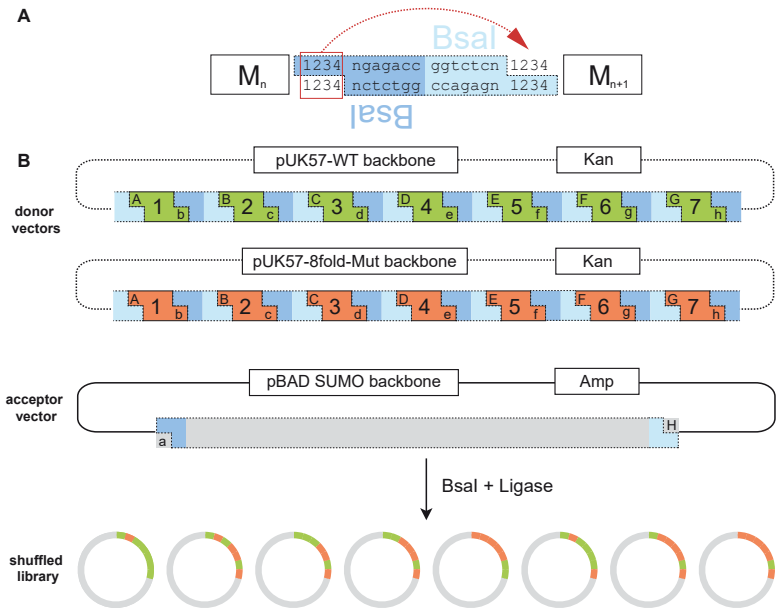

Figure 2. Design of the synthetic genes for Golden Gate gene shuffling. (a) BsaI recognition sites between two modules are flanked and mirrored. The four nucleotides at the end of one fragment are replicated at the beginning of the next one to avoid nucleotide loss after the ligation. (b) Donor vectors have the same fragment arrangement. The wild-type fragments are represented in green, while the fragments in orange have one mutation site each. The dotted sections (pUK57 backbone and BsaI sites) are lost after the ligation. The shuffled library consists of pBAD SUMO-HMFO vectors with a random combination and correct order of the 7 gene modules (with mutations)

of each module are replicated at the beginning of the following module to allow a scarless ligation. By performing the one pot Golden Gate cloning reaction on the mixture of the two donor vectors, containing the two synthetic genes, and the acceptor pBAD vector, all possible combinations of the 7 gene fragments are created in the pBAD-based expression vector. The Golden Gate gene shuffling library was analyzed by sequencing to confirm the heterogeneity and accuracy of the shuffling of gene fragments. The results showed that 97% of the colonies contained the correct restriction pattern and the shuffling efficiency was 65%. This indicates that per 100 clones, 65 contain non-redundant randomly shuffled sequences.

Table 1. Steady-State Parameters of the different HMFO variants on HMF [a]

HMFO	k_{cat} (s^{-1})	K_m (mM)	k_{cat}/K_m ($s^{-1}mM^{-1}$)
WT	13.7	1.52	9.03
7xHMFO	11.8	0.63	18.7

[a] Kinetic parameters were determined by measuring H_2O_2 formation in a coupled assay using HMF as substrate (Additional file 4: Figure S1).

Shuffled library screening. The gene shuffling library was tested to establish T_m^{app} of the variants and also their activity towards HMF. To be sure of screening all the possible combinations, the tested library size was 3.5 fold the number of possible combinations. The results of the ThermoFAD analysis showed that the 8xHMFO (I73V, H74Y, Q187E, G356H, V367L, T414K, A419Y, A435E) was the most thermostable variant with an improvement of 13 °C compared with the WT (T_m^{app} = 48.5 °C). Yet, an alignment of the best 9 multi-site mutants that presented an higher T_m^{app} together with a preserved ability to oxidize HMF demonstrated that the mutation Q187E had a negative effect on the activity (Additional file 3: Table S3). This shows the advantage of using a gene shuffling approach to evaluate the best thermostable and active mutant. Therefore the best multiple mutant was considered to be the 7xHMFO mutant (I73V, H74Y, G356H, V367L, T414K, A419Y, A435E) with a T_m^{app} of 60.5 °C and k_{cat} and K_m values comparable with the wild-type enzyme (Table 1) [10].

To further investigate the thermostable properties of the 7xHMFO mutant, its stability over time at 40 °C was investigated. The 7xHMFO variant presented a remarkable stability compared to the wild-type enzyme. While wild-type HMFO completely lost its activity after 2 days, the thermostable variant retained 50% of its activity even after 10 days of incubation at 40 °C (Additional file 5: Figure S2). Since HMFO is able to oxidize many different substrates, including compounds that are poorly soluble in water, we investigated the stability in the presence of different cosolvents. The 7xHMFO showed a much higher tolerance towards four commonly used cosolvents when compared with the wild-type enzyme (Figure 3). The 7xHMFO mutant with its higher thermostability, solvent-tolerance, and preserved catalytic activity represents an excellent template for further engineering.

Engineering of thermostable HMFO variant for FDCA production. To further tune the 7xHMFO variant towards conversion of HMF into FDCA we introduced two mutations (V367R and W466F) in the active

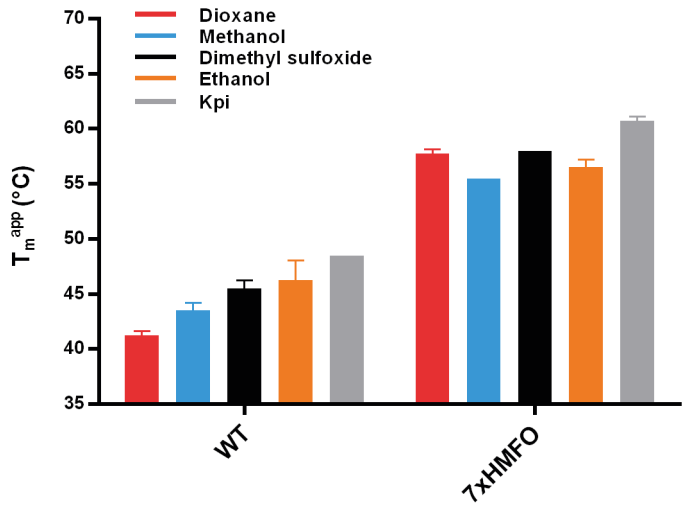

Figure 3. T_m^{app} in the absence or presence of 15% 1,4-dioxane, methanol, dimethyl sulfoxide, or ethanol. Kpi is the control in 50 mM phosphate buffer, pH 8.0

Table 2. T_m^{app} values of HMFO variants [a]

HMFO	T_m^{app} (°C)
WT	48.5
V367R W466F	39.5
7xHMFO[b]	60.5
8AxHMFO[c]	55.5
8BxHMFO[d]	51.5

[a] T_m^{app} values of HMFO variants (30 μM) obtained by ThermoFAD in phosphate buffer 50 mM pH 8.0. [b] The 7xHMFO variant includes the mutations: I73V, H74Y, G356H, V367L, T414K, A419Y, A435E. [c] The 8AxHMFO variant includes the mutations: I73V, H74Y, G356H, V367L, T414K, A419Y, A435E and W466F, [d] The 8BxHMFO variant includes the mutations: I73V, H74Y, G356H, V367R, T414K, A419Y, A435E and W466F.

site that have been shown to be beneficial for FDCA production from HMF [11]. Since V367 had already been mutated in the 7xHMFO variant (V367L) we included in the analysis also another 8xHMFO variant with only the W466F mutation. The variants were tested and as expected the additional mutation(s) introduced into the 7xHMFO decreased the T_m^{app}. Yet, the stability remained significantly higher than the wild-type enzyme (Table 2).

To determine whether the thermostable variants are more potent biocatalysts than the previously described wild-type and/or V367R

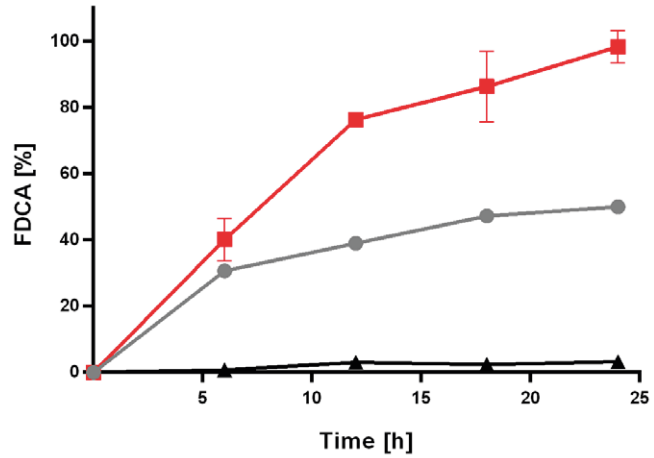

Figure 4. Production of FDCA from HMF at 25 °C by HMFO variants. WT (filled triangle), V367R W466F HMFO (filled circle), 8BxHMFO (I73V-H74Y, G356H, V367R, T414K, A419Y, A435E, and W466F) (filled square). Conversions were performed in duplicates in phosphate buffer 50 mM pH 8.0, HMFO 2.0 μM, HMF 5.0 mM, 25 °C

W466F HMFO mutant we tested the conversion rates using HMF as a substrate. The best thermostable variant for FDCA production turned out to be the newly engineered 8BxHMFO. The data revealed that this HMFO variant performs significantly better than the wild-type and the double mutant (Figure 4) (Additional file 6: Table S4).

At 25 °C an almost full conversion in 24 hours could be achieved while the conversion with the double mutant and the wild type enzyme remained below 50% and 5%, respectively. Since all the generated thermostable HMFO variants exhibit T_m^{app} values higher than 50 °C we decided to perform conversions also at 40 °C. At this temperature, only the 8BxHMFO mutant performed well (> 95% conversion in only 9 hours) (Additional file 7: Table S5). The k_{cat}/K_m of the 8BxHMFO is 0.1 $s^{-1}mM^{-1}$ which compared to the reported k_{cat}/K_m value of the double mutant is relatively low (2.2 $s^{-1}mM^{-1}$) (Additional file 8: Figure S3) [11]. This indicates that the higher conversion is largely due to an improved operational stability. The results indicate that this engineered version of HMFO can be used for longer time and can lead in this way to higher amounts of FDCA.

CONCLUSIONS

In this work we further developed the FRESCO protocol by developing a novel and efficient approach for combining individual stabilizing mutations. The Golden Gate gene shuffling described in this study was fundamental to rapidly identify the best combination of thermostabilizing mutations that led to a stable and active HMFO variant. The engineered 7xHMFO variant presented a T_m^{app} improvement of 12 °C compared with the wild-type enzyme together with an improved cosolvent tolerance. We could also demonstrate that this thermostable variant of HMFO can be used as template to introduce a destabilizing mutation in the active site. One of the resulting HMFO mutants displayed superior performance compared to previously reported HMFO variants in converting HMF in a three-step one-enzyme reaction into FDCA.

MATERIALS AND METHODS

All materials were acquired from Sigma-Aldrich unless otherwise specified.

Computational Methods. The FRESCO method was employed to obtain a thermostabilized variant of HMFO. Computational modeling was performed using the 4UDQ X-ray structure of HMFO (1.6 Å resolution). To avoid mutations that could interfere with the active site, only residues that were > 5 Å away from FAD were mutated [11]. The computational selection was started with calculating the predicted change of free folding energy ($\Delta\Delta G^{Fold}$) with FoldX (foldx.crg.es) and Rosetta-ddg (www.rosettacommons.org) [18,19-]. For Rosetta, the so-called row-3 protocol (described by Kellogg et al. in row 3 of their table 1) was invoked by using the following options: -ddg::weight_file soft_rep_design -ddg::iterations 50 -ddg::local_opt_only true -ddg::min_cst false -ddg::mean true -ddg::min false -ddg::sc_min_only false -ddg::ramp_repulsive false -ddg::opt_radius 8.0 [29]. For FoldX, the used options were --command=BuildModel --numberOfRuns=5. The single point mutations with a predicted $\Delta\Delta G^{Fold}$ < -5 kJ mol^{-1} were subsequently submitted to MD simulations under Yasara as previously described [18,19]. The averaged structures from the MD trajectories were visually inspected comparing the variant simulations with the wild type HMFO while examining backbone and side-chain flexibility, hydrogen bonds and hydrophobic exposure. This last *in silico* step is to further reduce the number of potentially thermostable variants to experimentally screen.

Genetic Engineering. For all the experiments the His6x-SUMO-HMFO fusion has been used as it has been demonstrated before that the SUMO protein fused at the N-terminus does not affect the activity nor the thermostability of HMFO [10].The gene single point variants, the double mutant I73V H74Y, the 8AxHMFO and the 8BxHMFO were obtained from pET SUMO-HMFO or pBAD SUMO-7xHMFO by whole-plasmid PCR with PfuUltra II Hotstart PCR Master Mix (Agilent). Template DNA was cleaved with DpnI (New England Biolabs) for at least 2 hours at 37 °C. *Escherichia coli* NEB 10β (New England Biolabs) chemically competent cells were transformed (heat shock at 41 °C for 45 seconds) and cells plated on 50 $\mu g \cdot mL^{-1}$ kanamycin or 100 $\mu g \cdot mL^{-1}$ ampicillin LB agar plates. All mutations were confirmed by sequencing.

Golden Gate Gene Shuffling. The 8-fold mutants were obtained using a gene shuffling approach. For this, we designed two synthetic gene versions of *hmfo*: one with 7 modules each containing one mutated region (the first module containing 2 mutations, and the 8 mutations are: I73V-H74Y, Q187E, G356H, V367L, T414K, A419Y, A435E) and the other synthetic gene with the same modules arrangement but without mutations, corresponding to the wild type DNA sequence. Each module had been designed to be flanked by BsaI recognition sites: NGAGACC at the beginning and GGTCTCN at the end. Moreover at the beginning of each fragment the last 4 base pairs (bp) of the previous module are repeated (or the 5'- 4 bp of the overhang region of the acceptor plasmid in the case of the first fragment and at the end of the 7^{th} fragment are replicated 4 bp of the 3'- ligation site of the receiving plasmid). The BsaI cutting sites have been chosen in order to be unique (at least 3 out of 4 nucleotides in the sticky end have to be different) and not palindromic to avoid unwanted ligations (Additional file 9: Gene Sequences). The synthetic genes have been ordered (GenScript) cloned in two pUK57. A derivative of pBAD SUMO vector designed with BsaI cutting site 5'-TGGTngagacc and ggtctcnCTTG-3') was used as receiving vector. The restriction-ligation reaction was set up in 20 µL volume with the components: pBAD SUMO 3.75 $ng \cdot \mu L^{-1}$, pUC57wt 2.5 $ng \cdot \mu L^{-1}$, pUC578xmutant 2.5 $ng \cdot \mu L^{-1}$, T4 DNA ligase buffer (Promega), T4 DNA ligase 1.5 $U \cdot \mu L^{-1}$ (Promega), BsaI 1 $U \cdot \mu L^{-1}$ (New England Biolabs); the thermocyler program was: incubation at 37 °C for 5 minutes and at 16 °C for 10 minutes repeated 50 times, followed by a final incubation at 50 °C for 10 minutes (final digestion) and at 80 °C for 10 minutes (enzyme inactivation). The restriction-ligation reaction (5 µL) were used to transform 100 µL of chemically competent NEB 10β cells plated on 100 $\mu g \cdot mL^{-1}$ampicillin LB agar plates. The *hmfo* variants were verified

first by colony PCR (DreamTaq Green PCR Master Mix, ThermoFisher) to determine the inserts size and then by sequencing.

Large scale expression and purification. For HMFO expression, a culture was started by inoculating 5 mL of preculture (LB supplemented with 50 $\mu g \cdot ml^{-1}$ kanamycin or 100 $\mu g \cdot ml^{-1}$ ampicillin) in 100 mL TB (Terrific Broth with the same antibiotic). In the case of pET constructs, protein expression was induced at OD_{600} 0.5 with 1.0 mM isopropyl β-d-1-thiogalactopyranoside (IPTG), and with 0.02% L-arabinose in the case of the pBAD SUMO-HMFO construct. The latter was obtained by cloning the HMFO DNA sequence using NdeI and HindIII (NEB) in pBAD SUMO. Cells were grown overnight at 24 °C 135 rpm and harvested at 5000 *g* for 10 min at 4 °C. The cells pellet was resuspended in 10 mL of 50 mM Tris HCl pH 8.0 with 150 mM NaCl and sonicated 3'' on 6'' off at 70% amplitude. The enzyme was purified from the cell free extract as described previously [8].

Small scale expression. The single point variants were expressed in *E. coli* BL21(DE3) cells with the pET SUMO-HMFO vector. The cultures were prepared using 600 µL of overnight culture (LB supplemented with 50 $\mu g \cdot ml^{-1}$ kanamycin) to inoculate 5 mL TB containing 50 $\mu g \cdot ml^{-1}$ kanamycin in a 24 well-plate. The multi-site variants were expressed with the pBAD SUMO-HMFO vector in *E. coli* NEB 10β cells; the cultures were made by inoculating 200 µL of overnight culture (LB supplemented with 100 $\mu g \cdot ml^{-1}$ ampicillin) in 800 µL of TB (100 $\mu g \cdot ml^{-1}$ ampicillin) in 96 well-plate. The cultures were incubated at 37 °C with a shaking at 300 rpm and induced with 1.0 mM IPTG (in case of *E. coli* BL21(DE3) cells carrying the pET SUMO-HMFO vector) or with 0.02% L-arabinose (*E. coli* NEB 10β cells carrying the pBAD SUMO-HMFO vector) at an optical density at 600 nm (OD_{600}) of 2.0. Expression continued overnight at 24 °C with shaking at 550 rpm.

Small scale purification. Cells were harvested by centrifugation at 2250 *g* for 20 minutes at 4 °C. The cell-free extract was obtained after cell lysation: the cell pellet was solubilized in 200 µL lysis buffer (lysozyme 1 $mg \cdot ml^{-1}$, deoxyribonuclease I 0.5 $mg \cdot ml^{-1}$, $MgCl_2$ 10 mM in 50 mM Tris HCl pH 8.0). The solubilized pellet was incubated for 30 minutes at 25 °C (shaking at 550 rpm) and then it was frozen in liquid nitrogen and centrifuged at 2250 *g* for 45 minutes at 4 °C. The soluble fraction was filtered (Whatman UNIFILTER 96-well Microplate, GE-Healthcare) at 7 *g* for 15 seconds at 4 °C and mixed with 100 µL of pre-equilibrated Ni-Sepharose resin (GE-Healthcare) for 15 minutes using an AcroPrep Advance 1 mL 96-well plate (Pall). The flow through was removed and the column was washed 2 times with 200 µL of 50 mM Tris HCl pH 8.0 with 150 mM NaCl, and one time with the same buffer containing 5 mM imidazole. The protein was eluted with 100 µL of 50 mm Tris HCl with 150 mM NaCl containing 500 mM imidazole. The eluate was desalted in 50 mM phosphate buffer pH 8.0 using PD MultiTrap G-25 plates (GE-Healthcare).

Thermostability assay. The melting temperature of HMFO cell free extract or purified variants was tested by the ThermoFAD method, which allows to determine the unfolding temperature based on the release of the flavin cofactor [8,24]. This assay was performed using 20 µL of CFE or 20 µL of purified enzyme in 50 mM phosphate buffer at pH 8.0. The ThermoFAD was also used to determine enzyme concentration after the small-scale purification based on the dT/fluorescence value using a calibration line. The calibration curve prepared with several WT concentrations proved that enzyme concentration does not affect the T_m^{app}.

Activity assays. All the activity assays were performed in 50 mM phosphate buffer pH 8.0 at 25 °C. The HMFO mutants I73V, H74Y, Q187E, G356H, V367L, T414K, A419Y, A435E were tested using enzyme activity towards vanillyl alcohol as reported previously [8]. The gene shuffling library was tested with the coupled H_2O_2 detection assay: horseradish peroxidase (HRP) (Sigma), 0.004 $U \cdot \mu L^{-1}$, 4-aminoantipyrine (0.1 mM), 3,5- dichloro-2-hydroxybenzenesulfonic acid (1 mM) and HMF (10 mM), measuring at 515 nm (ε_{515}=26 $mM^{-1}cm^{-1}$) the formation of pink product due to H_2O_2 production during the oxidation of HMF by HMFO. This HRP coupled assay was also used to determine k_{cat}, K_m, and the activity after the incubation at 40 °C for HMFO wild type and for the thermostable.

Product identification. The conversion performed by HMFO WT, HMFO V367R-W466F, HMFO I73V-H74Y-G356H-V367L-T414K-A419Y-A435E (7xHMFO), HMFO I73V-H74Y-G356H-V367L-T414K-A419Y-A435E-W466F (8AxHMFO), HMFO I73V-H74Y-G356H-V367R-T414K-A419Y-A435E-W466F (8BxHMFO), using 5.0 mM 5-(hydroxymethyl) furfural as a substrate were carried out at 25 °C or 40 °C, with shaking at 1000 rpm. After the conversion, the enzyme was inactivated at 80 °C for 10 minutes and eliminated by centrifugation. The products were analyzed by high-performance liquid chromatography as described previously [8].

REFERENCES

[1] A. Corma, S. Iborra, A. Velty, Chemical routes for the transformation of biomass into chemicals, Chem. Rev. 107 (6) (2007) 2411–2502.

[2] C. Moreau, M. Naceur, A. Gandini, Recent catalytic advances in the chemistry of substituted furans from carbohydrates and in the ensuing polymers, Topics in Catalysis 27 (2004) 11-30.

[3] S. Kima, M. Antunes, M. Pillinger, A. A. Valente, ChemInform Abstract: Ionic liquids as tools for the acid-catalyzed hydrolysis / dehydration of saccharides to furanic, ChemCatChem 3 (11) (2011) 1686.

[4] Z. Zhang, K. Deng, Recent advances in the catalytic synthesis of 2,5-furandicarboxylic acid and its derivatives, ACS Catal. 5 (2015) 6529–6544.

[5] P. Verdeguer, N. Merat, A. Gaset, Oxydation catalytique du HMF en acide 2,5-furane dicarboxylique, J. Mol. Catal. 85 (1993) 327–344.

[6] Y. Qu, J. Wang, Z. Zhang, S. Shi, D. Li, W. Shen, E. Shen, J. Zhou, Catalytic transformation of HODAs using an efficient meta-cleavage product hydrolase-spore surface display system, J. Mol. Catal. B Enzym. 102 (2014) 204–210.

[7] H. Yuan, J. Li, H. Shin, G. Du, J. Chen, Z. Shi, L. Liu, Improved production of 2,5-furandicarboxylic acid by overexpression of 5-hydroxymethylfurfural oxidase and 5-hydroxymethylfurfural/furfural oxidoreductase in *Raoultella ornithinolytica* BF60, Bioresour. Technol. 247 (2017) 1184-1188.

[8] W.P. Dijkman, M.W. Fraaije, Discovery and characterization of a 5-hydroxymethylfurfural oxidase from *Methylovorus sp.* strain MP688, Appl. Environ. Microbiol. 80 (2014) 1082–1090.

[9] J. Carro, P. Ferreira, L. Rodríguez, A. Prieto, A. Serrano, B. Balcells, A. Ardá, J. Jiménez-Barbero, A. Gutiérrez, R. Ullrich, M. Hofrichter, A.T. Martínez, 5-Hydroxymethylfurfural conversion by fungal aryl-alcohol oxidase and unspecific peroxygenase, FEBS J. 282 (2015) 3218–3229.

[10] W.P. Dijkman, M.W. Fraaije, Discovery and characterization of a 5-hydroxymethylfurfural oxidase from *Methylovorus sp.* strain MP688, Appl. Environ. Microbiol. 80 (2014) 1082–1090.

[11] W.P. Dijkman, C. Binda, M.W. Fraaije, A. Mattevi, Structure-based enzyme tailoring of 5-hydroxymethylfurfural oxidase, ACS Catal. 5 (2015) 1833–1839.

[12] J.K. Kristjansson, Thermophilic organisms as sources of thermostable enzymes, Trends Biotechnol. 7 (1989) 349–353.

[13] J.D. Bloom, S.T. Labthavikul, C.R. Otey, F.H. Arnold, Protein stability promotes evolvability, Proc. Natl. Acad. Sci. 103 (2006) 5869–5874.

[14] A.S. Bommarius, J.M. Broering, J.F. Chaparro-Riggers, K.M. Polizzi, High-throughput screening for enhanced protein stability, Curr. Opin. Biotechnol. 17 (2006) 606–610.

[15] N.J. Turner, Directed evolution drives the next generation of biocatalysts, Nat. Chem. Biol. 5 (2009) 567–573.

[16] V.G.H. Eijsink, A. Bjørk, S. Gåseidnes, R. Sirevåg, B. Synstad, B. Van Den Burg, G. Vriend, Rational engineering of enzyme stability, J. Biotechnol. 113 (2004) 105–120.

[17] K. Steiner, H. Schwab, Recent advances in rational approaches for enzyme engineering., Comput. Struct. Biotechnol. J. 2 (2012) e201209010.

[18] H.J. Wijma, R.J. Floor, P.A. Jekel, D. Baker, S.J. Marrink, D.B. Janssen, Computationally designed libraries for rapid enzyme stabilization, Protein Eng. Des. Sel. 27 (2014) 49–58.

[19] H.J. Wijma, M.J.L.J. Fürst, D.B. Janssen, A computational library design protocol for rapid improvement of protein Stability: FRESCO, in: U.T. Bornscheuer, M. Höhne (Eds.), Protein Eng. Methods Protoc., (2018) 69–85.

[20] H. Arabnejad, M.D. Lago, P.A. Jekel, R.J. Floor, A.W.H. Thunnissen, A.C.T. Van Scheltinga, H.J. Wijma, D.B. Janssen, A robust cosolvent-compatible halohydrin dehalogenase by computational library design, 30 (2017) 175–189.

[21] Y. Nosoh, T. Sekiguchi, Protein stability and stabilization through protein engineering, Biochem Mol Biol Edu. 21 (1993) 111.

[22] F. Forneris, R. Orru, D. Bonivento, L.R. Chiarelli, A. Mattevi, ThermoFAD, a Thermofluor-adapted flavin ad hoc detection system for protein folding and ligand binding, FEBS J. 276 (2009) 2833–2840.

[23] R.J. Floor, H.J. Wijma, D.I. Colpa, A. Ramos-Silva, P.A. Jekel, W. Szymański, B.L. Feringa, S.J. Marrink, D.B. Janssen, Computational library design for increasing haloalkane dehalogenase stability, ChemBioChem. 15 (2014) 1660–1672.

[24] W.M. Coco, W.E. Levinson, M.J. Crist, H.J. Hektor, a Darzins, P.T. Pienkos, C.H. Squires, D.J. Monticello, DNA shuffling method for generating highly recombined genes and evolved enzymes., Nat. Biotechnol. 19 (2001) 354–359.

[25] C. Engler, R. Kandzia, S. Marillonnet, A one pot, one step, precision cloning method with high throughput capability, PLoS One. 3 (2008) e3647.

[26] C. Engler, R. Gruetzner, R. Kandzia, S. Marillonnet, Golden gate shuffling: A one-pot DNA shuffling method based on type ils restriction enzymes, PLoS One. 4 (2009) e5553.

[27] F. Zhang, L. Cong, S. Lodato, S. Kosuri, G.M. Church, P. Arlotta, Efficient construction of sequence-specific TAL effectors for modulating mammalian transcription, Nat. Biotechnol. 29 (2011) 149–154.

[28] R. Guerois, J.E. Nielsen, L. Serrano, Predicting changes in the stability of proteins and protein complexes : a study of more than 1000 mutations, 2836 (2002) 369–387.

[29] E.H. Kellogg, A. Leaver-Fay, D. Baker, Role of conformational sampling in computing mutation-induced changes in protein structure and stability, Proteins Struct. Funct. Bioinforma. 79 (2011) 830–838.

SUPPORTING INFORMATION

Additional file 1: Table S1. $\Delta T_{app}{}^{m}$ of the best 17 single mutants. Results of the ThermoFAD assay performed on cell-free extract and purified enzyme.

Mutant	CFE ($\Delta T_m{}^{app}$ °C)	Purified enzyme ($\Delta T_m{}^{app}$ °C)
I73V	3.5	4.1
H74Y	2.9	2.9
G158S	1.3	0.9
H185Y	0.8	0.6
Q187E	5.0	2.6
S340T	0.4	0.9
G356H	2.4	3.9
S365T	1.5	0.9
V367L	2.0	1.4
G404D	1.8	0.6
G404Y	1.4	1.1
K407I	1.4	0.6
A419M	1.8	1.1
A419Y	1.8	1.6
A435E	2.1	1.9
T414K	2.0	1.4
G311A	1.6	1.1

Additional file 2: Table S2. Activity towards vanillyl alcohol of HMFO mutants I73V, H74Y, Q187E, G356H, V367L, T414K, A419Y, and A435E. All the activity assays were performed in 50 mM phosphate buffer pH 8.0 at 25 °C.

HMFO	k_{obs}(s^{-1})
WT	20.6
I73V	19.3
H74Y	20.3
Q187E	5.4
G356H	6.4
V367L	23.7
T414K	25.7
A419Y	24.4
A435E	16.6

Additional file 3: Table S3. Multiple mutant alignment of the 9 best performing multiple-mutants resulted from the gene shuffling (results of 96 plate expression and purification system).

I73Y H74Y	Q187E	G356H	V367L	T414K	A419Y	A435E	$T_m{}^{app}$ (°C)	k_{obs}(s^{-1})
	wt					wt	59	<10
	wt						60	<10
	wt		wt		wt		59.5	<10
	wt				wt		59.5	<10
	wt			wt	wt	wt	57	<10
	wt		wt		wt	wt	59.5	<10
	wt		wt	wt	wt		59	<10
	wt		wt	wt	wt	wt	59	<10
	wt		wt		wt		58	<10

Additional file 4: Figure S1. Michaelis–Menten graph of WT and 7xHMFO. Kinetic assay performed with HRP peroxidase in 50 mM phosphate buffer pH 8.0 at 25 °C using HMF as substrate.

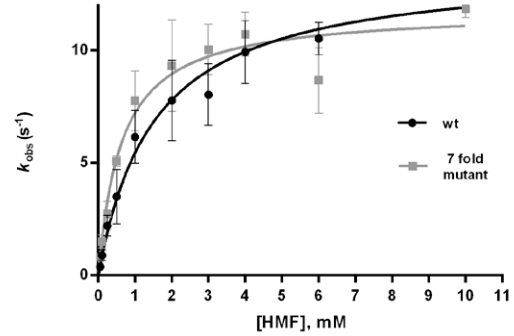

Best-fit values	wt	7xHMFO
k_{cat} (s^{-1})	13.72	11.79
K_m (mM^{-1})	1.518	0.6319
Std. Error		
k_{cat} (s^{-1})	0.70	0.64
K_m (mM^{-1})	0.24	0.14
95% Confidence Intervals		
k_{cat}	12.10 to 15.34	10.30 to 13.28
K_m	0.96 to 2.08	0.30 to 0.96
R^2	0.98	0.96

Additional file 5: Figure S2. Oxidation rates of HMF by HMFO wild-type and thermostable 7xHMFO variant after incubation at 40 °C [1 mM] in phosphate buffer 50 mM pH 8.0. The activity test was performed with HRP peroxidase assay using HMF as substrate.

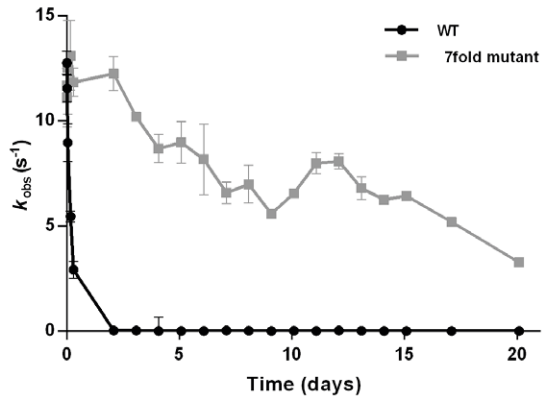

Additional file 6: Table S4. Percentages of products formed during the oxidation of 5 mM HMF by 2 μM of enzyme in phosphate buffer 50 mM pH 8.0 at 25 °C in Eppendorf ThermoMixer C while shaking at 1000 rpm. Average values of two experiments (standard deviations were < 27%, with an average standard deviation of 3.5%). Samples with only phosphate buffer, substrate, and WT enzyme where used as control.

Time (h)	Substrate/ Product (%)	WT	V367R W466F	8BxHMFO
6	**HMF**	0.0	54.2	18.7
6	**FFA**	79.6	3.4	2.7
6	**FDCA**	0.7	29.3	38.4
12	**HMF**	0.0	20.0	20.0
12	**FFA**	92.0	3.9	3.4
12	**FDCA**	3.0	37.0	73.0
18	**HMF**	0.0	40.3	11.4
18	**FFA**	100.9	3.2	1.8
18	**FDCA**	2.3	45.2	82.6
24	**HMF**	0.0	35.5	5.8
24	**FFA**	98.4	3.1	0.0
24	**FDCA**	3.1	47.9	94.1

Additional file 7: Table S5. Percentages of products formed during the oxidation of 5 mM HMF by 2 μM of enzyme in phosphate buffer 50 mM pH 8.0 at 40 °C in Eppendorf ThermoMixer C while shaking at 1000 rpm. Average values of two experiments (standard deviations were < 7%, with an average standard deviation of 1.0%). Samples with only phosphate buffer, substrate, and WT enzyme where used as control.

Time (h)	Substrate/Product (%)	WT	V367R W466F	8BxHMFO
3	**HMF**	69.2	97.6	22.5
3	**FFA**	21.8	0.4	9.2
3	**FDCA**	0.8	0.1	68.1
6	**HMF**	64.5	98.7	9.6
6	**FFA**	27.9	0.4	4.6
6	**FDCA**	0.0	0.1	76.0
9	**HMF**	62.3	96.8	7.6
9	**FFA**	29.2	0.2	3.9
9	**FDCA**	0.4	0.1	110.4
12	**HMF**	60.3	96.1	1.8
12	**FFA**	28.8	0.4	0.0
12	**FDCA**	0.3	0.2	101.6

Additional file 8: Figure S3. Michaelis–Menten graph of 8BxHMFO. Kinetic assay performed with HRP peroxidase in 50 mM phosphate buffer pH 8.0 at 25 °C using FFA as substrate.

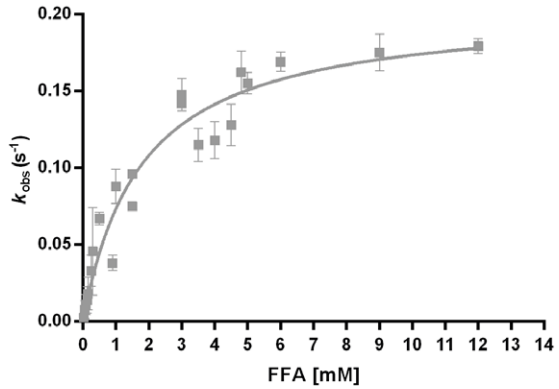

Additional file 9: Gene Sequences. Synthetic gene sequences for WT and 8xHMFO for the Golden Gate gene shuffling.

Gene name: HMFO-Wt, Length: 1738 bp, Vector name: pUC57-Kan, Cloning site: EcoRI/HindIII,
BsaI recognition sites
Nucleotides added for the scarless ligation

Sequence: GAATTCGGTCTCTT**GGTA**TGACTGATACGATTTTTGACTACGTGATTG
TTGGCGGTGGCACGGCGGGTAGCGTTCTGGCCAACCGTCTGTCCGCCCGTCCGGAGA
ATCGCGTGTTGCTGATTGAGGCCGGTATTGATACCCCGGAAAACAATATTCCGCCGG
AGATCCACGATGGCCTGCGCCCGTGGCTGCCGCGTCTGAGCGGTGATAAGTTCTTTT
GGCCGAATCTGACCATCCACCGTGCCGCGGAACACCCGGGTATCACGCGCGAGCCGC
AGTTCTATGAACAAGGCCGTCTGCTGGGCGGTGGTAGCAGCGTGAACATGGTCGTT
TCTAACCGTGGTCTGCCTCGCGACTATGACGAATGGCAGGCACTGGGCGCAGATGG
TTGGGATTGGCAGGGAGAGACCGGTCTCT**AGGG**TGTTCTGCCGTACTTCATCAAG
ACCGAGCGTGACGCGGACTACGGTGACGACCCGTTGCATGGCAATGCGGGTCCGA
TTCCGATCGGTCGCGTCGATTCGCGTCACTGGAGCGACTTCACGGTGGCGGCAACC
CAAGCTCTGGAAGCGGCTGGCCTGCCGAACATTCACGACCAAAACGCACGTTTTGA
TGACGGTTACTTCCCACCGGCATTTACGTTGAAAGGTGAAGAGCGCTTCAGCGCCGC
ACGCGGTTATCTGGATGCGAGCGTCCGTGTGCGTCCGAACCTGAGCCTGTGGACTGA
GAGCCGTGTCCTGAAGCTGCTGACCACTGGCAATGCAATCACCGGTGTGAGCGTGCT
GCGTGGTCGCGAAAGAGACCGGTCTCT**CGAA**ACCCTGCAAGTTCAAGCGCGCGAG
GTCATCCTGACCGCCGGTGCGTTGCAAAGCCCAGCGATTCTGTTGCGCACCGGCATCG
GCCCTGCGGCGGATCTGCACGCACTGGGTATTCCTGTTCTGGCAGACCGTCCGGGTG
TTGGTCGCAATCTGTGGGAGCACAGCTCTATCGGTGTGGTTGCCCCGCTGACCGAGCA
GGCACGTGCAGACGCCAGCACGGGTAAAGCCGGCTCTCGCCATCAACTGGGTATCCG
TGCGTCGTCCGGCGTAGATCCGGCGACGCCTAGCGACCTGTTTCTGCATATCGGTGCT
GATCCAGTCAGAGACCGGTCTCT**AGTC**AGCGGTCTGGCAAGCGCTGTGTTCTGGGTG
AACAAGCCAAGCTCCACCGGCTGGCTGAAGCTGAAGGACGCGGACCCGTTTAGCAG
AGACCGGTCTCT**TAG**CTACCCGGACGTAGACTTCAATCTGCTGAGCGATCCGCGCGA
CTTGGGTCGTCTGAAAGCGGGCCTGCGTCTGATCACCCATTACAGAGACCGGTCTCT
TTACTTCGCAGCGCCGTCCCTGGCGAAATATGGTTTGGCGCTGGCATTGAGCCGTTT
AGAGACCGGTCTCT**GTTT**TGCGGCACCGCAGCCGGGTGGTCCGCTGCTGAACGAC
CTGTTGCAGGACGAAGCCGCCCTGGAACGCTATTTGCGTACGAACGTCGGCGGTGTT
TGGCATGCGAGCGGCACGGCGCGTATCGGCCGTGCGGATGATTCCCAGGCTGTTGTC
GATAAAGCGGGTCGTGTGTACGGCGTCACCGGCCTGCGTGTTGCGGACGCAAGCATT
ATGCCGACCGTTCCGACCGCCAATACCAATCTGCCGACGCTGATGCTGGCTGAGAAA
ATTGCGGATGCGATTCTGACCCAGGCTTAA**CTTG**CGAGACCAAGCTT

Gene name: HMFO-Mut, Length: 1738 bp, Vector name: pUC57-Kan, Cloning site: EcoRI/HindIII,
BsaI recognition sites
Nucleotides added for the scarless ligation
Mutated nucleotides

Sequence:
GAATTCGGTCTCTT**GGTA**TGACTGATACGATTTTTGACTACGTGATTGTTGGCGGTG
GCACGGCGGGTAGCGTTCTGGCCAACCGTCTGTCCGCCCGTCCGGAGAATCGCGTGTT
GCTGATTGAGGCCGGTATTGATACCCCGGAAAACAATATTCCGCCGGAGATCCACG
ATGGCCTGCGCCCGTGGCTGCCGCGTCTGAGCGGTGATAAGTTCTTTTGGCCGAATC
TGACC**G**TC**T**ACCGTGCCGCGGAACACCCGGGTATCACGCGCGAGCCGCAGTTCTATG
AACAAGGCCGTCTGCTGGGCGGTGGTAGCAGCGTGAACATGGTCGTTTCTAACCGTG
GTCTGCCTCGCGACTATGACGAATGGCAGGCACTGGGCGCAGATGGTTGGGATTGGC
AGGGAGAGACCGGTCTCT**AGGG**TGTTCTGCCGTACTTCATCAAGACCGAGCGTGAC
GCGGACTACGGTGACGACCCGTTGCATGGCAATGCGGGTCCGATTCCGATCGGTCGC
GTCGATTCGCGTCACTGGAGCGACTTCACGGTGGCGGCAACCCAAGCTCTGGAAGCG
GCTGGCCTGCCGAACATTCACGAC**G**AAAACGCACGTTTTGATGACGGTTACTTCCC
ACCGGCATTTACGTTGAAAGGTGAAGAGCGCTTCAGCGCCGCACGCGGTTATCTGGA
TGCGAGCGTCCGTGTGCGTCCGAACCTGAGCCTGTGGACTGAGAGCCGTGTCCTGA
AGCTGCTGACCACTGGCAATGCAATCACCGGTGTGAGCGTGCTGCGTGGTCGCGAA
AGAGACCGGTCTCT**CGAA**ACCCTGCAAGTTCAAGCGCGCGAGGTCATCCTGACCGC
CGGTGCGTTGCAAAGCCCAGCGATTCTGTTGCGCACCGGCATCGGCCCTGCGGCGGA
TCTGCACGCACTGGGTATTCCTGTTCTGGCAGACCGTCCGGGTGTTGGTCGCAATCTG
TGGGAGCACAGCTCTATCGGTGTGGTTGCCCCGCTGACCGAGCAGGCACGTGCAGA
CGCCAGCACGGGTAAAGCCGGCTCTCGCCATCAACTGGGTATCCGTGCGTCGTCCGG
CGTAGATCCGGCGACGCCTAGCGACCTGTTTCTGCATATC**CA**TGCTGATCCAGTCAGA
GACCGGTCTCT**AGTC**AGCGGTCTGGCAAGCGCT**C**TGTTCTGGGTGAACAAGCCAA
GCTCCACCGGCTGGCTGAAGCTGAAGGACGCGGACCCGTTTAGCAGAGACCGGTCT
CT**TAGC**TACCCGGACGTAGACTTCAATCTGCTGAGCGATCCGCGCGACTTGGGTCGT
CTGAAAGCGGGCCTGCGTCTGATCA**AA**CATTACAGAGACCGGTCTCT**TTAC**TTCGC
A**TAT**CCGTCCCTGGCGAAATATGGTTTGGCGCTGGCATTGAGCCGTTTAGAGACCG
GTCTCT**GTTT**TG**A**GGCACCGCAGCCGGGTGGTCCGCTGCTGAACGACCTGTTGCAG
GACGAAGCCGCCCTGGAACGCTATTTGCGTACGAACGTCGGCGGTGTTTGGCATGCG
AGCGGCACGGCGCGTATCGGCCGTGCGGATGATTCCCAGGCTGTTGTCGATAAAGCG
GGTCGTGTGTACGGCGTCACCGGCCTGCGTGTTGCGGACGCAAGCATTATGCCGACC
GTTCCGACCGCCAATACCAATCTGCCGACGCTGATGCTGGCTGAGAAAATTGCGGA
TGCGATTCTGACCCAGGCTTAA**CTTG**CGAGACCAAGCT

Development of Alternative Recombinant Expression Systems for the Production of 5-hydroxymethylfurfural Oxidase

Caterina Martin and Marco W. Fraaije

Molecular Enzymology Group, University of Groningen, Nijenborgh 4, 9747AG, Groningen, The Netherlands

ABSTRACT

Two new strategies were pursued for heterologous production of 5-hydroxymethylfurfural oxidase (HMFO). The first method employed was spore surface display of HMFO by using *B. subtilis*. It was expected that this system allows easy application of the biocatalyst for the conversion of HMF. In addition, it was conceivable that surface display beneficially impacts the stability of HMFO.

Several surface display gene constructs were generated employing CRISPR-Cas9 and various sporulation conditions were evaluated. Unfortunately, none of the constructs lead to surface display of active HMFO. The second approach for heterologous expression involved the use of the yeast *P. pastoris* for intracellular and secreted expression of HMFO. Though functional expression was achieved in yeast, both intra- and extracellularly, the yield of active HMFO was not competitive when compared to the previously established *Escherichia coli* expression system.

Introduction

Every day the demand for sustainable plastic is becoming more pressing. In the scenario of replacing petrol-based polymers and materials, a furan building block is making its way to the market. 2,5-furandicarboxylic acid (FDCA) can be regarded as a renewable building block because it can be obtained through conversion of biomass-based carbohydrates. The first step in this process, a dehydration step, leads to the 5-hydroxymethylfurfural (HMF) [1]. FDCA can be produced from HMF through oxidation of this furan. For the latter process, various biocatalytic approaches have been investigated. The biocatalytic synthesis of FDCA can be achieved by using a single enzyme or using a cascade with multiple enzymes, using immobilized enzyme(s) or fermentative approaches [2,3]. Most of these biocatalytic studies focused on the identification of single biocatalysts or biocatalytic cascades, and only limited work has been reported on exploring industrial scale application of HMF-converting biocatalysts. The only enzyme known to be efficient in converting HMF to FDCA as single biocatalyst, is HMFO (EC 1.1.3.47) from *Methylovorus sp.* strain MP688. It represents a promising biocatalyst for FDCA production as extensively described in the introduction of this thesis and elsewhere in the literature [4,5]. Engineering of HMFO has been carried out in previous studies which resulted in the 8BxHMFO mutant. This variant was found to be more thermostable and displayed improved activity in converting HMF to FDCA when compared to than wild type HMFO. It has been demonstrated that this engineered HMFO can be used to synthetize FDCA in a biocatalytic, environmentally and industrially sustainable way [6]. For future industrial application, the costs of the biocatalysts should be minimized. This can be achieved by creating a robust variant but also an efficient production system will contribute to a cost-effective production. In this chapter, two approaches for expressing HMFO have been studied: (1) spore-based enzyme production and immobilization using *Bacillus subtilis*, and (2) HMFO secretion by the yeast *Komagataella phaffii* (also known as *Pichia pastoris*).

Bacillus subtilis is an organism that has been used already for decades as a production host [7,8]. Moreover, recently *B. subtilis* has been developed for the purpose of protein spore display [9–12]. Compared to other microbial cell-surface display systems such as those with phage, *E. coli* or yeast, *B. subtilis* spore display is safer, and the displayed enzymes are often more stable than their native counterparts [13] [14]. The folding of the proteins that will be displayed on the spores occurs inside the mother cells before sporulation. As a result, there is no need to transport the target protein across the membrane [15]. An additional advantage of using the *B. subtilis* spore display system is the

presence of molecular chaperones that facilitate the correct folding of the heterologous protein in the bacterial cytoplasm [16]. Another interesting aspect of spore display is that it leads to immobilization of the target protein on the spores. Immobilization of biocatalysts often results in a superior stability while spores will also allow easy recycling of the biocatalyst. Hence, expression of HMFO on spores would be an elegant approach to produce and immobilize the biocatalyst in one go.

As alternative approach for efficient production of HMFO, we also explored another known expression host: yeast. *P. pastoris* was chosen for establishing a system for high level of secretion of HMFO. Secretion of HMFO would allow facile production and usage of the biocatalyst as it would eliminate the need for costly procedures to isolate the biocatalyst. *P. pastoris* is known to support high expression levels of secreted protein. Production levels of more than 10 g/L are advertised on commercial websites (Validogen®) [17]. *P. pastoris* is a methylotrophic yeast that gained a lot of commercial interest in the last decade as one of the most important organisms to produce heterologous protein owing to an efficient protein secretion machinery and for its ability to perform post-translational modifications. Various tools for protein production have been developed, such as expression vectors and induction protocols [18]. A common strategy for heterologous protein expression in *P. pastoris* is by stable genome integration of the expression cassette and induction of expression by using methanol-regulated promoters of the methanol utilization pathway.

In this chapter, the results obtained for the expression of HMFO either on spores or secreted by yeast are presented. Although the results with expression in *B. subtilis* were disappointing, expression by *P. pastoris* was shown to be successful. Yet, the observed expression is still inferior when compared to the established intracellular expression in *E. coli*. More genetic engineering would be required to boost the expression in alternative recombinant expression hosts.

MATERIALS AND METHODS FOR EXPRESSION IN *B. SUBTILIS*

Bacterial strains, transformation and selection. *E. coli* NEB 10β cells were used for construction and amplification of the pJOE8999 vector. *E. coli* chemically competent cells were transformed by heat shock and selection was done using kanamycin at 50 μg ml^{-1}. The *B. subtilis* strain DB104 (*nprE18 nprR2 AaprA3*) double protease deficient strain was a kind gift from Prof. Dr. O.P. Kuipers [19]. The genomic DNA of this strain was used to amplify the regions necessary to construct the homologous recombination cassette, and it was used for transformation and sporulation experiments. *B. subtilis* transformation with pJOE8999 and selection were performed as previously described [20]. Homologous integration of the construct encoding coat proteins fused to HMFO was confirmed by colony PCR of the 5′ and 3′ regions using primers annealing to the chromosomal and HMFO regions.

Construction of the plasmid pJOE8999. The plasmid pJOE8999 was kindly donated by Prof. Dr. O.P. Kuipers [20]. The spacers (target sequence of sgRNA) were designed in order to target a small non-translated region at the 3′ terminus of the coat protein coding sequence that will be substituted by the HMFO sequence after the homologous recombination.

First the spacers were generated using single stranded oligonucleotides. The reaction mixtures were composed as follows: 20 μL of oligonucleotide forward [100 μM], 20 μL of oligonucleotide reverse [100 μM], 10 μL 5x T4 ligase buffer (Promega). The reaction mixtures were incubated in a thermocycler with the following program: 100 °C for 5 min and cooling down to 25 °C by a gradual decrease of 1 °C every 30 s. The spacer was cloned with Golden Gate cloning system into the pJOE8999 using BsaI restriction sites, and confirmed by sequencing.

The homology recombination cassette was cloned into the pJOE8999 carrying the spacer using NEBuilder® HiFi DNA Assembly or Gibson cloning method. First, it was necessary to amplify all the fragments. The *B. subtilis* genome was extracted and the regions 5′ and 3′ were amplified by PCR using primers overlapping with the vector in the SrfI cutting site and the HMFO. The 8BxHMFO coding sequence was amplified by PCR from a pBAD SUMO 8BxHMFO vector [21]. The NEBuilder® HiFi DNA Assembly reaction was used for the CotC,B,X,Z-HMFO fusions, and the Gibson assembly for CotG-HMFO constructs (no relevant reason behind this choice, as both cloning methods are similar; Gibson assembly requires more time, longer overlapping regions but is less expensive). The pJOE8999 was cut with SrfI or, amplified and digested with DpnI (Gibson assembly in case of CotG). The amplified 5′ and 3′ regions were digested with SrfI and DpnI (to eliminate the methylated template), while the HMFO gene was digested only with DpnI. The NEBuilder® HiFi DNA Assembly reaction and Gibson assembly were performed according to instructions by the manufacturer. The obtained construct was checked by sequencing.

Sporulation and endospore isolation. Sporulation was performed in adapted Shaeffer medium (Difco Nutrient Broth 8 g/L, $MgSO_4$ 1 mM, KCl 13 mM, $MnSO_4$*$4H_2O$ 0.13 mM, $CaCl_2$*$2H_2O$ 1 mM pH 7.0) at 37 °C or 30 °C at 135 rpm in an orbital shaker for 24-48 h until 95% of the population consisted of spores. Spores and sporangial

cells of *B. subtilis* were collected by centrifugation, resuspended and washed once in phosphate buffer 70 mM pH 7.0. The suspension was treated next with a 0.5% lysozyme solution with or without 1mM phenylmethylsulfonyl fluoride (PMSF) for 1 h at 37 °C. The suspension was centrifuged next 12 min at 3200x*g* after which the pellet was washed as follows: once with 1 M NaCl, once with 1 M KCl, and one time with phosphate buffer 50 mM pH 8.0. Subsequently, samples were centrifuged 4 min at 10.000 g and the purified spores obtained were resuspended in phosphate buffer and stored at 4 °C [22]. The spores were checked microscopically following the Schaeffer-Fulton method for staining endospores.

Product analysis. Conversions using the spores were performed in 500 µL of total reaction volume using 5 mM HMF as substrate and various amounts of spores in the presence or absence of 10 µM FAD at 25 °C at 400 rpm for 24 h in an Eppendorf ThermoMixer. Reactions were inactivated by heating the samples at 95 °C for 10 min and centrifuged. Products were analyzed as previously described [4].

MATERIAL AND METHODS FOR EXPRESSION IN *P. PASTORIS*

Vector assembly and yeast transformation. The 8BxHMFO-encoding gene was obtained as yeast codon-optimized double stranded DNA fragment from Integrated DNA Technologies (IDT) to enable intracellular expression, the DNA fragment was introduced into pBSY3Z by Gibson assembly employing SapI restriction sites, thereby yielding pBSY3Z-HMFO. Alternatively, it was amplified by PCR to add matching ends and then cut (MlyI) and cloned in the pBSYDCsec by Gibson assembly. The result was pBSYDCsec_blunt1-HMFO for extracellular secretion. All constructs were used to transform *E. coli* XL-1 blue and colonies from single transformants were grown in liquid medium and used next for plasmid DNA extraction. This was used to confirm the proper sequence by DNA sequencing. To obtain linearized plasmid DNA, pBSYDCsec_blunt1-HMFO was digested with SwaI, whereas pBSY3Z-HMFO was treated with SwaI, BamHI or a combination of both. The linearized vectors were purified and used to transform competent *P. pastoris* and then plated on YPD zeocin 25 µg/mL [23].

Protein expression. Expression was performed first on a small scale in 96 deep well plates to evaluate the best cassette integration site. To this end, the following media were used: (1) BYP (Buffered Yeast-Peptone:

Table 1: Induction scheme.

Time [h]	Step	Small scale (96 deep well plate)	Large scale (1L baffled flask)
0	-	Starting cell culture in 180 µL BYPD	Starting cell culture (2 mL/5 ml overnight culture) in 180 mL BYPD
~48	1st induction	250 µL BYPM2	20mL BMM10
~56	2nd induction	50 µL BYPM10	1 mL methanol
~72	3rd induction	50 µL BYPM10	2 mL methanol
~80	4th induction	50 µL BYPM10	2 mL methanol
~96	-	Harvest	Harvest

Protein expression was verified by SDS-PAGE analysis, while oxidase activity was assessed by HRP coupled oxidase assay using HMF as substrate [4].

20 g peptone and 10 g yeast extract in 700 mL dH_2O, autoclaved and added 200 mL 1.0 M phosphate pH 7.0 (autoclaved)), (2) BYPD (BYP with 100 mL dextrose 10x), (3) BYPM2 (10 mL methanol and 90 ml of water, BYP), or (4) BYPM10 (5 mL methanol and 95 mL of water, BYP).

Conversion of HMF. Conversions were set up as follows: 50 mM KPi pH 8.0, 48 h, 25 °C, 5 mM HMF, 300 rpm, 500 µL in 4 mL glass vial.
Sample preparation:

- Extracellular: 250 uL of cell-free supernatant from cells expressing HMFO (OD600 = 44.00)
- Extracellular Control: 250 µL of cell-free supernatant from *P. pastoris* wild type cells
- HMFO: 0.23 nM of purified HMFO in 50 mM pH 8.0
- HMFO+media: 0.23 nM of purified HMFO with 250 µL cell-free supernatant from *P. pastoris* wild type cells

RESULTS

B. SUBTILIS SPORE DISPLAY

PLASMID CONSTRUCTION AND GENE KNOCK-IN

Plasmids for *B. subtilis* transformations were obtained after two cloning steps. First the target sequence was introduced to obtain a complete sgRNA. Then the three PCR products corresponding to the 5' region, 3' region, and HMFO were ligated into the pJOE8999 to yield a complete vector for gene editing of the *B. subtilis* genome (Figure 1).

The homologous recombination cassette contained the 5′ and 3′ regions from the *B. subtilis* genome (coat protein specific) and the HMFO-encoding sequence. Seven plasmids for expression of seven different HMFO-coat protein fusions were built (Table 2). For fusion, five different Cot proteins were targeted: CotB, CotC, CotG, CotX, and CotZ. For fusion to CotG, three different linkers were tested.

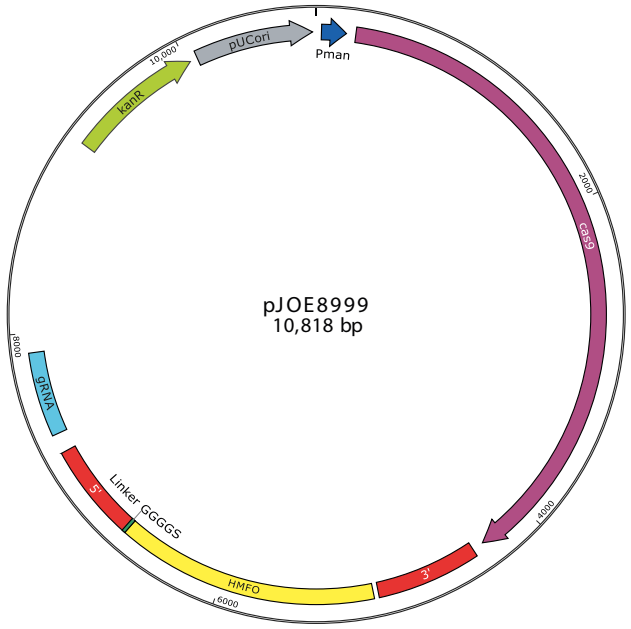

Figure 1. Map of complete pJOE8999. The pUC18 minimal origin, kanamycin resistance gene (*kanR*), cas9 under the control of the *B. subtilis* specific mannose-inducible Pman promoter, and sgRNA (with a spacer coat protein specific) transcribed from the semisynthetic promoter PvanP*.

Table 2. Coat proteins with the respective linker for Cot-HMFO fusions.

Coat protein	Linker (amino acids)
CotB	GGGGS
CotC	GGGGS
CotZ	GGGGS
CotX	GGGGS
CotG	GGGGS
CotG	GGGEAAAKGGG
CotG	-

The transformation of *B. subtilis* was successful, and the homologous integration was confirmed by PCR colony screening using primers annealing on the chromosome (in a region external to the homologous cassette) and on the HMFO sequence as illustrated in Figure 2. Two PCRs were performed to amplify 800 bp fragments of the 5′ and 3′ regions.

SPORULATION AND ENDOSPORE ISOLATION

Spores of the generated recombinant *B. subtilis* strains could be obtained as described above. Sporulation and endospore isolation were monitored microscopically. Micrographs confirmed sporulation and elimination of vegetative cells (Figure 3). Addition of PMSF or salt did not change the outcome. In every case sporulation and endospore

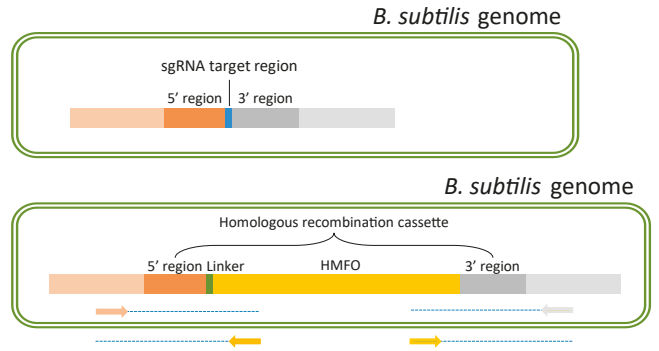

Figure 2. *B. subtilis* genome before and after homologous recombination. The top part of the figure shows the *B. subtilis* genome before the transformation with pJOE8999. The bottom part depicts the bacterial genome after the gene editing procedure. The arrows represent the primers used for the colony PCR of the 5′ and 3′ regions.

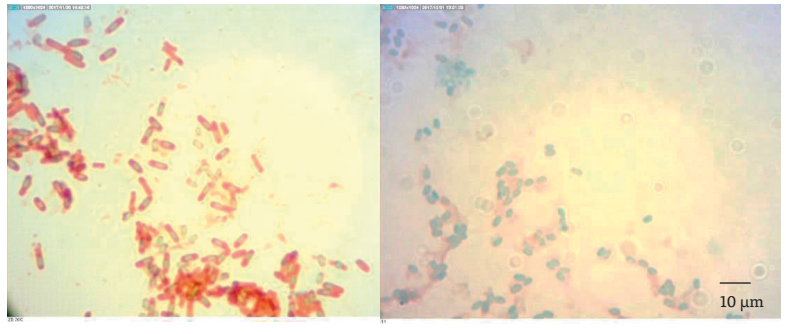

Figure 3. Microscope pictures of cells stained by the Schaeffer–Fulton method. The primary stain is malachite green, which dyes the endospores. The counterstain is safranin, which dyes the bacterial bodies. The left micrograph shows spores before the lysozyme treatment, and the right micrograph shows spores after the treatment.

isolation gave positive results concerning the integrity of the spore and the elimination of vegetative cells (Figure 3).

HMF CONVERSIONS

Conversion of HMF using isolated spores showed no apparent HMFO activity. There was some minor conversion (~1%) observed, most likely due to some unknown nonspecific oxidase or dehydrogenase present in the spores. In fact, a low conversion rate was found also in the negative control, using non-recombinant *B. subtilis* spores. There was no difference between cells carrying the different Cot-HMFO fusion constructs or non-recombinant cells: all could convert low amounts of HMF to FFA but no formation of FDCA was detected. To check whether HMFO was expressed as apo protein on the spores, the effect of adding FAD was tested. Nevertheless, the addition of 5 μM FAD did not lead to any improvement. These results suggest that no (functional) HMFO was displayed on the spores.

P. PASTORIS HMFO EXPRESSION AND HMF CONVERSION.

Next, the use of yeast for intracellular and extracellular HMFO expression was explored. In the case of intracellular expression, the activity assay was performed after cell lysis. Unfortunately, no activity could be detected, possibly due to poor expression levels in the 96 well plate format and/or an inhibitory effect from the lysis buffer in the HRP coupled assay. Subsequently, the colony with the best random integration site leading to the highest level of expression was identified by SDS-PAGE (Figure 4). This selection step is usually performed using minimal media instead of the relatively rich YP medium that contains yeast extract and peptone of which the composition can slightly vary from batch to batch. The choice of YP was determined by the fact that with minimal medium the expression level was relatively low. SDS-PAGE analysis of the extracts revealed overexpression of a protein with a molecular weight of about 68 kDa, which comes close to the theoretical molecular weight of HMFO (57 kDa). While the protein is one of the most abundant proteins in the cell extract

For most of the transformants, the expression is relatively poor when compared to expression of HMFO in *E. coli*.

As with extracellular expression SDS-PAGE, was used to identify a colony/transformant with the best integration site, resulting is secretion of HMFO. This revealed in some cases a clear overexpression of one particular protein (Figure 5). The observed protein seems to have a molecular weight that is higher (77.6 kDa) than the predicted molecular weight of HMFO (57 kDa) (Figure 5). Nevertheless, mass spectrometry (MS) analysis confirmed that the respective protein

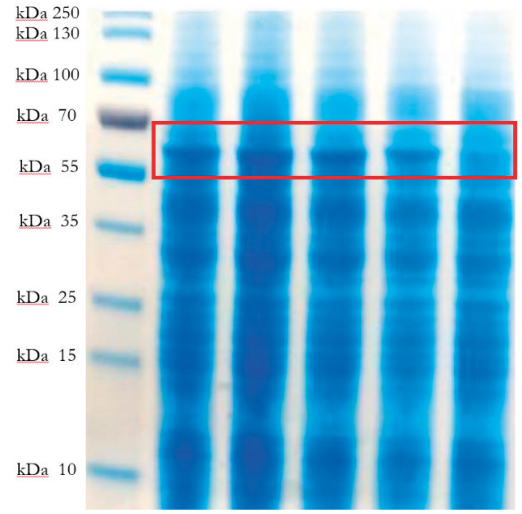

Figure 4. SDS-PAGE analysis of intracellular expression of HMFO by *P. pastoris* cells. The first lane is the protein ladder while the other lanes represent extracts from different cultures (using selected colonies).

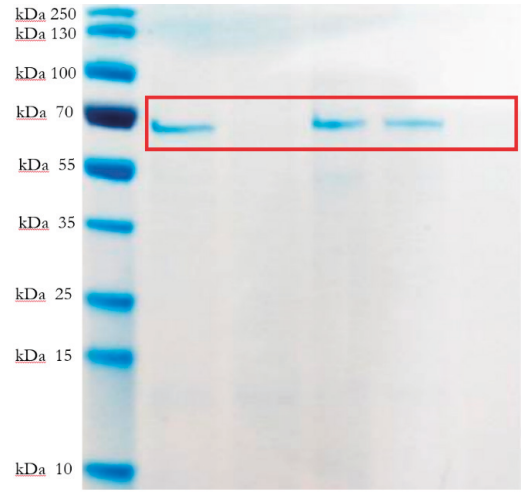

Figure 5. SDS-PAGE analysis of extracellular expression of HMFO by *P. pastoris* cells. The first lane is the protein ladder and the rest are protein samples of cell-free supernatants.

represents HMFO (see for details the Supporting Information). Analysis of the HMFO sequence for possible glycosylation sites with the web server NetNGlyc 1.0 suggests two possible glycosylation sites:

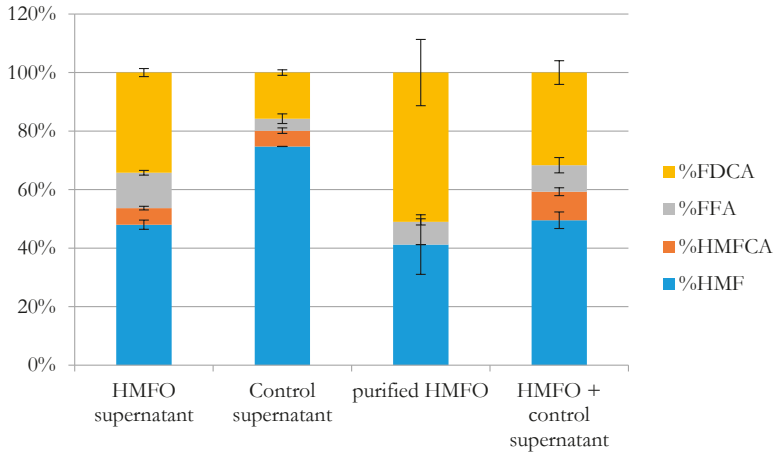

Figure 6. Conversion of HMF by HMFO expressed in the supernatant (extracellular fraction) of *P. pastoris* (left part) and purified HMFO from *E. coli* (HMFO and HMFO+supernatant).

N70 and N224. MS analysis gave almost complete coverage of the full HMFO sequence, except for a few short sequence regions which did not result in peptides measured by MS. Specifically no peptide encompassing N70 was detected. This suggests that this amino acid may be glycosylated when produced as secreted protein in yeast. This may explain the difference in molecular weight when compared with non-glycosylated HMFO.

The secreted HMFO appears rather pure and can be easily obtained as supernatant or filtrate from a culture. Since the extracellularly expressed HMFO is the most interesting to explore, we tested the supernatant containing secreted HMFO for HMF conversions. This revealed that cell-free supernatants containing extracellular HMFO were able to convert HMF to FDCA (Figure 6). However, also the cell-free supernatant of a control culture (wild type *P. pastoris*) was able to convert HMF (Figure 6). Interestingly, the conversions resulted in formation of some 5-(hydroxymethyl)furan-2-carboxylic acid (HMFCA). This oxidation product was not found in previous conversions in which HMFO was used. In fact, also a conversion of HMF with a known amount of HMFO was performed in parallel and confirmed that HMFO is not capable to form HMFCA. The conversions of the cell-free supernatants seem to be partly based on enzyme activities present in *P. pastoris*. The conversions also clearly confirm that some HMFO was secreted as active enzyme.

Since extracellular HMFO production is attractive, attempts were made to improve the yield of the secreted protein through optimizing culture conditions. Specifically, a different culture volume: flask volume ratio (1:20 instead of 1:10) to improve aeration and the addition of FAD (20 μM) in the culture were tested. Unfortunately, these changes did not have a significant effect. The final yield of secreted active protein was about 14 mg/L which is considerably lower than what is obtained by intracellular expression in *E. coli* (100-150 mg/L).

DISCUSSION

***B. subtilis* spore display of HMFO.** Surface display of enzymes has several well-known advantages in addition to the unrestricted access of the enzyme presented on the cell surface towards externally added substrates. Firstly, it allows the enzyme as an immobilized one because because cell can be easily recovered and recycled. Secondly, immobilization often increases the biocatalyst thermostability, which is obviously beneficial for industrial processes. To achieve HMFO expression on the surface of *B. subtilis* spores, the *hmfo* gene was introduced at the C-terminus of several genes known to encode for coat proteins (Cot). By choosing several Cot proteins, we tried to identify the best performing fusion. The selected coat proteins were CotB, CotC, CotG, CotX and CotZ, which represent some of the most commonly used surface anchoring targets since they are present in the outer or crust portion of the spore structure [16,24]. Common methods to achieve protein anchoring to spore coat proteins involve chromosomal expression in which genetic stability is assured by integration of the constructs into the non-essential *amyE* gene [25–28]. These strategies result in the co-presence of both chimeric spore coat fusion proteins and the native anchoring spore coat proteins on the spore surface. In this study introduction of the *hmfo* gene was targeted directly in the chromosomal location of the targeted coat proteins in order to achieve a high level expression of Cot-HMFO fusions on the spore surface by eliminating the competitive presence of the native coat protein. The expression of the various Cot-HMFO fusions would benefit from the native chromosomal location and the native promoter (sporulation induced). Moreover, this strategy would allow combining several fusions in order to get even more heterologous enzyme expressed on the spore surface using several spore coat proteins simultaneously. The chromosomal integrations were achieved by taking advantage of homology cross-over recombination and the CRISPR-Cas9 system for facile selection. The cross-over recombination genome editing technique is widely used to obtain

chromosomal expression [26,29,30]. Homologous recombination naturally occurs in *B. subtilis* as a bacterial strategy to perpetuate gene diversification and genome stability, and it can easily be used to achieve a targeted gene knock-in [31]. The homologous recombination was combined with the CRISPR-Cas9 system because the latter is a very efficient tool that comprises a markerless selection and facilitates the screening after the cross-over recombination [20]. The clustered regularly interspaced short palindromic repeat (CRISPR)-Cas system is a bacterial and archaeal adaptive immune system against phages and plasmids based on RNA sequence-specific detection [32]. CRISPR-Cas9 is a particular type of system involving Cas9, an endonuclease able to cleave target dsDNA thanks to the base-paired structure formed between thetrans-activating CRISPR RNA (tracrRNA) and the targeting crRNA [33]. The cleavage is site specific and is led by base-pairing of the crRNA and the target protospacer DNA including protospacer adjacent motif (PAM).

In this study we used the plasmid pJOE8999 to introduce the *hmfo* gene in frame with the genes encoding for CotB, CotC, CotG, CotX or CotZ [20]. This plasmid represents a shuttle vector that can be edited in *E. coli* and it does not replicate in *B. subtilis* allowing a simple genome editing of *B. subtilis* based on homology recombination and CRISPR-Cas9. This single-plasmid system represents a versatile tool for gene knock-out or knock-in purposes. The strategy based on homologous recombination of the Cot-HMFO fusion genes in the native coat locus differs from the commonly used recombination in the *amyE* locus as already mentioned in the introduction. The rationale for this approach was to use the native locus and promoter for Cot protein expression. This was thought to reduce the interference with the genome, that could lead to low expression levels, and to avoid the co-presence of chimeras and native coat proteins. The expression of a coat protein fusion in strains with null mutations for the targeted coat protein proved to be beneficial in the case of CotC [34]. The vector and method designed by J. Altenbuchner was an efficient and fast method to achieve the homologous recombination [20]. Different Cot proteins were targeted for two reasons: (1) to select the best performing fusion construct towards FDCA production, and (2) in a next step, different fusions could be combined to increase the amount of HMFO on the spores. We chose not to add a tag at the N- or C-terminus (e.g. for antibody detection) to avoid the risk of interfering with the protein folding. Moreover, because we were primarily interested in HMFO activity, we focused on establishing whether spores could catalyze the conversion of HMF to FDCA.

The linker used in case of all five coat protein was the GGGGS, a commonly used flexible linker with no defined structure [10,11,22,35–37]. Since CotG has been successfully used in several studies, we decided to try several linkers for the CotG-HMFO fusions. Except for the GGGGS linker, a construct was made without a linker and another construct contained a linker with a strong α-helical motif (–GGGEAAAKGGG-). The latter has been used in several cases [28,30,38]. Unfortunately, none of the Cot-HMFO constructs seems to be effective for functional HMFO display on the surface of *B. subtilis* spores. The lack of oxidase activity could be explained by the location of HMFO: being fused to the C-terminus of the coat proteins may result in localization of HMFO on the inner side of the spore. Yet, it is unlikely that this occurs in all cases (five different coat proteins) and one would still expect that it would lead to HMF conversion. Another reason behind the failure could be that HMFO is fused too close (even in the case of the long α-helix linker) to the spore surface and therefore there it blocks access of the substrate to the active site or a conformational change is induced which inactivates HMFO. The crystal structure of HMFO (PDB 4UDQ) shows that the N-terminus is quite well exposed and flexible. Therefore, it is unlikely that the linkage at the N-terminus would be a problem. Moreover, HMFO is usually expressed and purified as a fusion with a N-terminal His- or SUMO-tag to facilitate functional expression and purification. This shows that a N-terminal fusion can be tolerated. Other likely causes for the lack of activity is incorrect folding of HMFO during expression a Cot-fusion protein and/or loss of the FAD cofactor during the process of surface display. The surface display of apo HMFO may lead to unfolding, explained the inability to regain activity upon adding FAD.

The specific *B. subtilis* expression strain used in this study is *B. subtilis* DB104. This strain was selected because it is commonly used in industry as it lacks the alkaline protease (aprA3) and the neutral protease (nprE18). Hence, it displays a low extracellular protease activity [19]. We were able to obtain spores for each designed construct, proving that the fusion of HMFO to the specific Cot proteins does not affect the sporulation process. The reason behind the lack of HMFO activity is still not clear. Optimization of the sporulation protocol by lowering the sporulation time (from 48 h to 24 h) and temperature (from 37 °C to 30 °C) was explored to avoid a possible unfolding or proteolytic event. To limit proteolytic activity, we also tested the addition of PMSF in the lysozyme treatment. Yet, these precautions did not result in any detectable HMFO activity.

***P. pastoris* HMFO expression.** Active 8BxHMFO could be expressed intra- and extracellularly using *P. pastoris*. For secretion, the alpha-mating factor secretion tag was used [39]. The expression of HMFO was induced by the addition of methanol in the culture medium as an alternative carbon source once the glucose is consumed. The HMFO open reading frame is transcriptionally controlled by the CAT promotor, which is tightly repressed in the presence of glucose and strongly induced when methanol is present [40]. Although HMFO was clearly overexpressed as intracellular protein, based on SDS-PAGE analysis, the expression level was inferior when compared with expression in *E. coli*. The secreted expression of HMFO was more promising as SDS-PAGE revealed that HMFO was by far the most abundant protein in the supernatant. Clearly, extracellular expression is attractive for producing HMFO as hardly any processing is needed for isolating the enzyme. Interestingly the extracellular fraction of *P. pastoris* cells was found to catalyze conversion of HMF resulting in formation of some HMFCA as oxidation product. It suggests that *P. pastoris* harbors other enzymes that can convert HMF. The identity of this enzyme or multiple enzymes remains unknown. The fact that HMFCA is formed hints to an oxidative enzyme different from HMFO. These first attempts of secretion of HMFO by *P. pastoris* resulted in relatively low amounts of the enzyme. Future work should establish whether this approach for HMFO production through secretion can become more effective when compared with the use of *E. coli* as expression host.

CONCLUSIONS

The immobilization of HMFO through display on the surface of *B. subtilis* spores was not achieved. Attempts for establishing surface display of the oxidase using different coat protein anchors and linkers, different conditions for growth and sporulation, or addition of the FAD cofactor, were unsuccessful. The reason for this remains unclear but may be related to problems of protein folding, ineffective cofactor incorporation, and/or proteolysis.

Gratifyingly, intra- and extracellular expression using *P. pastoris* was found to be feasible, leading to functional HMFO. Secretion seems a viable alternative for HMFO production and deserves follow-up studies to optimize expression and to evaluate the recombinant enzyme.

REFERENCES

[1] S.P. Teong, G. Yi, Y. Zhang, Hydroxymethylfurfural production from bioresources: past, present and future, Green Chem. 16 (2014) 2015.

[2] H. Yuan, H. Liu, J. Du, K. Liu, T. Wang, L. Liu, Biocatalytic production of 2,5-furandicarboxylic acid: recent advances and future perspectives, Appl. Microbiol. Biotechnol. (2019) 527–543.

[3] L. Hu, A. He, X. Liu, J. Xia, J. Xu, S. Zhou, J. Xu, Biocatalytic Transformation of 5-Hydroxymethylfurfural into High-Value Derivatives: Recent Advances and Future Aspects, ACS Sustain. Chem. Eng. 6 (2018) 15915–15935.

[4] W.P. Dijkman, M.W. Fraaije, Discovery and characterization of a 5-hydroxymethylfurfural oxidase from *Methylovorus sp.* strain MP688, Appl. Environ. Microbiol. 80 (2014) 1082–1090.

[5] W.P. Dijkman, D.E. Groothuis, M.W. Fraaije, Enzyme-catalyzed oxidation of 5-hydroxymethylfurfural to furan-2,5-dicarboxylic acid, Angew. Chemie — Int. Ed. 53 (2014) 6515–6518.

[6] C. Martin, A. Ovalle Maqueo, H.J. Wijma, M.W. Fraaije, Creating a more robust 5-hydroxymethylfurfural oxidase by combining computational predictions with a novel effective library design, Biotechnol. Biofuels. 11 (2018) 56.

[7] L. Liu, Y. Liu, H.D. Shin, R.R. Chen, N.S. Wang, J. Li, G. Du, J. Chen, Developing *Bacillus spp*. as a cell factory for production of microbial enzymes and industrially important biochemicals in the context of systems and synthetic biology, Appl. Microbiol. Biotechnol. 97 (2013) 6113–6127.

[8] S.-L. Wong, Advances in the use of *Bacillus subtilis* for the expression and secretion of heterologous proteins, Curr. Opin. Biotechnol. 6 (1995) 517–522.

[9] J. Chen, L. Zhao, G. Fu, W. Zhou, Y. Sun, P. Zheng, J. Sun, D. Zhang, A novel strategy for protein production using non-classical secretion pathway in *Bacillus subtilis*, Microb. Cell Fact. 15 (2016) 69.

[10] H. Chen, R. Tian, Z. Ni, Q. Zhang, T. Zhang, Z. Chen, K. Chen, S. Yang, Surface display of the thermophilic lipase Tm1350 on the spore of *Bacillus subtilis* by the CotB anchor protein, Extremophiles. 19 (2015) 799–808.

[11] A. Hosseini-Abari, B.G. Kim, S.H. Lee, G. Emtiazi, W. Kim, J.H. Kim, Surface display of bacterial tyrosinase on spores of *Bacillus subtilis* using CotE as an anchor protein, J. Basic Microbiol. (2016) 1–7.

[12] H. Wang, R. Yang, X. Hua, W. Zhao, W. Zhang, Functional display of active β-galactosidase on *Bacillus subtilis* spores using crust proteins as carriers, Food Sci. Biotechnol. 24 (2015) 1755–1759.

[13] G.S. Hossain, H. Yuan, J. Li, H. dong Shin, M. Wang, G. Du, J. Chen, L. Liu, Metabolic engineering of *Raoultella ornithinolytica* BF60 for production of 2,5-furandicarboxylic acid from 5-hydroxymethylfurfural, Appl. Environ. Microbiol. 83 (2017).

[14] H. Wang, Y. Wang, R. Yang, Recent progress in *Bacillus subtilis* spore-surface display: concept, progress, and future, Appl. Microbiol. Biotechnol. 101 (2017) 933–949.

[15] Wong S. Advances in the use of *Bacillus subtilis* for the expression and secretion of heterologous proteins. Curr. Opin. Biotech. 6 (1995) 517–522 .

[16] J. Kim, W. Schumann, Display of proteins on *Bacillus subtilis* endospores, Cell. Mol. Life Sci. 66 (2009) 3127–3136.
[17] A. Mellitzer, C. Ruth, C. Gustafsson, M. Welch, R. Birner-grünberger, R. Weis, T. Purkarthofer, A. Glieder, Synergistic modular promoter and gene optimization to push cellulase secretion by *Pichia pastoris* beyond existing benchmarks, J. Biotechnol. 191 (2014) 187–195.
[18] M. Ahmad, M. Hirz, H. Pichler, H. Schwab, Protein expression in *Pichia pastoris*: Recent achievements and perspectives for heterologous protein production, Appl. Microbiol. Biotechnol. 98 (2014) 5301–5317.
[19] F. Kawamura, R.H. Doi, Construction of a *Bacillus subtilis* double mutant deficient in extracellular alkaline and neutral proteases, J. Bacteriol. 160 (1984) 442–444.
[20] J. Altenbuchner, Editing of the *Bacillus subtilis* genome by the CRISPR-Cas9 system, Appl. Environ. Microbiol. 82 (2016) 5421–5427.
[21] C. Martin, A.O. Maqueo, H.J. Wijma, M.W. Fraaije, Creating a more robust 5-hydroxymethylfurfural oxidase by combining computational predictions with a novel effective library design, Biotechnol. Biofuels, 11 (2018) 1–9.
[22] X. Xu, C. Gao, X. Zhang, B. Che, C. Ma, J. Qiu, F. Tao, P. Xu, Production of N-acetyl-D-neuraminic acid by use of an efficient spore surface display system, Appl. Environ. Microbiol. 77 (2011) 3197–3201.
[23] J. Lin-cereghino, W.W. Wong, S. Xiong, W. Giang, L.T. Luong, J. Vu, S.D. Johnson, G.P. Lin-cereghino, Condensed protocol for competent cell preparation and transformation of the mehylotropic yeast *Pichia pastoris*, Biotechniques. 38 (2005) 44–48.
[24] J.G. Pan, E.J. Kim, C.H. Yun, *Bacillus* spore display, Trends Biotechnol. 30 (2012) 610–612.
[25] N. Wang, C. Chang, Q. Yao, G. Li, L. Qin, L. Chen, K. Chen, Display of *Bombyx mori* Alcohol dehydrogenases on the *Bacillus subtilis* spore surface to enhance enzymatic activity under adverse conditions, PLoS One. 6 (2011).
[26] K. Hinc, R. Isticato, M. Dembek, J. Karczewska, A. Iwanicki, G. Peszyńska-Sularz, M. De Felice, M. Obuchowski, E. Ricca, Expression and display of UreA of *Helicobacter acinonychis* on the surface of *Bacillus subtilis* spores., Microb. Cell Fact. 9 (2010) 2.
[27] E.M.F. Mauriello, L.H. Duc, R. Isticato, G. Cangiano, H.A. Hong, M. De Felice, E. Ricca, S.M. Cutting, Display of heterologous antigens on the *Bacillus subtilis* spore coat using CotC as a fusion partner, Vaccine. 22 (2004) 1177–1187.
[28] A. Iwanicki, I. Piątek, M. Stasiłojć, A. Grela, T. Łęga, M. Obuchowski, K. Hinc, A system of vectors for *Bacillus subtilis* spore surface display, Microb. Cell Fact. 13 (2014) 30.
[29] R. Isticato, G. Esposito, R. Zilhão, S. Nolasco, G. Cangiano, M. De Felice, A.O. Henriques, E. Ricca, Assembly of Multiple CotC Forms into the *Bacillus subtilis* Spore Coat, J. Bacteriol. 186 (2004) 1129–1135.
[30] A. Negri, W. Potocki, A. Iwanicki, M. Obuchowski, K. Hinc, Expression and display of *Clostridium difficile* protein FliD on the surface of *Bacillus subtilis* spores, J. Med. Microbiol. 62 (2013) 1379–1385.

[31] S. Fernández, S. Ayora, J.C. Alonso, Bacillus subtilis homologous recombination: Genes and products, Res. Microbiol. 151 (2000) 481–486.
[32] P. Boyaval, S. Moineau, D. a Romero, P. Horvath, Against Viruses in Prokaryotes, Science 315 (2007) 1709–1712.
[33] M. Jinek, K. Chylinski, I. Fonfara, M. Hauer, J.A. Doudna, E. Charpentier, A Programmable Dual-RNA – Guided, 337 (2012) 816–822.
[34] R. Isticato, D.S. Di Mase, E.M.F. Mauriello, M. De Felice, E. Ricca, Amino terminal fusion of heterologous proteins to CotC increases display efficiencies in the *Bacillus subtilis* spore system, Biotechniques. 42 (2007) 151–156.
[35] J.H. Kim, C.S. Lee, B.G. Kim, Spore-displayed streptavidin: A live diagnostic tool in biotechnology, Biochem. Biophys. Res. Commun. 331 (2005) 210–214.
[36] H. Chen, B. Wu, T. Zhang, J. Jia, J. Lu, Z. Chen, Z. Ni, T. Tan, Effect of linker length and flexibility on the *Clostridium thermocellum* esterase displayed on *Bacillus subtilis* Spores, Appl. Biochem. Biotechnol. (2016) 1–13.
[37] H. Chen, T. Zhang, T. Sun, Z. Ni, Y. Le, R. Tian, Z. Chen, C. Zhang, *Clostridium thermocellum* nitrilase expression and surface display on *Bacillus subtilis* Spores, J. Mol. Microbiol. Biotechnol. 25 (2015) 381–387.
[38] K. Hinc, A. Iwanicki, M. Obuchowski, New stable anchor protein and peptide linker suitable for successful spore surface display in *B. subtilis*, Microb. Cell Fact. 12 (2013) 22.
[39] J. Kurjan, I. Herskowitz, Structure of a yeast pheromone gene (MFα): A putative α-factor precursor contains four tandem copies of mature α-factor, Cell. 30 (1982) 933–943.
[40] T. Vogl, L. Sturmberger, T. Kickenweiz, R. Wasmayer, C. Schmid, A.M. Hatzl, M.A. Gerstmann, J. Pitzer, M. Wagner, G.G. Thallinger, M. Geier, A. Glieder, A toolbox of diverse promoters related to methanol utilization: functionally verified parts for heterologous pathway expression in *Pichia pastoris*, ACS Synth. Biol. 5 (2016) 172–186.

SUPPORTING INFORMATION

Primer list for *B. subtilis* spore display of HMFO

PCR	Forward	Reverse
Spacer CotB	5'-TACGTGCCCTTTTTCAGTTAAAGG	5'-AAACCCTTTAACTGAAAAAGGGCA
Spacer CotC	5'-TACGGTGCACAAACAAAAAAGACC	5'-AAACGGTCTTTTTTGTTTGTGCAC
Spacer CotX	5'-TACGACCCACACCAAGTGGGGCAC	5'-AAACGTGCCCCACTTGGTGTGGGT
Spacer CotZ	5'-TACGGCTGTCCGGCAACATCAGCC	5'-AAACGGCTGATGTTGCCGGACAGC
Spacer CotG	5'-TACGTCATGACATATATCTAATAC	5'-AAACGTATTAGATATATGTCATGA
CotB 5' GGGGS	5'-GTCGACGGCCAACGAGGCCGCGTTAAACACAAATGAGGATG	5'-CGTAGTCAAAAATCGTATCAGTAGAACCGCCGCCACCAAATTTACGTTTCCAGTGATAGTCTATC
CotB 3'	5'-GCGGATGCGATTCTGACCCAGGCTTAAGTGAAAGGTTTGAATCAATTCCTTAACA	5'-CTAGAAAGGCCTTATTGGCCCAAGAGGGCAGTTTTGTATAC
CotC 5' GGGGS	5'-GTCGACGGCCAACGAGGCCTTCTTAGGCAGGTGGCATTG	5'-CGTAGTCAAAAATCGTATCAGTAGAACCGCCGCCACCGTAGTGTTTTTTATGCTTTTTATACTCTACAACATAATC
CotC 3'	5'-GCGGATGCGATTCTGACCCAGGCTTAATTCATAAGTGAGCGCATTC	5'-CTAGAAAGGCCTTATTGGCCCGTACTGTTCAGGTAGAC
CotX 5' GGGGS	5'-GTCGACGGCCAACGAGGCCAGAAGAAGCAGCCGCACAAG	5'-CGTAGTCAAAAATCGTATCAGTAGAACCGCCGCCACCGAGGACAAGAGTGATAACTAGGATGG
CotX 3'	5'-GCGGATGCGATTCTGACCCAGGCTTAAATCAATGAGCTGCGGAAAAAC	5'-CTAGAAAGGCCTTATTGGCCTACAGCTTCACGCACGC
CotZ 5' GGGGS	5'-GTCGACGGCCAACGAGGCCAAGGCGATACCTTAAGTGTTTGC	5'-CGTAGTCAAAAATCGTATCAGTAGAACCGCCGCCACCATGATGATGTGTACGATTGATTAATCGAGG
CotZ 3'	5'-GCGGATGCGATTCTGACCCAGGCTTAAGTTAAAAACCGAGCGGGTG	5'-CTAGAAAGGCCTTATTGGCCCTGATTTTCAGCTTTCTGTCATATAG
CotG 5'	5'-TTTAAAAGGAGGATTTCAAATTGGGCCACTATTCCCATTCT	5'-TCGTATCAGTTTTGTATTTCTTTTTGACTACCCAGC
CotG 5' GGGGS	5'-TTTAAAAGGAGGATTTCAAATTGGGCCACTATTCCCATTCT	5'-CAGTAGAACCGCCGCCACCTTTGTATTTCTTTTTGACTACCCAGC

PCR	Forward	Reverse
CotG 5' GGGEAAAKGGG	5'-TTTAAAAGGAGGATTTCAAATTGGGCCACTATTCCCATTCT	5'-CCTTTGGCGGCCGCTTCGCCGCCACCTTTGTATTTCTTTTTGACTACCC
CotG 3'	5'-GCGATTCTGACCCAGGCTTAAGGTATCCTAACGATAAAGGCG	5'-GTTTCTTCTATTTAAATAGTCCTTCTCTTCAGCTGGGACGAATCAGT
HMFO (CotB)	5'-GGTGGCGGCGGTTCTACTGATACGATTTTTGACTACG	5'-TTAAGCCTGGGTCAGAATCG
HMFO (CotC)	5'-GGTGGCGGCGGTTCTACTGATACGATTTTTGACTACG	5'-TTAAGCCTGGGTCAGAATCG
HMFO (CotX)	5'-GGTGGCGGCGGTTCTACTGATACGATTTTTGACTACG	5'-TTAAGCCTGGGTCAGAATCG
HMFO (CotZ)	5'-GGTGGCGGCGGTTCTACTGATACGATTTTTGACTACG	5'-TTAAGCCTGGGTCAGAATCG
HMFO (CotG)	5'-GAAATACAAAACTGATACGATTTTTGACTACGTGATT	5'-CGCCTTTATCGTTAGGATACCTTAAGCCTGGGTCAGAATCGC
HMFO (CotG GGGGS)	5'-GGTGGCGGCGGTTCTACTGATACGATTTTTGACTACGTGATT	5'-CGCCTTTATCGTTAGGATACCTTAAGCCTGGGTCAGAATCGC
HMFO (CotG GGGGS)	5'-CGAAGCGGCCGCCAAAGGTGGTGGCACTGATACGATTTTTGACTACGTG	5'-CGCCTTTATCGTTAGGATACCTTAAGCCTGGGTCAGAATCGC
pJOE8999 (CotG)	5'-ACTGATTCGTCCCAGCTGAAGAGAAGGACTATTTAAATAGAAGAAAC	5'-AGAATGGGAATAGTGGCCCAATTTGAAATCCTCCTTTTAAAAATATGTTA
Colony CotB-HMFO 5'	5'-ATTGGTCTGGCTGGGAGA	5'-CACCGCCAACAATCACGT
Colony CotB-HMFO 3'	5'-GCCAATACCAATCTGCCGA	5'-CCATTATCATCATTCCGCTGACT
Colony CotC-HMFO 5'	5'-CGTTTGTATCATTTCCGGCAGAG	5'-CACCGCCAACAATCACGT
Colony CotC-HMFO 3'	5'-GCCAATACCAATCTGCCGA	5'-TTCCGCTTGTTGCCCTAAA
Colony CotX-HMFO 5'	5'-GACTTACAAGCTAAATCACAAGCGC	5'-CACCGCCAACAATCACGT
Colony CotX-HMFO 3'	5'-GCCAATACCAATCTGCCGA	5'-CCGACATTTCCGAAGGCG
Colony CotZ-HMFO 5'	5'-CAACACTGTCTATTTTACGCCCG	5'-CA CGCCAACAATCACGT
Colony CotZ-HMFO 3'	5'-GCCAATACCAATCTGCCGA	5'-GTTCTTGTTCAGCGATATGTCCC
Colony CotG-HMFO 5'	5'-CCGGATCATCGTCCCATATATCC	5'-CACCGCCAACAATCACGT
Colony CotG-HMFO 3'	5'-GCCAATACCAATCTGCCGA	5'-GAGAGGCGAGACTGATGG

GBLOCK FOR P. PASTORIS HMFO EXPRESSION:

8BxHMFO-encoding gene, codon optimized for yeast

5'CACTTCAATTACTTGAAATTCACCATAACACTTGCTCTAGTCAAGACTTACAATTA
AAATGACCGATACTATTTTCGACTACGTTATTGTTGGTGGTGGTACTGCTGGTTCCG
TTTTGGCTAACAGATTGTCCGCAAGACCAGAAAACAGAGTCCTGCTTATTGAGGCTG
GTATCGACACTCCAGAAAATAACATCCCACCTGAAATTCACGACGGATTGCGTCCT
TGGTTGCCAAGATTGTCCGGAGACAAATTCTTCTGGCCAAACCTTACCGTCTACAGA
GCTGCTGAACATCCTGGTATTACCAGAGAGCCACAGTTCTACGAACAAGGAAGAT
TGTTGGGAGGAGGATCTTCAGTTAACATGGTTGTCTCTAACAGAGGTTTACCAAGAG
ATTACGACGAGTGGCAAGCTCTGGGTGCTGATGGTTGGGACTGGCAGGGAGTCCTGC
CTTATTTCATCAAAACCGAGCGTGACGCTGACTACGGAGACGACCCATTACATGGAA
ACGCTGGACCAATTCCAATTGGTAGAGTCGACTCCCGTCATTGGTCAGATTTCACTGT
GGCTGCCACTCAAGCCCTTGAGGCCGCTGGACTGCCTAACATTCACGACCAAAACGC
TAGATTCGATGACGGTTACTTTCCTCCAGCTTTCACCTTAAAGGGTGAGGAGAGATTC
TCTGCTGCAAGAGGTTACTTGGACGCATCAGTGAGAGTCCGTCCAAACTTGTCTTTG
TGGACCGAGTCTAGAGTCCTGAAACTGCTTACCACCGGTAACGCCATTACTGGTGTG
TCCGTCCTTAGAGGTCGTGAAACTCTTCAGGTTCAAGCTAGAGAAGTCATTCTGACC
GCTGGTGCATTACAGTCTCCTGCTATTTTGTTGAGAACTGGTATTGGACCAGCTGCTG
ATTTACACGCTCTTGGTATCCCTGTTCTTGCTGATAGACCTGGTGTCGGTCGTAACCTT
TGGGAACACTCTTCTATTGGTGTTGTGGCTCCACTGACCGAGCAAGCAAGAGCTGA
TGCTTCTACTGGTAAGGCCGGTTCTCGTCACCAGTTGGGTATCAGAGCTTCATCTGG
AGTTGATCCAGCAACCCCTTCCGATCTGTTCTTGCACATTCACGCTGACCCTGTGTC
TGGTCTGGCATCAGCTAGATTCTGGGTCAACAAGCCATCTTCCACCGGTTGGTTGAA
GCTGAAGGACGCTGATCCTTTTTCTTACCCTGACGTTGATTTCAACTTGTTGTCAGA
CCCTAGAGACTTGGGTAGACTTAAGGCCGGTTTGAGATTGATCAAGCACTACTTCG
CTTATCCTTCCTTAGCAAAGTACGGATTGGCCTTGGCCCTTTCCAGATTCGAGGCTC
CTCAACCAGGAGGTCCTTTGCTGAACGACTTATTGCAAGACGAAGCTGCATTGGAA
AGATACTTGAGAACCAACGTCGGTGGTGTCTTTCACGCTTCTGGTACTGCAAGAATC
GGTCGTGCAGATGACTCTCAGGCAGTCGTTGATAAGGCTGGTAGAGTTTATGGTGTTA
CCGGTTTGAGAGTTGCAGACGCTTCCATCATGCCAACCGTTCCAACCGCTAACACCA
ACTTGCCAACTTTGATGTTAGCCGAAAAGATTGCTGATGCTATCTTGACTCAGGCATA
AGCGGCCGCTCAAGAGGATGTCAGAATGCCATTTG

PRIMER LIST FOR *P. PASTORIS* HMFO EXPRESSION

To clone HMFO in pBSYDCsec (template: gBlock HMFO codon optimized for yeast):

5'-GGTGTCTCTCTCGAGAAGAGAGAGGCCGAAGCTAGATTCCCATCTATTTTCACC
GCTGTC

5'-TCTCAGGCAAATGGCATTCTGACATCCTCTTGATTATGCCTTAGGCTTAATGGAT
TGTGG

SECRETED 8BXHMFO MASS-SPECTROMETRY ANALYSIS

Probability Legend:
over 95%
80% to 94%
50% to 79%
20% to 49%
0% to 19%

Bio View:
25 Proteins in 25 Clusters

#	Visible?	Starred?	sp|HMFO|HMFO	Accession Number	Alternate ID	Molecular Weight	Protein Grouping Ambiguity	HMFO
1	☑	☆	**sp|HMFO|HMFO**	**HMFO**		**57 kDa**		**730**
2	☑	☆	Uncharacterized protein OS=Komagataella phaffii (strain GS115 / ATCC 20864) OX=64422...	C4R3H3_KOMPG...	PAS_chr3_...	32 kDa		54
3	☑	☆	Uncharacterized protein OS=Komagataella phaffii (strain GS115 / ATCC 20864) OX=64422...	C4R3C4_KOMPG...	PAS_chr3_...	63 kDa		44
4	☑	☆	Daughter cell-specific secreted protein with similarity to glucanases, endo-1,3-beta-glucan...	C4QW71_KOMP...	PAS_chr1-1...	110 kDa		26
5	☑	☆	Cell wall protein with similarity to glucanases OS=Komagataella phaffii (strain GS115 / ATC...	C4QZH9_KOMPG...	PAS_chr2-1...	49 kDa		24
6	☑	☆	Protein of the SUN family (Sim1p, Uth1p, Nca3p, Sun4p) that may participate in DNA replica...	C4R2Z5_KOMPG...	PAS_chr2-2...	45 kDa		24
7	☑	☆	ATPase involved in protein import into the ER, also acts as a chaperone to mediate protein...	C4QZS3_KOMPG	PAS_chr2-1...	74 kDa		18
8	☑	☆	Uncharacterized protein OS=Komagataella phaffii (strain GS115 / ATCC 20864) OX=64422...	C4QZV5_KOMPG...	PAS_chr2-1...	182 kDa		18
9	☑	☆	Cell wall protein with similarity to glucanases OS=Komagataella phaffii (strain GS115 / ATC...	C4QVL7_KOMPG...	PAS_chr1-3...	36 kDa		16
10	☑	☆	Amine oxidase OS=Komagataella phaffii (strain GS115 / ATCC 20864) OX=644223 GN=PAS...	C4R098_KOMPG...	PAS_chr2-1...	90 kDa		16
11	☑	☆	Uncharacterized protein OS=Komagataella phaffii (strain GS115 / ATCC 20864) OX=64422...	C4R8H7_KOMPG...	PAS_chr4_...	64 kDa		10
12	☑	☆	Uncharacterized protein OS=Komagataella phaffii (strain GS115 / ATCC 20864) OX=64422...	C4R1Q1_KOMPG...	PAS_chr2-1...	31 kDa		10
13	☑	☆	Putative GPI-anchored protein OS=Komagataella phaffii (strain GS115 / ATCC 20864) OX=...	C4R4T0_KOMPG...	PAS_chr3_...	31 kDa		10
14	☑	☆	Kex2 proprotein convertase OS=Komagataella phaffii (strain GS115 / ATCC 20864) OX=64...	C4R095_KOMPG...	PAS_chr2-1...	87 kDa		8
15	☑	☆	Uncharacterized protein OS=Komagataella phaffii (strain GS115 / ATCC 20864) OX=64422...	C4R0Z8_KOMPG...	PAS_chr2-1...	24 kDa		8
16	☑	☆	Endochitinase OS=Komagataella phaffii (strain ATCC 76273 / CBS 7435 / CECT 11047 / NRR...	F2QUR1_KOMPC	CTS1	72 kDa		8
17	☑	☆	1,3-beta-glucanosyltransferase OS=Komagataella phaffii (strain GS115 / ATCC 20864) OX...	C4R9F4_KOMPG...	PAS_c034_...	54 kDa		8
18	☑	☆	Glycoprotein involved in cell wall beta-glucan assembly OS=Komagataella phaffii (strain GS...	C4R635_KOMPG...	PAS_chr3_...	28 kDa		6
19	☑	☆	Alpha-1,2-mannosyltransferase OS=Komagataella phaffii (strain GS115 / ATCC 20864) OX...	C4QX95_KOMPG...	PAS_chr1-4...	77 kDa		6
20	☑	☆	Uncharacterized protein OS=Komagataella phaffii (strain GS115 / ATCC 20864) OX=64422...	C4QXM2_KOMP...	PAS_chr1-4...	31 kDa		6
21	☑	☆	Protein disulfide isomerase, multifunctional protein resident in the endoplasmic reticulum lu...	C4R938_KOMPG...	PAS_chr4_...	53 kDa		4
22	☑	☆	Cell wall glycoprotein linked protein OS=Komagataella phaffii (strain ATCC 76273 / CBS 743...	A0A1G4KPI2_K...	CCW14	23 kDa		2
23	☑	☆	Endo-beta-1,3-glucanase, major protein of the cell wall, involved in cell wall maintenance O...	C4QYF3_KOMPG...	PAS_chr1-4...	34 kDa		2
24	☑	☆	Uncharacterized protein OS=Komagataella phaffii (strain GS115 / ATCC 20864) OX=64422...	C4R2E2_KOMPG...	PAS_chr2-2...	38 kDa		2
25	☑	☆	Cell wall protein that functions in the transfer of chitin to beta(1-6)glucan OS=Komagatael...	C4QWP6_KOMP...	PAS_chr1-1...	49 kDa		2

3

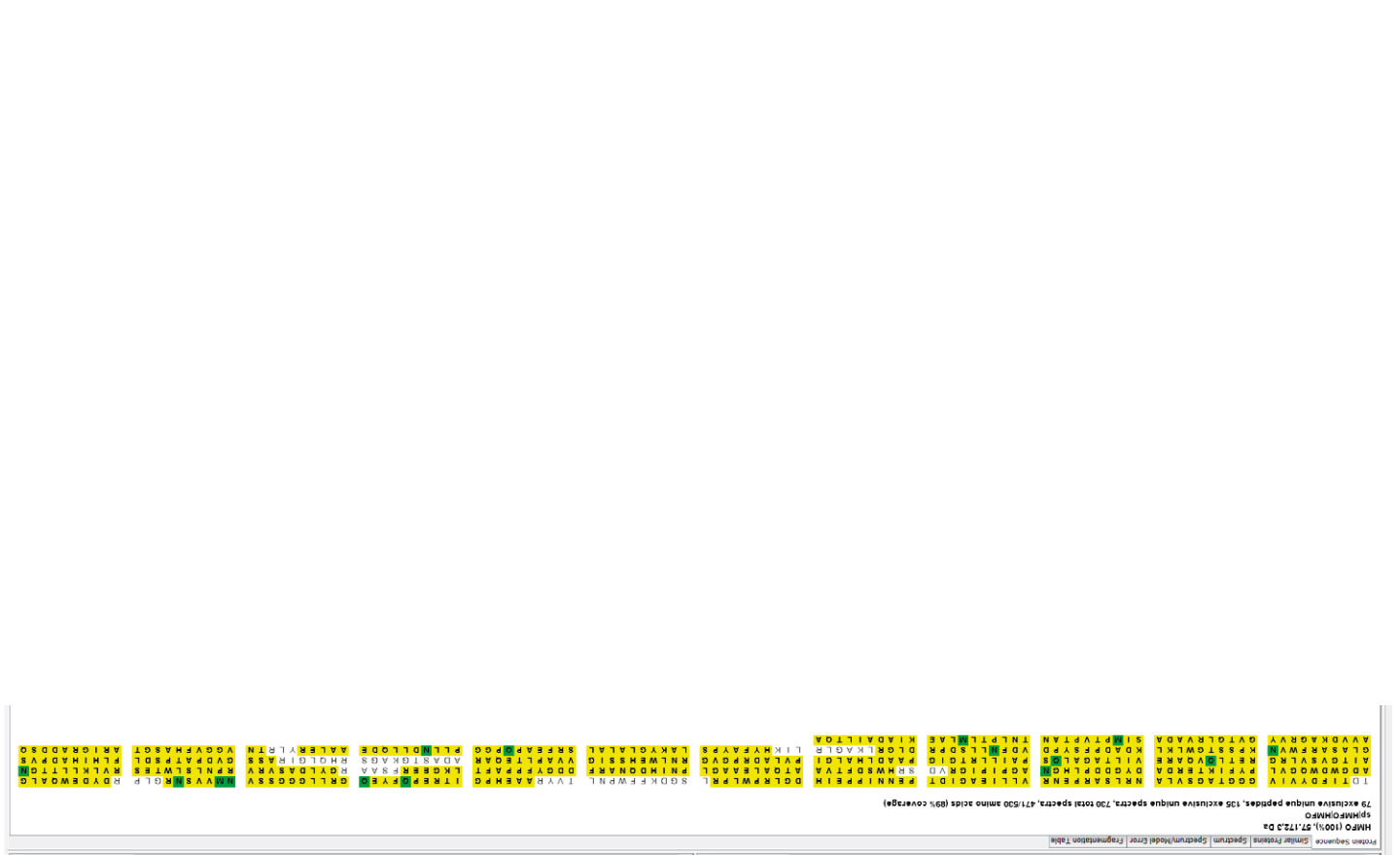

4

Production of Hydroxy Acids through Selective Double Oxidation of Diols by a Flavoprotein Alcohol Oxidase

Caterina Martin, Milos Trajkovic and Marco W. Fraaije*

Molecular Enzymology Group, University of Groningen,
Nijenborgh 4, 9747AG, Groningen, The Netherlands

*Corresponding author

Published in:
Angewandte Chemie Internationl Edition, (2020) (59) 4869-4872

ABSTRACT

Flavoprotein oxidases can catalyze oxidations of alcohols and amines by merely using molecular oxygen as the oxidant, making this class of enzymes appealing for biocatalysis. The FAD-containing (FAD=flavin adenine dinucleotide) alcohol oxidase from *P. chrysosporium* facilitated double and triple oxidations for a range of aliphatic diols. Interestingly, depending on the diol substrate, these reactions result in formation of either lactones or hydroxy acids. For example, diethylene glycol could be selectively and fully converted into 2-(2-hydroxyethoxy) acetic acid. Such a facile cofactor-independent biocatalytic route towards hydroxy acids opens up new avenues for the preparation of polyester building blocks.

INTRODUCTION

Oxygen-containing heterocycles (*O*-heterocycles) form a class of compounds proven to be relevant in the polymers, fuel, and medical fields.[1–4] Some of these *O*-heterocycles such as lactones, and in particular 1,4-dioxan-2-one can be used for synthesis of biodegradable polyesters that find countless clinical applications thanks to their biocompatibility and strength properties.[5,6] Bioabsorbable polymers derived from 1,4-oxathian-2-one possess similar characteristics to polydioxanone, but they are not as studied and commercially used, probably because of the poor yield in the synthesis of 1,4-oxathian-2-one.[7] The chemical routes to synthetize some of these compounds often require expensive transition-metal catalysts (Au or Pd catalysts), which increase the production costs.[8] Moreover biodegradable polymers for biomedical applications need to be metal free.[9] Enzymatic synthesis of lactones as polyester building blocks gained great interest as an environmentally sustainable alternative to current chemical methods. The most common biocatalysts to produce lactones are Baeyer-Villiger monooxygenases (BVMOs) and alcohol dehydrogenases (ADHs).[10–13] These two classes of enzymes require cofactor NAD(P)H regeneration, making these strategies less suitable for commercial applications. Oxidases are an attractive class of enzymes for the production of bulk chemicals since they use oxygen either as an oxidant without the need to regenerate cofactors.[14] Alcohol oxidases are a subclass of oxidative enzymes containing either a copper or flavin adenine dinucleotide (FAD) as a prosthetic group that often has a broad substrate spectrum, including primary and secondary alcohols, aldehydes, and ketones.[15] A remarkable example of the power of flavoprotein oxidases is the 5-hydroxymethylfurfural (HMF) oxidase discovered and engineered by our group. This FAD-containing biocatalyst can oxidize 5-hydroxymethylfurfural to 2,5-furandicarboxylic acid in three consecutive oxidations.[16,17] Another recent demonstration of the biocatalytic potential of a flavoprotein alcohol oxidase was recently reported by Turner and co-workers. They showed that choline oxidase can be engineered towards a wider substrate acceptance, for the selective oxidation of primary alcohols to aldehydes.[18]

The FAD-containing alcohol oxidase from the white-rot basidiomycete *Phanerochaete chrysosporium* (*Pc*AOX) was recently characterized and engineered by our group for improved activity towards glycerol.[19] The rational engineering study resulted in the variant F101S optimized for glycerol conversion. The aim of this work was to explore and expand the potential of this improved variant. Herein,

the attention was directed to diols which represent an industrially important class of chemical compounds as they are relatively cheap and can be transformed into either lactones or hydroxy acids, which in turn are building blocks for biodegradable polymers. Except for a focus on diols as substrates, we also tested other alcohols (primary and secondary) and aminoalcohols. Such a large variety of different substrates was explored to probe the substrate acceptance profile of F101S-*Pc*AOX, but also to understand how catalyzes the double oxidation of alcohols into carboxylic acids. The most striking discovery is the ability of F101S-*Pc*AOX to selectively perform double oxidations on one of two hydroxy groups for a subset of diols.

The initial experiments were performed with a small set of diols, aimed to verify which variant of *Pc*AOX (wild-type *Pc*AOX or the F101S variant) was more active (see the Supporting information). NMR analysis proved to be the best method for analysis of these types of compounds. This approach is fast and it allowed a quantitative and qualitative analysis of the formed products. Table 1 presents the list of substrates tested and the product yields as determined by ^{1}H NMR spectroscopy.

The results revealed that the F101S mutant outperformed the wild-type enzyme, which is in line with its wider active site. F101S-*Pc*AOX (referred to as AOX* in the rest of the manuscript) was selected for further investigation.

AOX* showed activity towards the shortest tested diol (1,3-propanediol), but a mixture of products was obtained. The enzyme is likely to convert this substrate into a very active aldehyde and/or dialdehyde species. The substrate **1** (1,4-butanediol) was oxidized by AOX* into a mixture of two products: the corresponding γ-butyrolactol and γ-butyrolactone (Table 1). The lactol product intermediate was the main component and existed in the buffer environment as mixture of hemiacetal and hydroxylaldehyde (ratio 10:1). The unanticipated finding that AOX* converted **1** into the lactone (by a double oxidation) motivated us to perform product analysis of other aliphatic diols. The substrate **2** was crucial to understanding the reaction mechanism.

For **2**, complete conversion was observed, resulting in the doubly oxidized product. This result shows that AOX* performs two consecutive oxidations of the primary alcohol group, even in the presence of a secondary alcohol moiety. The product of the double oxidation was obtained as mixture of the lactone form (γ-valerolactone) and the hydrolyzed form (4-hydroxypentanoic acid) in a ratio of 4:1. Analogous to the conversion of **1**, the double oxidation of **2** presumably proceeds by formation of the corresponding lactol (5-methyltetrahydrofuran-2-ol). To verify the ability of AOX* to act on both compounds, the steady-state

Table 1. Results of AOX*-catalysed conversions of diols and other alcohols [a].

Entry	Substrate	Intermediate	Product	Product [%]
1	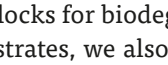	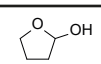		11 (63 intermediate)
2	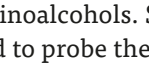	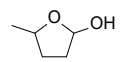	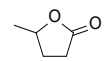	>99[b]
3	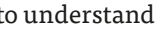		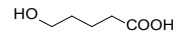	>99
4	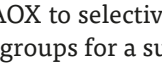		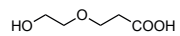	>99
5			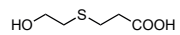	>99
6	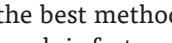	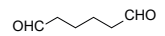	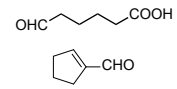	64[c] (36 aldol)
7		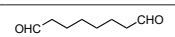	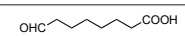	>99[c]
8		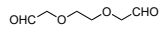	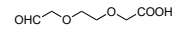	>99[d]
9	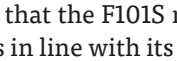	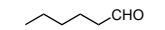	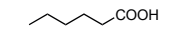	>99
10		/	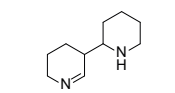	>99
11	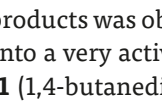	/	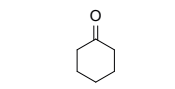	21
12	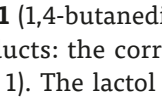	/	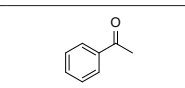	15
13	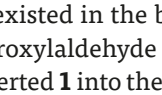	/	/	0

[a] Reaction conditions: substrate (20 mM), enzyme (40 μM), and 100 mM potassium phosphate buffer pH 7.5 for 48 h at 35 °C. Yields were determined based on ^{1}H NMR spectroscopy. ^{1}H NMR spectroscopy was performed after the addition of D_2O (15% v/v). [b] Ratio cyclic to open product 4:1. [c] Ratio of *gem*-diol and aldehyde form of carboxylic acid (ratio ~1:1). [d] Ratio of *gem*-diol and aldehyde form of carboxylic acid (ratio~10:1).

kinetic parameters for these and other alcohols were determined (see Table 2). This data indeed confirmed that AOX* can act on aliphatic

diols and the lactol (5-methyltetrahydrofuran-2-ol), demonstrating that the catalytic route proceeds through initial lactol formation and subsequent additional oxidation to the lactone.

The substrates **3**, **4,** and **5** were selected as examples for 1,5-diols (Table 1). For all three substrates, complete conversion was obtained and the corresponding products of the double oxidation for these diols were obtained in the form of 5-hydroxycarboxylic acids as single products. No other products (lactone, diacid, or aldehyde acid) were observed by ^{1}H NMR spectroscopy. These results are in contrast to the products formed with **1** and **2**, which are obtained in the lactone form. Additional experiments were performed to explain this apparent difference. We investigated the stability of the commercially available 1,4-dioxan-2-one (the lactone form of the product of substrate **4**). This compound was found to swiftly hydrolyze in buffer (Scheme 1). In buffer, in less than half hour it completely hydrolyzed to the hydroxy acid (reaction conditions: 100 mM KPi buffer pH = 7.5; see Supporting Information), indicating that as soon as the lactone is formed upon oxidation of either **3**, **4,** or **5**, the formed lactone rapidly hydrolyzes into the stable hydroxy acid. We also monitored the conversion of **4**, thus revealing that the first detectable product intermediate exists in its hemiacetal form. According to these data, we conclude that the AOX*-catalyzed double oxidation of aliphatic diols proceeds by formation of the corresponding hemiacetal which is subsequently oxidized into the lactone, which is prone to hydrolysis into the corresponding 5-hydroxy acids (Scheme 1).

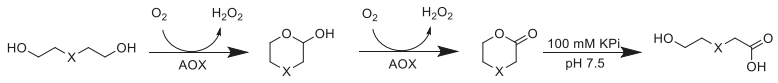

Scheme 1 Catalytic route for oxidation of the 1,5-diols **3**, **4** and **5** by AOX*. X=C, S, or O.

The substrate **6** (Table 1) was also tested, because the corresponding product lactone (ε-caprolactone) is of value as a polymer building block. [20] Somewhat unforeseen, AOX* was found to oxidize both hydroxy groups into aldehyde groups resulting in the production of adipaldehyde. In the employed buffer, adipaldehyde spontaneously reacted by aldol condensation (non-enzymatic reaction; see Supporting Information) while also some further oxidation into 6-oxohexanoic acid was observed. Similarly, to substrate **6**, 1,8-octanediol (**7**) and triethylene glycol (**8**) underwent oxidation at both hydroxy groups, yielding the corresponding dialdehydes, which were then further oxidized into oxocarboxylic acids. For these two substrates the aldol condensation product was not obtained, probably because of the unfavorable formation of a seven-membered-ring product. For the latter substrates (**6**-**8**), AOX* performed a triple oxidation by oxidizing the *gem*-diol form of the formed dialdehydes. NMR analysis also confirmed that these aliphatic aldehydes are significantly hydrated (10-50%) in the employed buffer. For the selective oxidation of only one hydroxy group, as observed for **3**-**5**, formation of a very stable hemiacetal intermediate seems to be crucial. If the hemiacetal is not formed upon the first oxidation, the enzyme will oxidize the other hydroxy group, resulting in the dialdehyde. Subsequently, one aldehyde group is oxidized to the carboxylic acid via the *gem*-diol. Once that the carboxylic acid is obtained, the enzyme does not accept this compound for the further oxidation towards a diacid. Along these lines, the substrate **9** was found to yield hexanoic acid, supporting our hypothesis that AOX* can further oxidize the initially formed aldehyde via its *gem*-diol. Different from the other substrates, **9** and the intermediate product formed from **9** (**Int-9**) exhibited substrate inhibition (see Table 2; see the Supporting Information), which may be due to alternative binding pockets for these relatively apolar substrates when compared with the tested diols.

The aminoalcohol (**10**) was used to explore the substrate promiscuity of AOX* (Table 1). Interestingly, complete conversion was observed for **10**. From the ^{1}H NMR spectra it can be concluded that the reaction occurred as selective single oxidation on the hydroxy group. A singlet at d=7.88 ppm clearly indicated that the product exists as an imine (*in situ* formed spontaneously from aminoaldehyde). The ^{1}H NMR spectra appeared complex and the product could not be extracted with ethyl acetate to confirm the product by GC-MS analysis. Nevertheless Braekman and coworker describe that Δ-piperideine under reaction conditions (pH 7.5) analogous to ours preferably dimerizes to form tetrahydroanabasine, which correlates with our ^{1}H NMR spectra.[21]

It is known that alcohol oxidases can oxidize secondary alcohols, though with poor efficiency. We selected just a few to test AOX* (substrates **11**, **12**, and **13**; Table 1). Cyclohexanol (**11**) was oxidized to cyclohexanone with a low yield. Initially, we tested racemic 1-phenylethanol and its conversion was rather low, similar to cyclohexanol. We then tested separately each enantiomer of this alcohol (substrates **12** and **13**). Remarkably, AOX* was highly selective towards the *S*-enantiomer of 1-phenylethanol (no conversion for the *R*-enantiomer).

The steady-state kinetic parameters for a selection of the discovered AOX* substrates were determined (Table 2).

The observed values for **2** and its corresponding lactol (**Int-2**) support the proposed catalytic mechanism of the double oxidation going

Table 2. Apparent Steady-State Kinetic Parameters for AOX*[a].

Entry	Substrate	K_M[a]	K_i[b]	k_{cat}[a]	k_{cat}/K_M
1	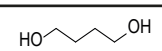	198	n.d.	6.74	34.1
2	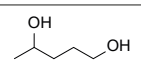	52.6	n.d.	1.28	24.3
Int-2	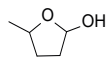	95.5	n.d.	1.13	11.8
3	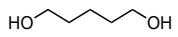	69.6	n.d.	3.48	50.0
4	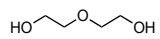	12.3	n.d.	0.73	59.2
5	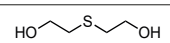	119	n.d.	3.56	29.9
6	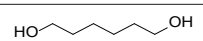	12.9	n.d.	4.07	316
9	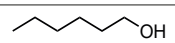	3.0	56	0.56	187
Int-9	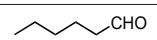	0.20	5.5	0.15	750

[a] Values obtained using the HRP-coupled assay in 50 mM potassium phosphate, pH 7.5. K_M values are presented in units of mM, k_{cat} values are presented in units of s^{-1}, and k_{cat}/K_M values are presented in units of $M^{-1}\,s^{-1}$. [b] The notation n.d. (not detected) used to indicate that no substrate inhibition was observed.

through the lactol intermediate. The rate-limiting step (lower k_{cat}/K_M) seems to be the second oxidation step, the oxidation of the lactol. This step was confirmed for substrate **1** and also by shorter conversion experiments for substrates **2**-**5**. Shorter incubations revealed the accumulation of the respective lactols.

The substrates **4** and **5** were also tested as substrates with several other flavoprotein alcohol oxidases: alditol oxidase (HotAldO) from *Acidothermus cellulolyticus* 11B, chitooligosaccharide oxidase (ChitO) from *Fusarium graminearum*, 5-hydroxymethylfurfural oxidase (HMFO) wild type and variant 8BxHMFO from *Methylovorus sp.* strain MP688, methanol oxidase from *Hansenula sp*. (EC 1.1.3.13), glucose oxidase form *Aspergillus niger* (EC 1.1.3.4), and choline oxidase wild-type and an engineered choline oxidase variant (AcCO6) from *Arthrobacter chlorophenolicus*. [16,17,22–24] Except for (AcCO6), all these oxidases did not convert **4** and **5**. The six-fold mutant of choline oxidase, AcCO6, proved to facilitate the double oxidation of **4** and **5**, albeit with low yields: 5% product (38% lactol intermediate) with **4**, and 28% of product (68% lactol intermediate) with **5**, using the same reaction conditions as with AOX*. Furthermore, AcCO6 was found to suffer from severe substrate inhibition.

In conclusion, this work demonstrates the potential of AOX* as a biocatalyst to produce, in one pot, hydroxy acids from 1,5-diols through a selective double oxidation. Diethylene glycol and thiodiglycol can be converted into the corresponding hydroxy acids, which represent interesting building blocks for biodegradable polymers. Similarly, 1,4-diols are converted into the respective lactones. The final oxidation products obtained, γ-butyrolactone and γ-valerolactone are used in the polymer industry.[4] [25] The catalytic mechanism of AOX* with these diols involves the *in situ* formation of stable hemiacetals. Longer diols can also be oxidized by AOX*, resulting in the corresponding oxocarboxylic acids through a triple oxidation. For all these AOX*-catalyzed oxidation cascade reactions, no external cofactor is required. These results suggest that AOX* holds a great promise as a biocatalyst for selective oxidations.

EXPERIMENTAL SECTION

AOX* was expressed in *E. coli* NEB 10β as His-tag-SUMO phusion using a pBAD expression vector and purified using affinity chromatography as described before.[19] Kinetic parameters were determined using a HRP-coupled assay as described before.[19] ^{1}H NMR spectra were recorded on an Agilent 400-MR spectrometer (^{1}H and ^{13}C resonances at 400 MHz and 100 MHz, respectively). Chemical shifts are reported in parts per million (ppm) and coupling constants (J) are reported in hertz (Hz).

REFERENCES

[1] P.H. Plesch, Some aspects of the polymerisation of 1,3-dioxacycloalkanes, Polym. Heterocycles (Ring Opening), Pergamon (1977) 287–293.

[2] P.K. Singh, O. Silakari, The current status of o-heterocycles : a synthetic and medicinal overview, ChemMedChem. 13 (2018) 1071–1087.

[3] Z. Lu, Biomolecular chemistry for efficient gene delivery, Org. Biomol. Chem. 15 (2017) 6567–6574.

[4] M. Gagliardi, A. Bifone, Ring-opening copolymerization thermodynamics and kinetics of γ-valerolactone/ε-caprolactone, PLoS One. 13 (2018) 1–15.

[5] N. Goonoo, R. Jeetah, A. Bhaw-luximon, D. Jhurry, Polydioxanone-based bio-materials for tissue engineering and drug/gene delivery applications, Eur. J. Pharm. Biopharm. 97 (2015) 371–391. https://doi.org/10.1016/j.ejpb.2015.05.024.

[6] J.A. Von Fraunhofer, R.S. Storey, I.K. Stone, B.J. Masterson, Tensile strength of suture materials, J. Biomed. Mater. Res. 19 (1985) 595–600.

[7] A.C. Company, M. Street, Polyesters Derived from 1,4-Oxathian-Z-Ones, J. Polym. Sci. 23 (1985) 843–849.

[8] A. Deiters, S.F. Martin, Synthesis of oxygen- and nitrogen-containing heterocycles by ring-closing metathesis, Chem. Rev. 104 (2004) 2199–

[9] H. Nishida, M. Yamashita, M. Nagashima, T. Endo, Y. Tokiwa, Synthesis of metal-free poly(1,4-dioxan-2-one) by enzyme-catalyzed ring-opening polymerization, J. Polym. Sci. 38 (2000) 1560–1567.

[10] F. Hollmann, S. Kara, D.J. Opperman, Y. Wang, Biocatalytic synthesis of lactones and lactams, Chem. Asian J. 13 (2018) 3601–3610.

[11] C.D. Dithugoe, J. van Marwijk, M.S. Smit, D.J. Opperman, An alcohol dehydrogenase from the short-chain dehydrogenases/reductases family of enzymes for the lactonization of 1,6-hexanediol, ChemBioChem. 20 (2018) 96–102.

[12] S. Kara, D. Spickermann, J.H. Schrittwieser, A. Weckbecker, C. Leggewie, I.W.C.E. Arends, F. Hollmann, Access to lactone building blocks via horse liver alcohol dehydrogenase-catalyzed oxidative lactonization, ACS Catal. 3 (2013) 2436–2439.

[13] L. Huang, G.V. Sayoga, F. Hollmann, S. Kara, Horse Liver Alcohol dehydrogenase-catalyzed oxidative lactamization of amino alcohols, ACS Catal. 8 (2018) 8680–8684.

[14] P.N.R. Vennestrøm, C.H. Christensen, S. Pedersen, J. Grunwaldt, J.M. Woodley, Next-generation catalysis for renewables : Combining enzymatic with inorganic heterogeneous catalysis for bulk chemical production, ChemCatChem. 2 (2010) 249–258.

[15] E. Romero, J.R. Gómez Castellanos, G. Gadda, M.W. Fraaije, A. Mattevi, Same substrate, many reactions: oxygen activation in flavoenzymes, Chem. Rev. (2018)

[16] W.P. Dijkman, D.E. Groothuis, M.W. Fraaije, Enzyme-catalyzed oxidation of 5-hydroxymethylfurfural to furan-2,5-dicarboxylic acid, Angew. Chemie - Int. Ed. 53 (2014) 6515–6518.

[17] C. Martin, A. Ovalle Maqueo, H.J. Wijma, M.W. Fraaije, Creating a more robust 5-hydroxymethylfurfural oxidase by combining computational predictions with a novel effective library design, Biotechnol. Biofuels. 11 (2018) 56.

[18] R.S. Heath, W.R. Birmingham, M.P. Thompson, A. Taglieber, L. Daviet, N.J. Turner, An engineered alcohol oxidase for the oxidation of primary alcohols, ChemBioChem 2019,. 20 (2019) 276–281.

[19] Q.-T. Nguyen, E. Romero, W. Dijkman, S.P. de Vasconcellos, C. Binda, A. Mattevi, M.W. Fraaije, Structure-based engineering of *Phanerochaete chrysosporium* alcohol oxidase for enhanced oxidative power towards glycerol, Biochemistry. 57 (2018) 6209–6218.

[20] A.L. Sisson, D. Ekinci, A. Lendlein, The contemporary role of ε-caprolactone chemistry to create advanced polymer architectures, Polymer (Guildf). 54 (2013) 4333–4350.

[21] A. Rouchaud, J.C. Braekman, Synthesis of new analogues of the tetraponerines, European J. Org. Chem. 5 (2009) 2666–2674.

[22] R.T. Winter, D.P.H.M. Heuts, E.M.A. Rijpkema, E. van Bloois, H.J. Wijma, M.W. Fraaije, Hot or not? Discovery and characterization of a thermostable alditol oxidase from *Acidothermus cellulolyticus* 11B, Appl. Microbiol. Biotechnol. 95 (2012) 389–403.

[23] A.R. Ferrari, M. Lee, M.W. Fraaije, Expanding the substrate scope of chitooligosaccharide oxidase from *Fusarium graminearum* by structure-inspired mutagenesis, Biotechnol. Bioeng. 112 (2015) 1074–1080.

[24] I.J. van der Klei, L. V Bystrykh, W. Harder, Alcohol oxidase from *Hansenula polymorpha* MIE 4732, Hydrocarb. Methylotrophy, Academic Press, (1990) 420–427.

[25] M. Danko, J. Mosnázek, Ring-opening polymerization of γ-butyrolactone and its derivatives: A review, Polimery. 62 (2017) 272–282.

SUPPORTING INFORMATION

Kinetic analyses. The employed assay measures the reaction rate thanks to the hydrogen peroxide generated by AOX during the substrate conversion. Hydrogen peroxide is used by HRP (horse radish peroxidase) (40 U/mL) to catalyze the oxidative coupling reaction of 4-aminoantipyrine (0.1 mM) and 3,5-dichloro-2-hydroxybenzenesulfonic acid (1.0 mM). This reaction results in the formation of a pink quinoid product that can be detected and quantified using a spectrophotometer (ε515 =26 $mM^{-1}cm^{-1}$). The K_M values are presented in mM, kcat values are presented in s^{-1}, and k_{cat}/K_M values are presented in $M^{-1}\,s^{-1}$. For obtaining K_M and k_{cat} values, the data were fit using a regular Michaelis-Menten equation: $k_{obs}=k_{cat}*[S]/K_M + [S]$.

In the case of observed substrate inhibition, the following modified Michaelis-Menten formula was used: $K_{obs}=k_{cat}*[S]/K_M + [S]*(1+[S]/K_I)$.

F101S 1,5 pentanediol

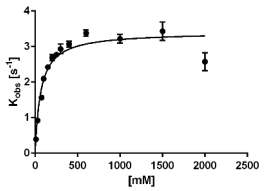

K_M
69.6±13.90
k_{cat}
3.48±0.15
k_{cat}/K_M
50.0

WT 1,5 pentanediol

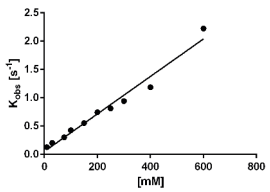

K_M
>600
k_{cat}
>2.22
k_{cat}/K_M
3.3±0.01

F101S diethylene glycol

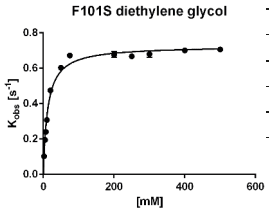

K_M
12.3±0.96
k_{cat}
0.73±0.01
k_{cat}/K_M
59.3

WT diethylene glycol

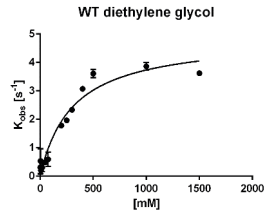

K_M
307.6±74.30
k_{cat}
4.88±0.45
k_{cat}/K_M
16.0

F101S thiodiglycol

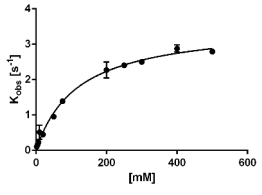

K_M
119.0±14.80
k_{cat}
3.56±0.15
k_{cat}/K_M
29.9

WT thiodiglycol

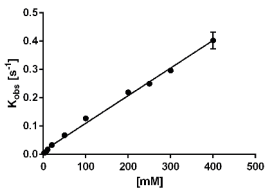

K_M
>400
k_{cat}
>0.4
k_{cat}/K_M
1.0±0.01

F101S 1,4 pentanediol

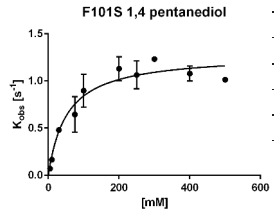

K_M
52.6±14.10
k_{cat}
1.28±0.08
k_{cat}/K_M
24.3

F101S 1,4 pentanediol intermediate

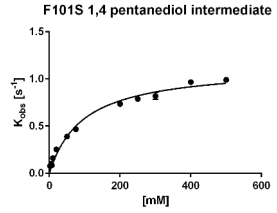

K_M
95.5±14.89
k_{cat}
1.13±0.05
k_{cat}/K_M
11.8

F101S 1,4 butanediol

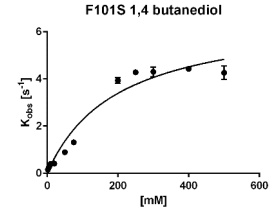

K_M
198±66.60
k_{cat}
6.74±0.94
k_{cat}/K_M
34.1

F101S 1,6 hexanediol

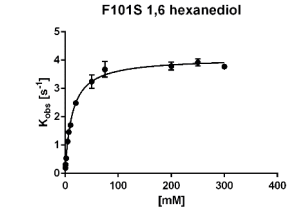

K_M
12.9±0.67
k_{cat}
4.07±0.05
k_{cat}/K_M
316

F101S 1-hexanol

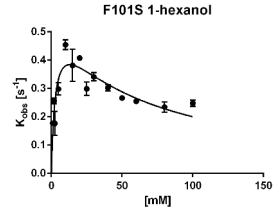

K_M
3.0±1.2
k_{cat}
0.56±0.09
K_i
56±23
k_{cat}/K_M
187

F101S hexanal

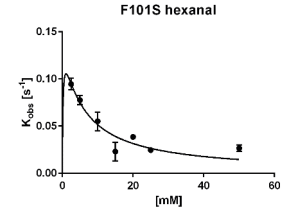

K_M
0.20±2.4
k_{cat}
0.15±0.14
K_i
5.5±7.6
k_{cat}/K_M
750

ENZYMATIC REACTION OF SUBSTRATES AND ANALYSIS OF PRODUCTS

Each reaction mixture contained 20 mM substrate, 40 μM enzyme in 100 mM KPi buffer, pH 7.5 (final reaction volume was 0.4 mL). The reaction was performed in a closed 4 mL glass vial at 35 °C during 24 or 48 h. After that, the reaction was diluted by adding 100 μL of D_2O (20% v/v) and the product was analyzed by ^1H NMR without further purification. Yields were determined based on ^1H NMR. All the reactions were done in duplicates. The control reaction was performed under the same reaction conditions without adding alcohol oxidase.

NMR SPECTRA

Substrate 1 (1,4-butanediol)

Substrate 1 (1,4-butanediol) ^{1}H NMR (400 MHz, D_2O) δ 3.63 – 3.34 (m, 2H), 1.60 – 1.31 (m, 2H).
Substrate 1-int (tetrahydrofuran-2-ol) ^{1}H NMR (400 MHz, D_2O) δ 5.35 (dd, *J* = 4.8, 1.8 Hz, 1H), 3.85 (dt, *J* = 7.9, 5.2 Hz, 1H), 3.67 (dd, *J* = 7.9, 7.0 Hz, 1H), 1.93 – 1.64 (m, 4H).
Product 1 (γ-butyrolactone) ^{1}H NMR (400 MHz, D_2O) δ 4.29 (t, *J* = 7.2 Hz, 2H), 2.43 (d, *J* = 8.0 Hz, 2H), 2.18 – 2.08 (m, 2H).

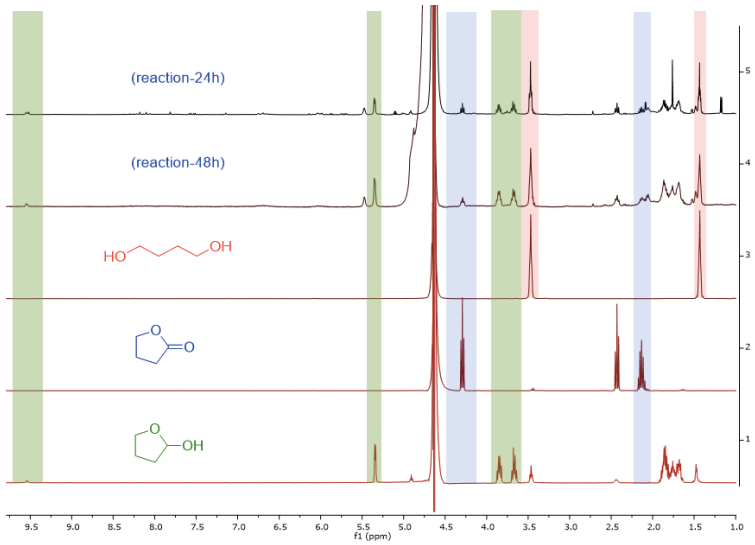

Substrate 2 (1,4-pentanediol)

Substrate 2 (1,4-pentanediol) ^{1}H NMR (400 MHz, D_2O) δ 3.70 (h, *J* = 6.2 Hz, 1H), 3.46 (t, *J* = 6.4 Hz, 2H), 1.53 – 1.30 (m, 4H), 1.02 (d, *J* = 6.4 Hz, 3H).
Substrate 2 (5-methyltetrahydrofuran-2-ol – *major isomer*) ^{1}H NMR (400 MHz, D_2O) δ 5.36 (dd, *J* = 5.2, 2.6 Hz, 1H), 4.19 (dd, *J* = 12.3, 6.3 Hz, 1H), 2.11 – 1.93 (m, 2H), 1.72 – 1.59 (m, 1H), 1.42 – 1.30 (m, 1H), 1.05 (d, *J* = 6.3 Hz, 3H).
Product 2 (γ-valerolactone) ^{1}H NMR (400 MHz, D_2O) δ 2.58 – 2.41 (m, 2H), 2.32 – 2.21 (m, 1H), 1.84 – 1.65 (m, 1H), 1.24 (d, *J* = 6.2 Hz, 3H).

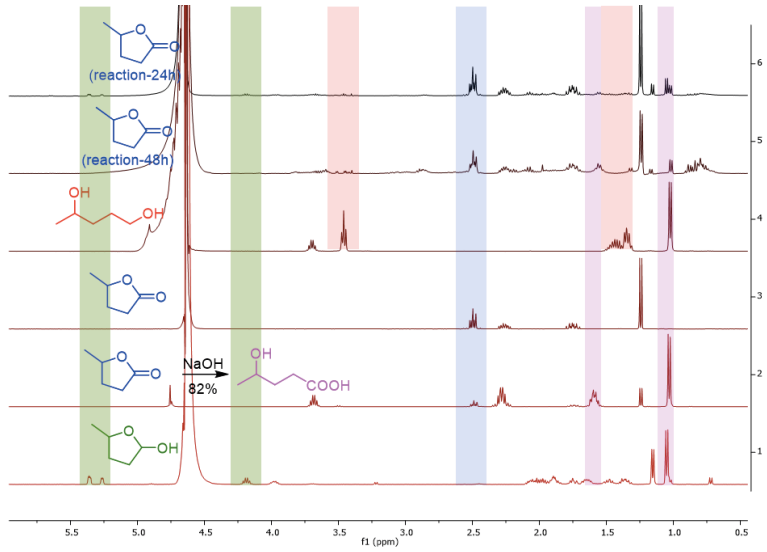

Substrate 3 (1,5-pentanediol)

Substrate 3 (1,5-pentanediol) ^{1}H NMR (400 MHz, D_2O) δ 3.46 (t, *J* = 6.6 Hz, 4H), 1.41 (p, *J* = 7.0 Hz, 4H), 1.27 – 1.17 (m, 2H).
Product 3 (5-hydroxypentanoic acid) ^{1}H NMR (400 MHz, D_2O) δ 3.46 (t, *J* = 6.2 Hz, 2H), 2.05 (t, *J* = 7.0 Hz, 2H), 1.48 – 1.35 (m, 4H).

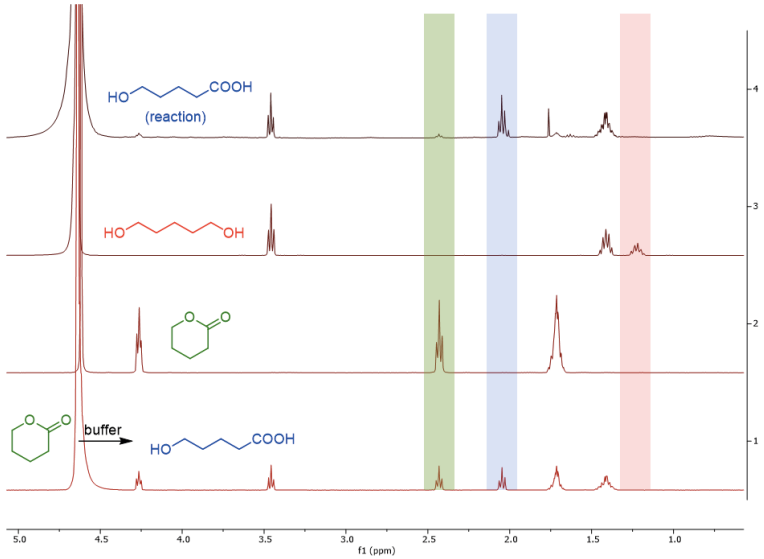

Substrate 4 (diethylene glycol)

Substrate 4 (diethylene glycol) ^{1}H NMR (400 MHz, D_2O) δ 3.61 – 3.57 (m, 4H), 3.51 – 3.47 (m, 4H).
Product 4 (2-(2-hydroxyethoxy)acetic acid) ^{1}H NMR (400 MHz, D_2O) δ 3.80 (s, 2H), 3.61 – 3.56 (m, 2H), 3.50 – 3.45 (m, 2H).

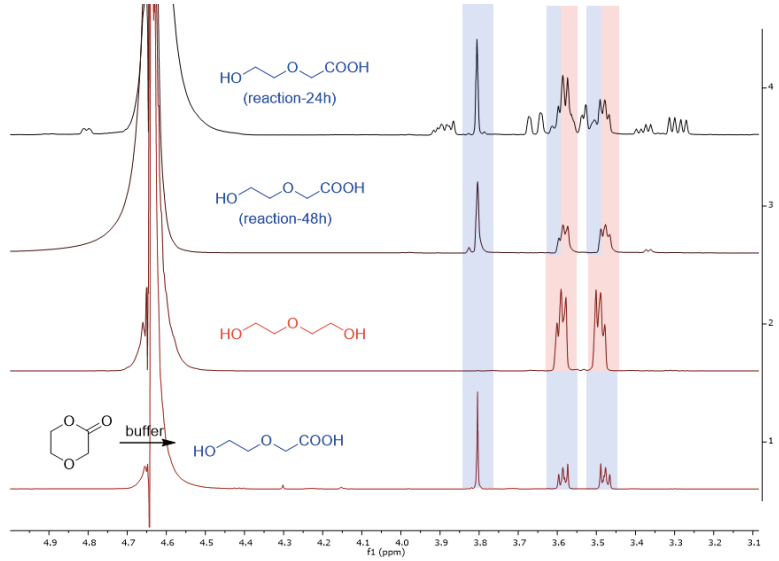

Substrate 5 (thiodiglycol)

Substrate 5 (thiodiglycol) ^{1}H NMR (400 MHz, D_2O) δ 3.60 (t, *J* = 6.3 Hz, 4H), 2.60 (t, *J* = 6.2 Hz, 4H).
Product 5 (2-((2-hydroxyethyl)thio)acetic acid) ^{1}H NMR (400 MHz, D_2O) δ 3.60 (t, *J* = 6.3 Hz, 2H), 3.07 (s, 2H), 2.58 (t, *J* = 6.3 Hz, 2H).

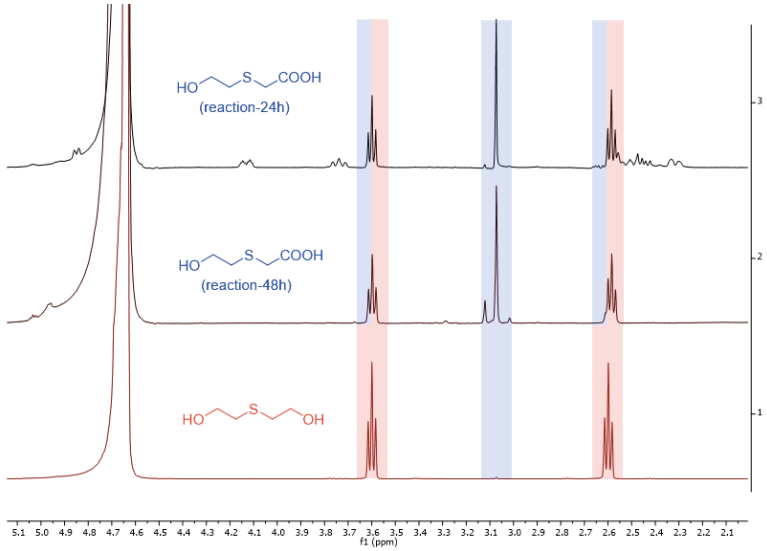

Substrate 6 (1,6-hexanediol)

Substrate 6 (1,6-hexanediol) ^{1}H NMR (400 MHz, D_2O) δ 3.45 (t, *J* = 6.6 Hz, 4H), 1.39 (p, *J* = 6.7 Hz, 4H), 1.23 – 1.17 (m, 4H).
Substrate 6-int (6,6-dihydroxyhexanal) ^{1}H NMR (400 MHz, D_2O) δ 9.52 (s, 1H), 4.89 (t, *J* = 5.6 Hz, 1H), 2.46 – 2.37 (m, 2H), 1.54 – 1.41 (m, 4H), 1.30 – 1.19 (m, 2H).
Product 6a (cyclopent-1-ene-1-carbaldehyde) ^{1}H NMR (400 MHz, D_2O) δ 9.50 (s, 1H), 7.07 (bs, 1H), 2.55 – 2.46 (m, 2H), 2.39 – 2.28 (m, 2H), 1.92 – 1.77 (m, 2H).
Product 6b ^{1}H NMR (400 MHz, D_2O) δ 9.52 (s, 0.5H), 4.88 (t, *J* = 5.3 Hz, 0.5H), 2.44 – 2.37 (m, 1H), 2.04 (td, *J* = 7.2, 3.1 Hz, 2H), 1.51 – 1.37 (m, 4H), 1.27 – 1.16 (m, 1H).

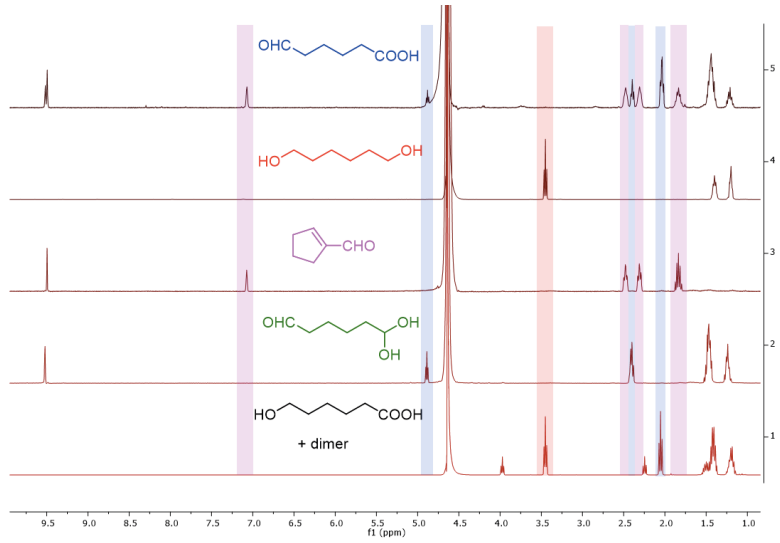

Substrate 7 (1,8-octanediol)

Substrate 7 (1,8-octanediol) ^{1}H NMR (400 MHz, D_2O) δ 3.44 (t, *J* = 6.7 Hz, 4H), 1.43 – 1.35 (m, 4H), 1.21 – 1.13 (m, 8H).
Product 7 (8-oxooctanoic acid) ^{1}H NMR (400 MHz, D_2O) δ 9.51 (s, 0.5H), 4.88 (t, *J* = 5.6 Hz, 0.5H), 2.37 (t, *J* = 7.4 Hz, 1H), 2.02 (t, *J* = 7.4 Hz, 2H), 1.51 – 1.35 (m, 4H), 1.27 – 1.09 (m, 5H).

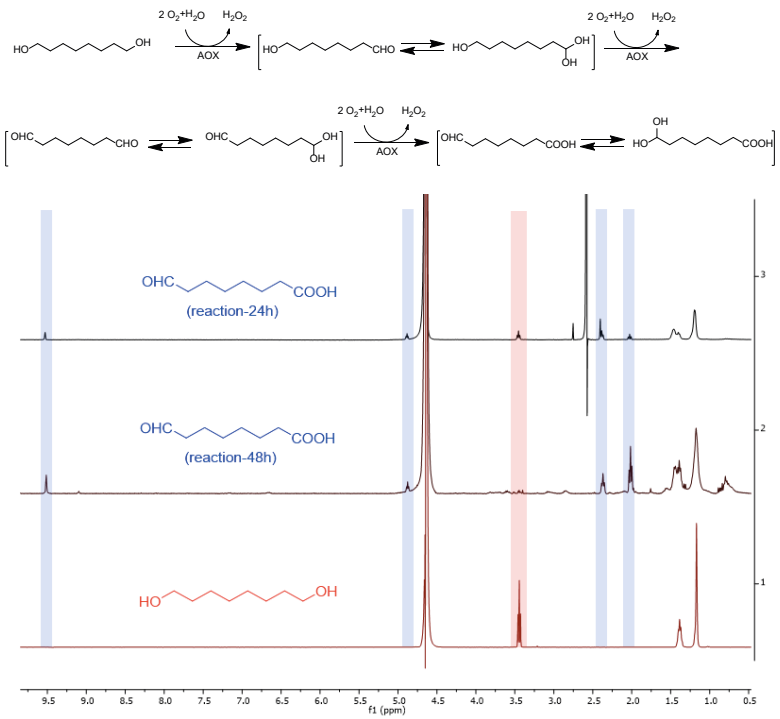

Substrate 8 (triethylene glycol)

Substrate 8 (triethylene glycol) ^{1}H NMR (400 MHz, D_2O) δ 3.60 – 3.57 (m, 4H), 3.56 (s, 4H), 3.52 – 3.48 (m, 4H).
Product 8 (2-(2-(2,2-dihydroxyethoxy)ethoxy)acetic acid) ^{1}H NMR (400 MHz, D_2O) δ 5.03 (t, *J* = 5.0 Hz, 1H), 3.80 (s, 2H), 3.61 – 3.47 (m, 4H), 3.37 (d, *J* = 5.0 Hz, 2H).

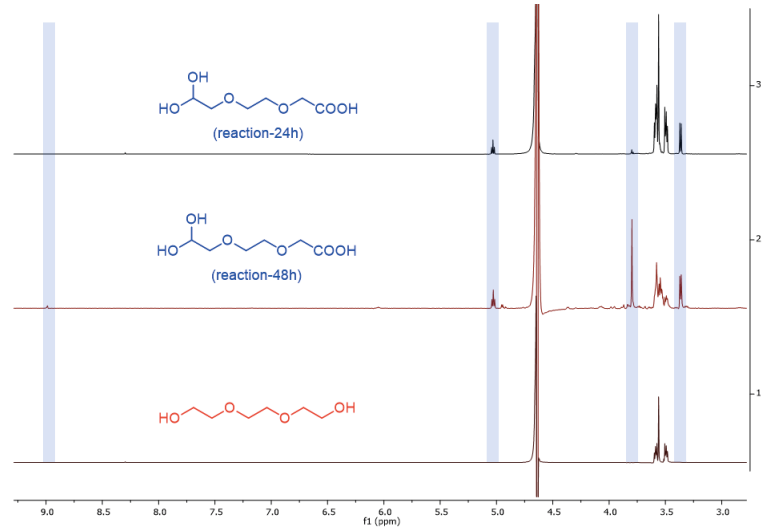

Substrate 9 (1-hexanol)

Substrate 9 (1-hexanol) ^{1}H NMR (400 MHz, D_2O) δ 3.44 (t, *J* = 6.7 Hz, 2H), 1.38 (p, *J* = 5.8 Hz, 2H), 1.22 – 1.11 (m, 6H), 0.75 – 0.67 (m, 2H).
Product 9 (hexanoic acid) ^{1}H NMR (400 MHz, D_2O) δ 2.01 (t, *J* = 7.4 Hz, 2H), 1.39 (p, *J* = 7.2 Hz, 2H), 1.25 – 1.05 (m, 4H), 0.71 (t, *J* = 6.8 Hz, 2H).

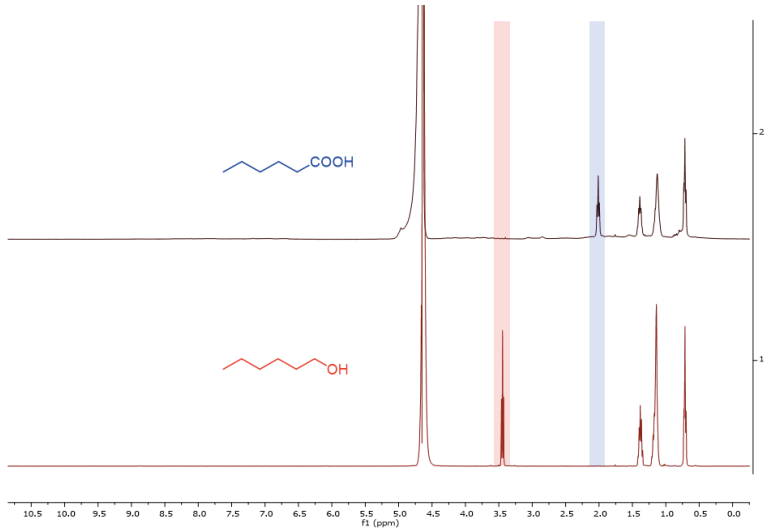

Substrate 10 (5-amino-1-pentanol)

Substrate 10 (5-amino-1-pentanol) ^{1}H NMR (400 MHz, D_2O) δ 3.46 (t, *J* = 6.5 Hz, 2H), 2.85 (d, *J* = 6.8 Hz, 2H), 1.53 (p, *J* = 7.6 Hz, 2H), 1.47 – 1.38 (m, 2H), 1.32 – 1.20 (m, 2H).
Product 10 (5-(piperidin-2-yl)-2,3,4,5-tetrahydropyridine) ^{1}H NMR (600 MHz, D_2O) δ 7.97 (s, 1H), 3.89 (t, *J* = 5.9 Hz, 2H), 3.82 (t, *J* = 6.2 Hz, 2H), 3.16 (t, *J* = 6.3 Hz, 2H), 2.78 (t, *J* = 6.4 Hz, 2H), 2.62 (t, *J* = 6.5 Hz, 2H), 2.58 (t, *J* = 7.6 Hz, 2H), 1.93 – 1.88 (m, 2H), 1.80 – 1.69 (m, 2H).

Substrate 11 (cyclohexanol)

Substrate 11 (Cyclohexanol) ^{1}H NMR (400 MHz, D_2O) δ 3.52 – 3.42 (m, 1H), 1.78 – 1.66 (m, 2H), 1.61 – 1.51 (m, 2H), 1.43 – 1.32 (m, 1H), 1.19 – 0.91 (m, 5H).
Product 11 (Cyclohexanone) ^{1}H NMR (400 MHz, D_2O) δ 2.23 (t, *J* = 6.6 Hz, 4H), 1.75 – 1.64 (m, 4H), 1.58 – 1.52 (m, 2H).

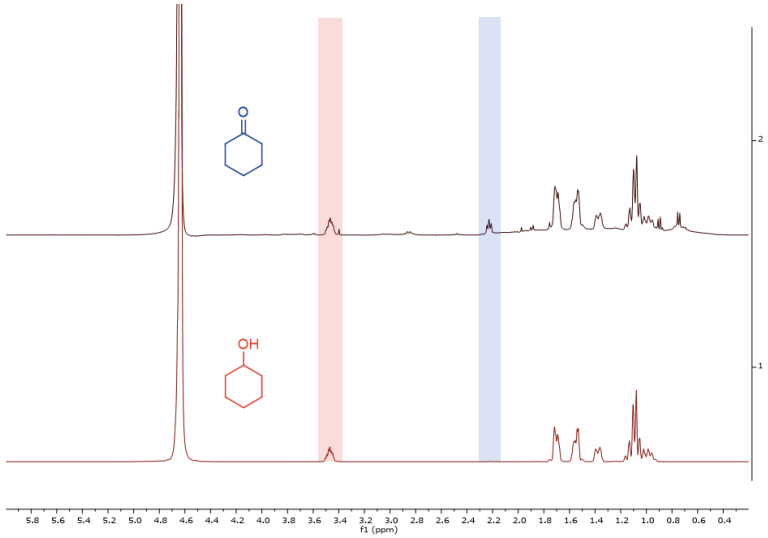

Substrate 12 and 13 ((S or R)-1-phenylethan-1-ol)

Substrate 12 and 13 ((S or R)-1-phenylethan-1-ol) ^{1}H NMR (400 MHz, D_2O) δ 7.36 – 7.15 (m, 5H), 4.50 – 4.35 (m, 1H), 1.32 (d, *J* = 6.6 Hz, 3H).
Product 12 and 13 (Acetophenone) ^{1}H NMR (400 MHz, D_2O) δ 7.86 (d, *J* = 7.7 Hz, 2H), 7.55 (t, *J* = 7.5 Hz, 1H), 7.41 (t, *J* = 7.6 Hz, 2H), 2.52 (s, 3H).

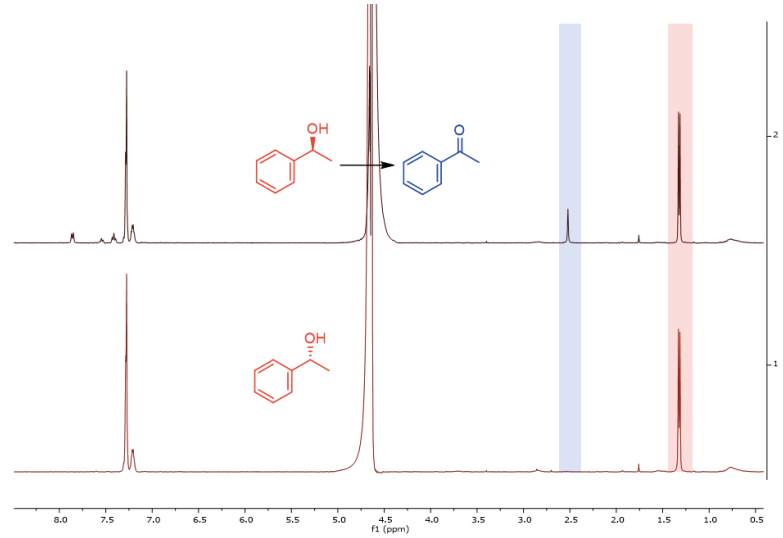

Facile Stereoselective Reduction of Prochiral Ketones using an F_{420}-dependent Alcohol Dehydrogenase

Caterina Martin, Gwen Tjallinks, Milos Trajkovic and Marco W. Fraaije*

Molecular Enzymology Group, University of Groningen, Nijenborgh 4, 9747AG, Groningen, The Netherlands

*Corresponding author

Published in:
ChemBioChem 2020

ABSTRACT

Effective synthetic procedures for the synthesis of optically pure alcohols are highly valuable. A commonly employed method involves the biocatalytic reduction of prochiral ketones. This is typically achieved using nicotinamide cofactor-dependent reductases. In this work we demonstrate that a rather unexplored class of enzymes can also be used for this. We used an F_{420}-dependent alcohol dehydrogenase (ADF) from *Methanoculleus thermophilicus* which was found to reduce various ketones into enantiopure alcohols. The respective S-alcohols were obtained in excellent enantiopurity (>99% e.e.). Furthermore, we discovered that the deazaflavoenzyme can be used as a self-sufficient system by merely using a sacrificial cosubstrate (isopropanol) and a catalytic amount of cofactor F_{420} or the unnatural cofactor FOP to achieve full conversions. This study reveals that deazaflavoenzymes complement the biocatalytic toolbox for enantioselective ketone reductions.

INTRODUCTION

The biocatalytic production of chiral alcohols is feasible by employing different classes of enzymes: oxidoreductases (EC 1), hydrolases (EC 3), and lyases (EC 4).[1] Several methods allow for the production of chiral alcohols and an effective method involves the enantioselective reduction of prochiral ketones by alcohol dehydrogenases (ADHs). ADHs have gained great interest due to their enantioselectivity, allowing for the development of many biotechnological applications.[2] The applicability of ADHs is somewhat limited due to their cofactor dependence: most ADHs rely on the nicotinamide cofactors NADH or NADPH for performing reductions.[3] Often, cofactor regeneration is achieved by using an enzyme-coupled process.[4] We explored another type of ADH: an F_{420}-dependent ADH. Such type of ADH had never been explored for biocatalytic reductions of ketones. The deazaflavin cofactor F_{420} was discovered in 1972, first in methanogens and later also in actinobacteria and other bacteria.[5–7] The redox active part of the cofactor resembles the isoalloxazine ring of the canonical flavin cofactors (Figure 1). The differences are the lack of the N5, different groups on the benzylic moiety, and the poly-γ-glutamate lactyl tail instead of the adenine part of FAD. The absence of N5 (a carbon instead) dictates that the cofactor is an obligatory hydride transfer agent, similar to the nicotinamide cofactors. The F_{420} cofactor displays an absorption maximum at 420 nm, hence its name. The redox potential of this redox cofactor is exceptionally low: –380 mV (220 mV for FAD and –320 mV NAD(P)).[5]

While flavin and nicotinamide cofactors are readily available together with a huge number of enzymes utilizing these cofactors, the biocatalytic exploration of F_{420}-dependent is lagging behind. This is partly due to the fact that the deazaflavin cofactor was difficult to obtain. The deazaflavin cofactor can be isolated from F_{420}-producing

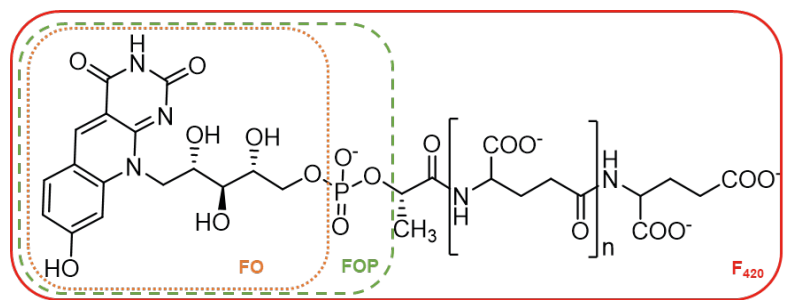

Figure 1 Structural formula of the F_{420} deazaflavin cofactor. Also, other deazaflavins are indicated: FO and FOP.

microbes, such as *Mycobacterium smegmatis*. Although it involves a laborious process and yields small amounts, it is nowadays available for biocatalytic studies. Furthermore, we have recently demonstrated that a truncated version of the cofactor, lacking the poly-γ-glutamate lactyl tail (FOP, see Figure 1), is also accepted as cofactor by F_{420}-dependent enzymes.[8] FOP represents an unnatural deazaflavin cofactor for which a relatively easy synthetic procedure has been developed. Another bottleneck for using F_{420}-dependent enzymes has been the lack of knowledge of and access to such biocatalysts. Particularly, these redox enzymes seem promising for performing selective reductions by virtue of the unique low redox potential deazaflavin cofactor. This would require regeneration of the reduced deazaflavin cofactor. This demand for $F_{420}H_2$-regenerating enzymes has been satisfied by the recent discovery of several deazaflavoenzymes. Especially the availability of several F_{420}-dependent glucose-6-phosphate dehydrogenases is attractive for this.[9]

In the last decade the interest in exploring deazaflavoenzymes for biocatalysis has increased.[10,11] F_{420}-dependent enzymes were shown to be involved in the production of antibiotics, and could be used for the asymmetric reduction of prochiral imines and enones.[12–15] In this work we explored an F_{420}-dependent ADH (ADF) for its ability to perform enantioselective reductions of prochiral ketones. The F_{420}-dependent alcohol dehydrogenase from *Methanoculleus thermophilicus* was chosen for this. ADF is a relatively small enzyme (37 kDa) which was first described in 1989. It can be recombinantly produced in *Escherichia coli* and its crystal structure has been elucidated.[12,16] Previously it was shown that ADF converts small aliphatic secondary alcohols into ketones. It was shown that during this oxidation step a hydride is transferred in a stereoselective manner from the alcohol to the *Si*-face of the F_{420} cofactor (to the C5 atom). It was demonstrated that the enzyme is able to oxidize isopropanol to acetone and the reverse reaction.[12] This was a clear indication that the enzyme may act as an enantioselective ketone reductase through an enantioselective hydride transfer.[16]

MATERIALS AND METHODS

Reagents and chemicals were purchased from Sigma-Aldrich (St. Louis, MO, USA) unless indicated otherwise.

F_{420} production. F_{420} was isolated from *Mycobacterium smegmatis* as described before.[17] The production strain *M. smegmatis* mc^2 4517 was a kind gift from Dr. G. Bashiri from the University of Auckland, New Zealand.

Expression and purification of F_{420}-dependent ADF and FGD. An Adf-encoding gene fragment was ordered codon optimized for *Escherichia coli* and cloned into a pBAD to have the construct expressed with a C-terminal His-tag. Expression was performed using *Escherichia coli* NEB 10β. Cells carrying the plasmid were grown in Terrific broth (TB) supplemented with 50 μg mL^{-1} ampicillin until OD_{600} was 0.8 and expression was induced with L-arabinose 0.02% at 24 °C overnight. Cells were harvested by centrifugation at 5000 × g for 20 min at 4 °C. Cell pellets were resuspended in 250 mM sodium phosphate buffer pH 7.0 containing 1 mM phenylmethylsulfonyl fluoride and 10% v/w glycerol. The cells were lysed by sonication, using a Sonics Vibra-Cell VCX 130 sonicator with a 3 mm stepped microtip (5s on, 5s off, 70 % amplitude, 7 min). Cell debris were pelleted by centrifugation at 12000 × g for 20 min at 4 °C. The supernatant was applied to Ni-Sepharose High Performance (GE Healthcare) pre-equilibrated with 250 mM sodium phosphate pH 7.0, 10% v/w glycerol. The washing buffer was 250 mM sodium phosphate pH 7.0, 10% v/w glycerol, 10 mM imidazole and the elution buffer was 250 mM sodium phosphate pH 7.0, 10% v/w glycerol, 500 mM imidazole. The eluted protein was desalted using a desalting column pre-equilibrated with 250 mM sodium phosphate pH 7.0, 10% v/w glycerol. FGD was purified as previously described.[9] Purity of ADF and FGD was assessed with SDS-PAGE analysis and protein concentrations were measured by using the Bradford assay.

Conversions of ketones. For ketone reductions, reaction mixtures contained 200 μL of 250 mM sodium phosphate pH 7.0, 10% glycerol, 1% DMSO, 2.0 mM substrate, 2.0 mM ethyl benzene (internal standard), 20 μM ADF, 40 μM F_{420} or 40 μM FOP, and 200 mM isopropanol or 20 mM glucose-6-phosphate with 10 μM FGD. The reaction was performed in a 1.5 mL Eppendorf tube in an Eppendorf Thermomixer at 25 °C and 500 rpm for 24 h. The reaction was extracted twice using 200 μL of ethyl acetate. The reactions passed over anhydrous magnesium sulfate and finally analyzed using GC (details in the Supporting Information).

Substrate docking. Molecular docking was performed in YASARA Structure (version 19.12.14). [18] The crystal structure of ADF (1.8 Å resolution; PDB 1RHC [16]) was used. Substrates were built using YASARA, energy minimization was performed, and VINA was employed to perform the docking. [19] Docking was accomplished using the docking simulation macro 'dock_run.mrc' with a 5 Å cube cell size

around the C5 atom of F_{420}, 100 runs, 2 Å cluster RMSD and using the YAMBER forcefield. [20] YASARA was used to visualize the results. Pymol was used for preparing the figures.

Steady-state activity assays for F_{420}-dependent alcohol dehydrogenase ADF with isopropanol. The employed assay measures the rate at which F_{420} is reduced (ε_{400} =25.7 $mM^{-1}cm^{-1}$). The buffer used was 250 mM sodium phosphate (pH 7.0), 10% v/w glycerol. For obtaining K_M and k_{cat} values, the data were fit using a regular Michaelis-Menten equation: $k_{obs}=k_{cat}*[S]/K_M + [S]$. Data in the Supporting Information.

Isopropanol tolerance assay. The tolerance of ADF towards isopropanol was probed by measuring its apparent melting temperature by ThermoFluor. [21] Using a real-time PCR the temperature at which ADF unfolds in the presence of different concentrations of isopropanol was measured. For the measurements, 250 mM sodium phosphate pH 7.0, 10% glycerol, 1x Sypro Orange, and 10 μM ADF was used. Data in the Supporting Information.

RESULTS AND DISCUSSION

Substrate exploration. First, we explored the substrate scope of ADF to find out whether it is able to accept alcohols different from isopropanol. Alcohol oxidation activity could be easily monitored by measuring the decrease of absorbance of F_{420} (the reduced form does not absorb at 420 nm). ADF did not convert the following alcohols: 2-heptanol, 5-amino-1-pentanol, 1-amino-2-propanol, 3-chloro-1,2-propanediol, 1-phenyl-1,2-ethanediol, 1-indanol, acetoin, carveol, cyclohexylmethanol, tetrahydropyran-2-methanol, 3-butyn-2-ol. Nevertheless, we could identify a set of aromatic and aliphatic alcohols that were not reported before as substrate of ADF. The corresponding ketones were investigated as prochiral substrates for ADF (Figure 2).

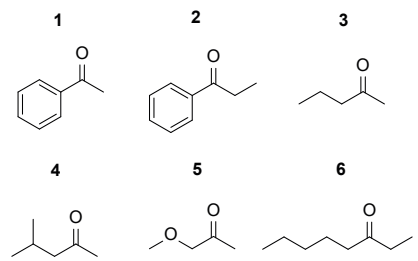

Figure 2. Ketones used for the biocatalytic exploration of ADF.

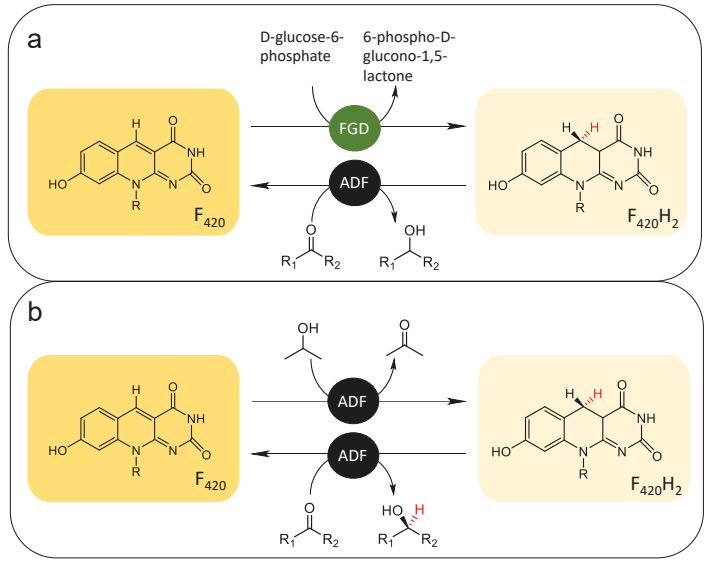

Scheme 1. Coupled reactions for the reduction of prochiral ketones by ADF. ADF: F_{420}-dependent alcohol dehydrogenase, FGD: F_{420}-dependent glucose-6-phosphate dehydrogenase. (a) D-glucose-6-phosphate is used by FGD to regenerate $F_{420}H_2$. (b) Self-sufficient use of ADF for ketone reductions with isopropanol as cosubstrate to regenerate $F_{420}H_2$.

Conversions using F_{420}-dependent glucose-6-phosphate dehydrogenase to regenerate F_{420}. For the first test conversions, we used the F_{420}-dependent glucose-6-phosphate dehydrogenase (FGD) from *Rhodococcus jostii* RHA1 (FGD) together with ADF (Scheme 1a).[9] Gratifyingly, it was found that the enzyme was able to fully and stereoselectively reduce methyl ketones to the corresponding (*S*)-alcohols. For most ketones, excellent enantioselectivity was observed (>99% *e.e.*), except for substrate 3 (92% *e.e.*) and substrate 6 (racemic product) (Table 1).

Substrates docking. In silico docking studies were performed to understand the molecular basis for the (*S*)-stereoselectivity of ADF. For acetophenone (**1**) and methoxyacetone (**5**) docking suggested that the structurally favorable product is in both cases indeed the *S*-enantiomer. This can be explained by examining the role and position of the active-site residues. Previous studies postulated that His39, Trp43, Glu12 and Glu108 are crucial for substrate binding and catalysis.[16] In the reduction reaction, a hydride transfer from the C5 atom of $F_{420}H_2$ to the ketone carbon with a simultaneous or stepwise proton addition from His39 to the ketone oxygen occurs. Hence, the specific orientation of substrate

Table 1. Reduction of prochiral ketones by ADF [a].

Entry	Substrate	Cofactor	Cofactor regeneration [b]	Conversion (%)	*e.e.* (%)
1EF$_{420}$	**1**	F$_{420}$	FGD	96	>99 (*S*)
1IF$_{420}$	**1**	F$_{420}$	-	95	>99 (*S*)
1IFop	**1**	FOP	-	5	n.d.*
2EF$_{420}$	**2**	F$_{420}$	FGD	77	>99 (*S*)
2IF$_{420}$	**2**	F$_{420}$	-	80	>99 (*S*)
2IFop	**2**	FOP	-	3	n.d.*
3EF$_{420}$	**3**	F$_{420}$	FGD	>99	92 (*S*)
3IF$_{420}$	**3**	F$_{420}$	-	>99	72 (*S*)
3IFop	**3**	FOP	-	94	>99 (*S*)
4EF$_{420}$	**4**	F$_{420}$	FGD	87	>99 (*S*)
4IF$_{420}$	**4**	F$_{420}$	-	93	>99 (*S*)
4IFop	**4**	FOP	-	2	n.d.*
5EF$_{420}$	**5**	F$_{420}$	FGD	>99	>99 (*S*)
5IF$_{420}$	**5**	F$_{420}$	-	>99	>99 (*S*)
5IFop	**5**	FOP	-	>99	>99 (*S*)
6EF$_{420}$	**6**	F$_{420}$	FGD	>99	0
6IF$_{420}$	**6**	F$_{420}$	-	>99	0
6IFop	**6**	FOP	-	>99	0

[a] Values obtained using 250 mM sodium phosphate pH 7.0, 10% glycerol, 1% DMSO, 2.0 mM substrate, 2.0 mM ethyl benzene (internal standard), 20 μM ADF, 40 μM F$_{420}$ or 40 μM FOP. [b] For cofactor regeneration, 20 mM glucose-6-phosphate with 10 μM FGD ('FGD') or 200 mM isopropanol ('-') was used. Details are in the Supporting Information. *Conversions were too low for an accurate determination of *e.e.*

towards the F$_{420}$ cofactor and His39 is decisive in the enantioselective outcome of the reaction. Docking of acetophenone revealed that Trp43 together with Val193, Trp229, Trp246, Cys249 and Phe255 form a hydrophobic pocket which snugly accommodates the aromatic ring of the substrate (Figure 3). As a result, acetophenone binds in the active site in such a way that only the (*S*)-enantiomer can be formed: the hydride can only be transferred to the *Re*-face of the substrate. Positioning of acetophenone necessary to form the (*R*)-enantiomeric alcohol is prevented because its aromatic ring cannot be accommodated in the active site in any other conformation. Docking of methoxyacetone resulted in an analogous optimal binding pose in which the apolar pocket next to the deazaflavin cofactor plays a crucial role in positioning the substrate such that hydride attack will occur on the *Re*-face of the substrate, assisted by proton transfer by His39. This will, again, only allow formation of (*S*)-1-methoxy-2-propanol, as experimentally observed.

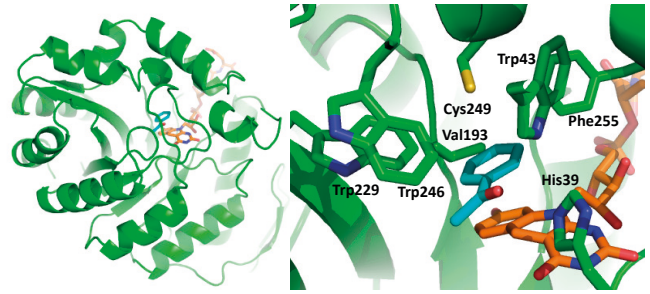

Figure 3. Binding pose of acetophenone (**1**) in ADF (PDB:1RHC). Left: overall structure of ADF with docked substrate (cyan) and F$_{420}$ (orange) highlighted in sticks. Right: close-up of binding of acetophenone.

CONVERSIONS USING ISOPROPANOL AS COSUBSTRATE TO REGENERATE F$_{420}$

The second aim of this work was to establish an efficient cofactor regeneration system. While the used glucose-6-phosphate dehydrogenase is effective in recycling F$_{420}$H$_2$, such cofactor regeneration system still requires an addition enzyme and a relatively expensive cosubstrate. Therefore, we explored whether ADF can be used as reductase and dehydrogenase in one pot, using a sacrificial alcohol as cosubstrate. For this, we tested the use of isopropanol as it had been reported to be a good ADF substrate. In order to determine the highest concentration of isopropanol tolerated in conversions, we first assessed the thermostability of ADF in the presence of different amounts of isopropanol and its kinetic parameters with isopropanol. ADF was found to be relatively tolerant towards isopropanol with only a slight change in apparent melting temperature up to 200 mM isopropanol (T_m varied from 57.5 to 56.0 °C, see Supporting Information). The steady-state kinetic analysis confirmed that isopropanol is an effective substrate with a K_M value of 1.26 mM and a k_{cat} of 1.68 s^{-1} (see Supporting Information). A concentration of 200 mM of isopropanol was selected to probe it as cosubstrate for the ADF-catalyzed reduction of prochiral ketones. Remarkably, the use of isopropanol as cosubstrate worked extremely well. In fact, there was no difference between the use of glucose-6-phosphate dehydrogenase and glucose-6-phosphate or merely isopropanol for cofactor regeneration (Table 1). This shows that the use of isopropanol as coupled substrate is a valid and simple alternative to use ADF as enantioselective ketone reductase.

Conversions using FOP as alternative cofactor. Finally, we also explored whether F$_{420}$ can be replaced by an unnatural deazaflavin

cofactor: FOP. We have recently shown that FOP can be prepared in a relatively easy manner and is often accepted by F_{420}-dependent enzymes. The results obtained using FOP as alternative cofactor with ADF and isopropanol as cosubstrate revealed that ADF can also operate with this alternative deazaflavin (Table 1). Yet, the use of FOP resulted in lower conversions for some of the ketones tested, while the enantioselectivity was largely retained. The inferior performance, when compared with F_{420}, probably reflects a poor recognition of FOP by ADF.

CONCLUSIONS

In conclusion, the finding that ADF can reduce various prochiral ketones in a highly (*S*)-stereoselective manner unveils a new biocatalytically relevant class of enzymes: F_{420}-dependent ketone reductases. They can be regarded as alternatives to nicotinamide cofactor-dependent enzymes. Moreover, we demonstrate that isopropanol can be used as cheap cosubstrate for cofactor recycling, rendering ADF self-sufficient. With the crystal structure of ADF available and many genes encoding for ADF homologs in the genome sequence database, it will be exciting to explore other variants for more demanding selective reductions.

REFERENCES

[1] K. Goldberg, K. Schroer, S. Lütz, A. Liese, Biocatalytic ketone reduction - a powerful tool for the production of chiral alcohols - Part I: Processes with isolated enzymes, Appl. Microbiol. Biotechnol. 76 (2007) 237–248.

[2] Y.G. Zheng, H.H. Yin, D.F. Yu, X. Chen, X.L. Tang, X.J. Zhang, Y.P. Xue, Y.J. Wang, Z.Q. Liu, Recent advances in biotechnological applications of alcohol dehydrogenases, Appl. Microbiol. Biotechnol. 101 (2017) 987–1001.

[3] E. Tassano, M. Hall, Enzymatic self-sufficient hydride transfer processes, Chem. Soc. Rev. 48 (2019) 5596–5615.

[4] W. Hummel, M.R. Kula, Dehydrogenases for the synthesis of chiral compounds., Eur. J. Biochem. 184 (1989) 1–13.

[5] R.S. Cheeseman, P. Toms-Wood, A. Wolfe, Isolation and Properties of a Fluorescent compound, Factor 420, from *Methanobacterium* strain M.o.H., J. Bacteriol. 112 (1972) 1887–1891.

[6] L. Daniels, N. Bakhiet, K. Harmon, Widespread distribution of a 5-deazaflavin cofactor in actinomyces and related Bacteria, Syst. Appl. Microbiol. 6 (1985) 12–17.

[7] B. Ney, F.H. Ahmed, C.R. Carere, A. Biswas, A.C. Warden, S.E. Morales, G. Pandey, S.J. Watt, J.G. Oakeshott, M.C. Taylor, M.B. Stott, C.J. Jackson, C. Greening, The methanogenic redox cofactor F_{420} is widely synthesized by aerobic soil bacteria, ISME J. 11 (2017) 125–137.

[8] J. Drenth, M. Trajkovic, M.W. Fraaije, Chemoenzymatic synthesis of an unnatural deazaflavin cofactor that can fuel F_{420}-dependent enzymes, ACS Catal. 9 (2019) 6435–6443.

[9] Q.T. Nguyen, G. Trinco, C. Binda, A. Mattevi, M.W. Fraaije, Discovery and characterization of an F_{420}-dependent glucose-6-phosphate dehydrogenase (Rh-FGD1) from *Rhodococcus jostii* RHA1, Appl. Microbiol. Biotechnol. 101 (2017) 2831–2842.

[10] M. Taylor, C. Scott, G. Grogan, F_{420}-dependent enzymes - Potential for applications in biotechnology, Trends Biotechnol. 31 (2013) 63–64.

[11] M.L. Mascotti, H. Kumar, Q.T. Nguyen, M.J. Ayub, M.W. Fraaije, Reconstructing the evolutionary history of F_{420}-dependent dehydrogenases, Sci. Rep. 8 (2018) 1–10.

[12] F. Widdel, R.S. Wolfe, Expression of secondary alcohol dehydrogenase in methanogenic bacteria and purification of the F_{420}-specific enzyme from *Methanogenium thermophilum* strain TCI, Arch. Microbiol. 152 (1989) 322–328.

[13] W. Li, S. Chou, A. Khullar, B. Gerratana, Cloning and characterization of the biosynthetic gene cluster for tomaymycin, an sjg-136 monomeric analog, Appl. Environ. Microbiol. 75 (2009) 2958–2963.

[14] M.C. Taylor, C.J. Jackson, D.B. Tattersall, N. French, T.S. Peat, J. Newman, L.J. Briggs, G. V. Lapalikar, P.M. Campbell, C. Scott, R.J. Russell, J.G. Oakeshott, Identification and characterization of two families of $F_{420}H_2$-dependent reductases from mycobacteria that catalyse aflatoxin degradation, Mol. Microbiol. 78 (2010) 561–575.

[15] S. Mathew, M. Trajkovic, H. Kumar, Q.T. Nguyen, M.W. Fraaije, Enantio- and regioselective: ene-reductions using $F_{420}H_2$-dependent enzymes, Chem. Commun. 54 (2018) 11208–11211.

[16] S.W. Aufhammer, E. Warkentin, H. Berk, S. Shima, R.K. Thauer, U. Ermler, Coenzyme binding in F_{420}-dependent secondary alcohol dehydrogenase, a member of the bacterial luciferase family, Structure. 12 (2004) 361–370.

[17] D. Isabelle, D.R. Simpson, L. Daniels, Large-Scale Production of Coenzyme F_{420}-5 , 6 by Using *Mycobacterium smegmatis* Appl. Environ. Microbiol. 68 (2002) 5750–5755.

[18] C. Guilbert, T.L. James, Docking to RNA via Root-mean-square-deviation-driven Energy Minimization with Flexible Ligands and Flexible Targets, J. Chem. Inf. Model. 48 (2008) 1257–1268.

[19] O. Trott, A.J. Olson, AutoDock Vina: Improving the Speed and Accuracy of Docking with a New Scoring Function, Efficient Optimization, and Multithreading, J. Comput. Chem. 32 (2012) 174–182.

[20] E. Krieger, T. Darden, S.B. Nabuurs, A. Finkelstein, G. Vriend, Making Optimal Use of Empirical Energy Functions: Force-field Parameterization in Crystal Space, Proteins Struct. Funct. Genet. 57 (2004) 678–683.

[21] F. Forneris, R. Orru, D. Bonivento, L.R. Chiarelli, A. Mattevi, ThermoFAD, a Thermofluor-adapted flavin ad hoc detection system for protein folding and ligand binding, FEBS J. 276 (2009) 2833–2840.

SUPPORTING INFORMATION

STEADY STATE KINETICS ANALYSES

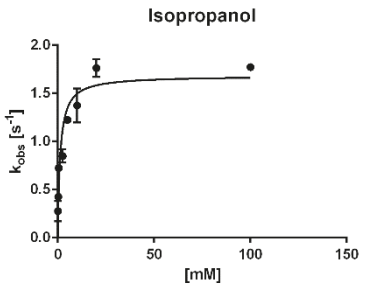

K_M
1.26±0.52 mM
k_{cat}
1.68±0.14 s^{-1}
k_{cat}/ K_M
1.33 $s^{-1}mM^{-1}$

ISOPROPANOL TOLERANCE

Table 1. Thermostability of ADF in the presence of isopropanol

Isopropanol Concentration (mM)	T_m^{app} (°C)
50	57.5±0
100	57.5±0
200	56.0±0
500	53.5±0
1000	49.5±0

CONVERSIONS

SUBSTRATE 1

Analyzed using: Agilent Technologies 7890A GC system with column CP Chiralsil Dex CB (Agilent). Program: 40 °C to 130 °C in 5 min, hold 130 °C 10 min, 130 °C to 180 °C in 10 min, hold 180 °C in 5 min.

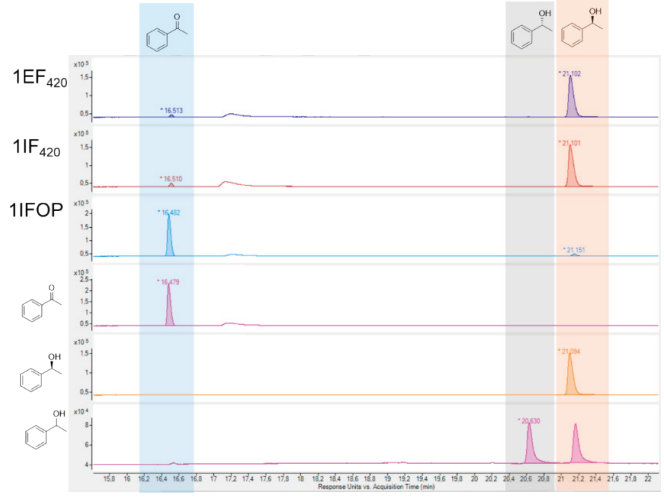

SUBSTRATE 2

Analyzed using: Agilent Technologies 7890A GC system with column CP Chiralsil Dex CB (Agilent). Program: 40 °C to 130 °C in 5 min, hold 130 °C 10 min, 130 °C to 180 °C in 10 min, hold 180 °C in 5 min.

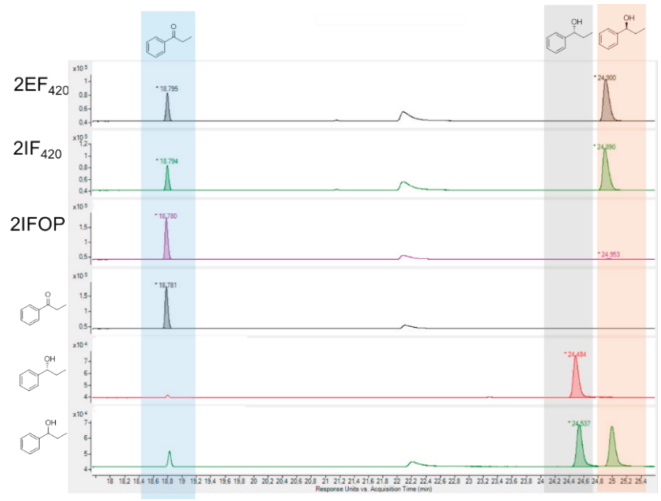

SUBSTRATE 3

Analyzed using: Agilent Technologies 7890A GC system with column CP Chiralsil Dex CB (Agilent). Program: 40 °C to 120 °C in 3 min, 120 °C to 40 °C in 10 min.

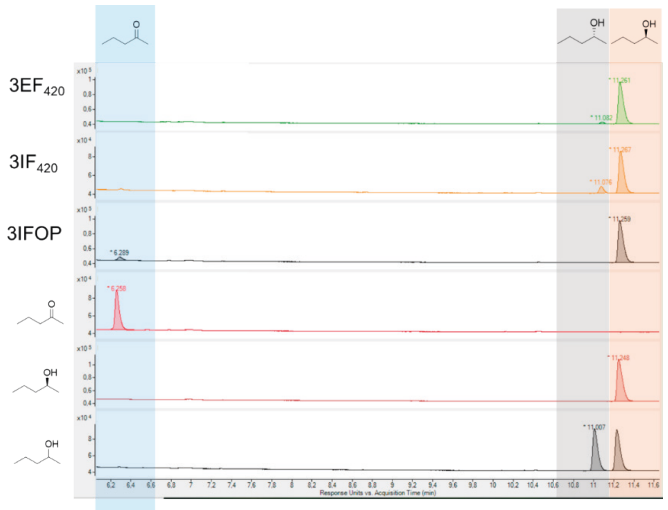

SUBSTRATE 4

Analyzed using: Agilent Technologies 7890A GC system with column CP Chiralsil Dex CB (Agilent). Program: 40 °C to 140 °C in 5 min, 140 °C to 40 °C in 10 min.

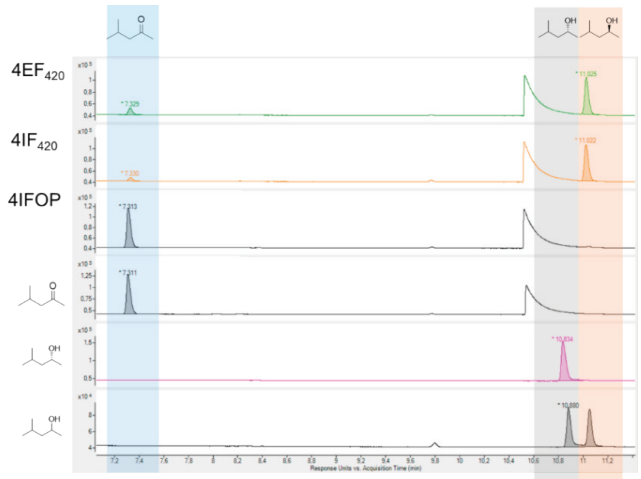

SUBSTRATE 5

Analyzed using: Agilent Technologies 7890A GC system with column FS-Hydrodex-B-TBDAc (Aurora Borealis) Program: 40 °C to 190 °C in 5 min, 190 °C to 40 °C in 10 min.

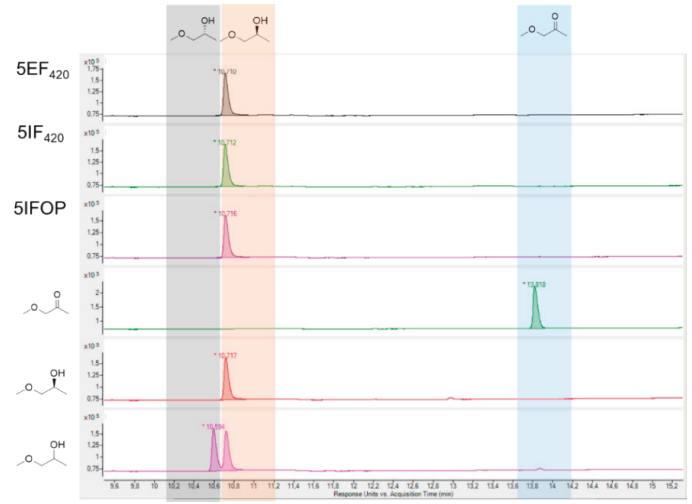

SUBSTRATE 6

Analyzed using: Agilent Technologies 7890A GC system with column FS-Hydrodex-B-TBDAc (Aurora Borealis) Program: 40 °C to 190 °C in 5 min, 190 °C to 40 °C in 10 min.

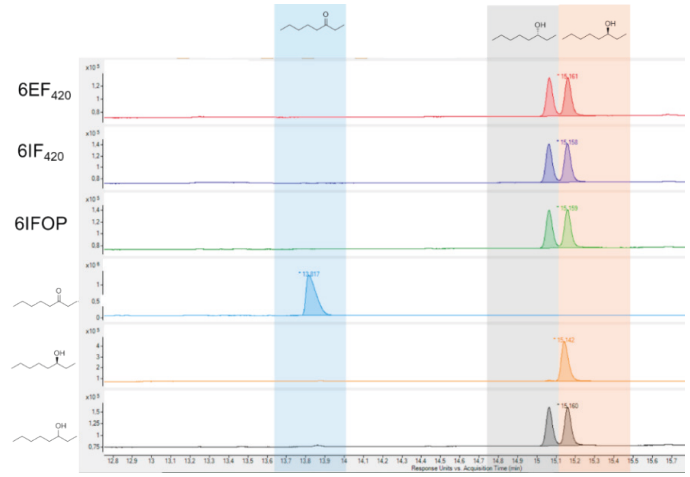

EN

Summary

SUMMARY

Work described in this thesis focused on studying and developing flavo- and deazaflavoenzymes in the context of biocatalysis**.** In recent years, biocatalytic oxidations perfomed by flavin-dependent enzymes have gained great interest in academia and industry. Some flavoprotein oxidases are well-known and widely applied in biotechnology. Yet, there are many flavoprotein oxidases that have never been considered for biocatalysis. Based on structural features, flavoprotein oxidases can be classified into six distinct families as described in **Chapter 1**. Even though they are redox enzymes, flavoprotein oxidases are relatively easy to use as they do not require the use of expensive cofactors or cofactor regeneration systems. They harbor a tightly bound flavin cofactor and merely rely on molecular oxygen (O_2) as electron acceptor. Their applications include synthesis of valuable compounds and use in biosensors. Several oxidase examples of the GMC-type oxidase family are been described in detail to provide a more exhaustive view on their applications, but also of the process and the purposes for which these enzymes have been engineered in recent years.

Chapter 2 reports on the engineering of the FAD-containing HMF-oxidase (HMFO) towards improved thermostability. HMFO from *Methylovorus sp.* strain MP688 was discovered in 2014 and represents an effective biocatalyst for the production of FDCA from HMF. In fact, it is the only known enzyme that is able to perform efficiently such a triple oxidation of HMF. In a previous study HMFO was already optimized to produce FDCA by molding the active site in order to improve the last and rate-limiting oxidation step. Unfortunately, this optimized variant, despite a good catalytic performance, displayed a relatively low thermostability. This chapter describes the work performed that resulted in a HMFO variant with a high thermostability. For generating more thermostable enzyme variants, a computational protocol, FRESCO, has been developed. This *in silico* method uses a protein structure and, using protein folding free-energy calculations and molecular dynamics simulations, predicts mutations that should render the target protein more thermostable. The FRESCO-predicted point mutations for HMFO were tested in the laboratory which yielded a number of relatively thermostable mutants. In a next step, the stabilizing mutations were combined in order to create a highly thermostable HMFO variant. For identifying the best combination of mutations, a novel gene shuffling method was developed. The identified thermostable HMFO variant displayed a melting temperature that is 12 °C higher than that of the wild-type enzyme. By including the mutations that are beneficial for

catalyzing the last oxidation step leading to FDCA, the final variant (8BxHMFO) was obtained which was shown to result in significantly higher conversions of HMF info FDCA.

Another study to improve the applicability of HMFO is described in **Chapter 3**. The aim was to optimize the heterologous expression of the enzyme, making its production and application more efficient. To achieve this, two strategies were pursued.

The first approach to improve the efficiency of HMFO utilization was to immobilize the biocatalyst using an *in vivo* system. *B. subtilis* was selected for its ability to sporulate. The generated spores can display a biocatalyst that it is fused with a spore-coat protein. HMFO-fusions were designed to obtain stable expression by genomic integration of 8BxHMFO fused with 5 different spore-coat proteins. The *hmfo* was integrated in the genome of *B. subtilis* in a target locus by homology recombination and the screening was facilitated by CRISPR-Cas9 selection. Integration was efficient, but for all generated variants there was either no expression or no expression of active HMFO. Optimization efforts were directed on helping HMFO folding by adding FAD and on spore treatment optimization. Further investigation is necessary to establish the cause of absence of expression/activity. Most probably misfolding is causing the observed issues.

The second approach to improve heterologous expression of HMFO was by secretion using the yeast *Pichia pastoris*. *P. pastoris* is known for allowing, in some cases, high level production of secreted proteins. The expression of HMFO in *P. pastoris* was accomplished by genomic integration of a cassette containing an antibiotic resistance gene for selection, a methanol-regulated promoter and the 8BxHMFO-encoding sequence with or without the alpha-mating factor for secretion or intracellular expression. Both expression systems were succesfull; expression of intracellular and secreted HMFO was demonstrated and it was possible to convert HMF to FDCA by using whole cells or concentrated supernatant. Unfortunately, the expression levels were not competitive to the heterologous expression previously optimized in *E. coli*.

In **Chapter 4,** another remarkable flavoprotein oxidase was explored. It is the case of alcohol oxidase from *Phanerochaete chrysosporium* (AOX). This biocatalyst was recently discovered and engineered in our group. In the study reported in this thesis, the biocatalytic potential of this enzyme was further expanded. By testing a large set of potential substrates, it was discovered that the oxidase has a very relaxed substrate acceptance profile and intriguing catalytic properties. The most striking discovery was the capability of AOX to perform selective double oxidations of short aliphatic diols to obtain hydroxy acids or lactones by *in situ* formation of stable hemiacetals. Also, longer diols could be oxidized by AOX, resulting in the corresponding oxocarboxylic acids through a triple oxidation. Some of the chemicals produced, such as γ-butyrolactone and γ-valerolactone, are valuable building blocks for biodegradable polymers.

In **Chapter 5**, the potential of F_{420}-dependent enzymes for ketone reductions was studied. A specific deazaflavoprotein alcohol dehydrogenase (ADF) was found to be able to reduce various prochiral ketones in a highly enantioselective manner. This unveils a new class of F_{420}-dependent redox enzymes (alcohol dehydrogenases that can be used for ketone reductions) that represent alternatives to the well-known and widely applied nicotinamide cofactor-dependent enzymes. The potential of this discovery is enhanced by the demonstration that isopropanol can be used as cheap cosubstrate for cofactor recycling, making ADF self-sufficient. Moreover, a semi-synthetic cofactor was tested as alternative to F_{420}: FOP. Despite the low conversion rates in some cases (probaby due to poor recognition of FOP by ADF) the enantioselectivity was largely retained.

Samenvatting

translated by Gwen Tjallinks

SAMENVATTING

Het werk wat beschreven wordt in dit proefschrift focust zich op het bestuderen en ontwikkelen van flavo- en deazaflavoenzymen in het kader van biokatalyse. In de afgelopen jaren hebben bio-katalytische oxidaties uitgevoerd door flavine-afhankelijke enzymen grote belangstelling gekregen in de academische wereld en industrie. Ondanks het feit dat sommige flavoproteïne oxidases welbekend zijn en veelvuldig worden toegepast in de biotechnologie, zijn er vele flavoproteïne oxidases die nog nooit overwogen zijn voor biokatalyse.

Flavine-afhankelijke oxidases zijn geclassificeerd in zes verschillende enzymfamilies gebaseerd op hun structurele eigenschappen, zoals beschreven in **Hoofdstuk 1**. Flavoproteïne oxidases zijn relatief gemakkelijk te gebruiken omdat ze voor activiteit geen additionele dure cofactoren of cofactor recycling systemen nodig hebben. Ze bevatten een sterk gebonden flavine cofactor en hebben alleen moleculaire zuurstof (O_2) nodig als elektronenacceptor. Verschillende van deze oxidases worden toegepast in de synthese van waardevolle chemicaliën en gebruikt in biosensoren. Meerdere oxidases van de GMC-oxidase familie worden in dit hoofdstuk in detail beschreven om zo een completer beeld van hun toepassingen te schetsen. Daarnaast wordt ook het proces en de doeleinden waarvoor deze enzymen zijn aangepast (engineered) toegelicht.

In **Hoofdstuk 2** wordt er gekeken naar het maken van een aangepaste versie van een flavine-bevattend HMF-oxidase (HMFO) voor verbeterde thermostabiliteit. HMFO van de bacterie *Methylovorus sp.* MP688 werd in 2014 ontdekt en vertegenwoordigt een effectieve en unieke biokatalysator voor de productie van FDCA uit HMF. Het is het enige bekende enzym dat in staat is om de drievoudige oxidatie van HMF uit te voeren. In een eerdere studie was HMFO al geoptimaliseerd voor de productie van FDCA door het aanpassen van het katalytische centrum (active site) om zo de laatste en snelheidsbeperkende oxidatiestap te verbeteren. Helaas vertoonde deze geoptimaliseerde variant, ondanks goede katalytische prestaties, een relatief lage thermostabiliteit. Dit hoofdstuk beschrijft de uitgevoerde werkzaamheden die hebben geresulteerd in een HMFO-variant met een beduidend hogere thermostabiliteit. Om meer thermostabiele enzymvarianten te genereren, is een recent ontwikkeld computerprotocol (FRESCO) gebruikt. Deze *in silico* methode maakt gebruik van een opgehelderde eiwitstructuur (in dit geval van HMFO) en voorspelt, met behulp van vrije energie berekeningen en moleculaire dynamica-simulaties, mutaties die het

eiwit meer thermostabiel zouden moeten maken. De door FRESCO voorspelde puntmutaties voor HMFO werden in het laboratorium getest, wat een aantal relatief thermostabiele mutanten opleverde. In een volgende stap werden de stabiliserende mutaties gecombineerd om een zeer thermostabiele HMFO-variant te creëren. Om de beste combinatie van mutaties te identificeren, werd een nieuwe methode voor *gene-shuffling* ontwikkeld. De geïdentificeerde thermostabiele HMFO-variant vertoonde een smelttemperatuur die 12 °C hoger is dan die van het wildtype enzym. Door de mutaties die gunstig zijn voor het katalyseren van de laatste oxidatiestap toe te voegen, werd de laatste variant (8BxHMFO) verkregen. Deze geoptimaliseerde variant van HMFO resulteerde in significant hogere conversies van HMF naar FDCA.

Een andere studie om de toepasbaarheid van HMFO te verbeteren, wordt beschreven in **Hoofdstuk 3**. Het doel was om de heterologe expressie van het enzym te optimaliseren, waardoor de productie en toepassing ervan efficiënter wordt. Om dit te bereiken werden twee strategieën gevolgd.

De eerste aanpak om de efficiëntie van HMFO productie te verbeteren, was om de biokatalysator te immobiliseren met behulp van een *in vivo* systeem. *Bacillus subtilis* is gebruikt om HMFO op de oppervlakte van sporen te verankeren. Verschillende constructen zijn gemaakt en met behulp van CRISPR-Cas9 in het genoom aangebracht. De integratie in het genoom was efficiënt, maar voor alle gegenereerde varianten was er geen expressie of geen expressie van actief HMFO. Optimalisatie-inspanningen waren gericht op het bevorderen van het vouwen van HMFO door de FAD cofactor toe te voegen en op het optimaliseren van de behandelde sporen. Meer onderzoek is nodig om de oorzaak van afwezigheid van expressie/activiteit vast te stellen. Hoogstwaarschijnlijk veroorzaakt het verkeerd vouwen van het eiwit de waargenomen problemen.

De tweede aanpak om heterologe expressie van HMFO te verbeteren was door uitscheiding met behulp van de gist *Pichia pastoris*. Van *P. pastoris* is het bekend dat het in sommige gevallen een hoge productie van uitgescheiden eiwitten mogelijk maakt. De expressie van HMFO in *P. pastoris* werd bereikt door genomische integratie van een cassette met een antibioticumresistentie-gen voor selectie, een methanol-gereguleerde promotor en de 8BxHMFO-coderende sequentie met of zonder de *alfa-mating* factor voor secretie of intracellulaire expressie. Beide expressiesystemen waren succesvol; expressie van intracellulaire en uitgescheiden HMFO werd aangetoond en het was mogelijk om HMF om te zetten in FDCA door gebruik te maken van hele cellen of geconcentreerd supernatant. Helaas waren de expressieniveaus niet vergelijkbaar met de heterologe expressie die eerder al was behaald in *Escherichia coli*.

In **Hoofdstuk 4** werd een ander opmerkelijke flavoproteïne oxidase onderzocht, namelijk het alcohol oxidase uit *Phanerochaete chrysosporium* (AOX). Deze biokatalysator is onlangs ontdekt. In de studie die in dit proefschrift wordt beschreven, werd het biokatalytische potentieel van dit enzym verder uitgebreid. Door een groot aantal potentiële substraten te testen, werd ontdekt dat het oxidase een zeer breed acceptatie profiel en intrigerende katalytische eigenschappen heeft. De meest opvallende ontdekking was het vermogen van AOX om selectieve dubbele oxidaties uit te voeren van korte alifatische diolen om hydroxyzuren of lactonen te verkrijgen door *in situ* vorming van stabiele hemiacetalen. Ook konden langere diolen worden geoxideerd door AOX, wat resulteert in oxocarbonzuren door een drievoudige oxidatie. Sommige van de geproduceerde chemicaliën, zoals γ-butyrolacton en γ-valerolacton, zijn waardevolle bouwstenen voor biologisch afbreekbare polymeren.

In **Hoofdstuk 5** werd het potentieel van F_{420}-afhankelijke enzymen voor selectieve reductie van ketonen bestudeerd. Een specifiek deazaflavoproteïne alcohol dehydrogenase (ADF) bleek in staat te zijn om verschillende prochirale ketonen op een enantioselectieve manier te reduceren. Dit heeft een nieuwe klasse van F_{420}-afhankelijke redox-enzymen onthuld (alcohol dehydrogenases die kunnen worden gebruikt voor keton reductie), die alternatieven vertegenwoordigen voor de bekende en algemeen toegepaste nicotinamide-cofactor-afhankelijke enzymen. Het potentieel van deze ontdekking wordt vergroot door het feit dat isopropanol kan worden gebruikt als goedkoop cosubstraat voor cofactor-recycling, waardoor ADF zelfvoorzienend wordt. Bovendien werd een semi-synthetische cofactor getest als alternatief voor F_{420}: FOP. Ondanks de lage conversies in sommige gevallen (waarschijnlijk vanwege de slechte herkenning van FOP door ADF) bleef de enantioselectiviteit grotendeels behouden.

Curriculum Vitae

CURRICULUM VITAE

I was born on the 20th of October 1991 and grew up in Motta di Livenza (Treviso, Italy). In 2011 I started my studies at the University of Padova (Italy), and obtained the Bachelor Degree in Biotecnology in 2014 with the thesis: "Production of genetically modiefied plants and gene pyramidization" (final grade 101/110). After, I continued at the University of Padova with the master program in Industrial Biotechnology graduating in September 2016 with the thesis: "Production of enginerized proteins for advanced EPR studies: human neuroglobin and ribonuclease A" (final grade 110 *cum laude*/110).

In October 2016 I started a PhD program in the Molecular Enzymology group of Prof. Marco Fraaije at the University of Groningen. This research was financed by NWO and focused on the study of flavoenzymes and deazaflavoenzymes. In particular I worked with FAD-dependent 5-hydroxymethylfurfural oxidase (HMFO) and alcohol oxidase (AOX). The aim was to improve HMFO thermostability and the production for industrial purposes and to explore the oxidative capability of AOX. In parallel to flavodependent enzymes I studied how to improve the relevance of deazaflavoenzymes, a underestimated class of enzymes due to the poor availability of the F_{420} cofactor, by showing how these enzymes can be used for enantioselective demanding reactions. Currently I am working as research scientist for GECCO Biotech .

LIST OF PUBLICATIONS

C. Martin, A.O. Maqueo, H.J. Wijma, M.W. Fraaije, Creating a more robust 5-hydroxymethylfurfural oxidase by combining computational predictions with a novel effective library design, Biotechnol. Biofuels (2018) 56.

M.J.L.J. Fürst, **C. Martin**, N. Lončar, M.W. Fraaije, Experimental Protocols for Generating Focused Mutant Libraries and Screening for Thermostable Proteins, Methods Enzymol. 608 (2018) 151–187.

M.G. Dal Farra, S. Richert, **C. Martin**, C. Larminie, M. Gobbo, E. Bergantino, C.R. Timmel, A.M. Bowen, M. Di Valentin, Light-induced pulsed EPR dipolar spectroscopy on a paradigmatic hemeprotein, ChemPhysChem. 20 (2019) 931–935

C. Martin, M. Trajkovic, M.W. Fraaije, Production of hydroxy acids through selective double oxidation of diols by a flavoprotein alcohol oxidase, Angew. Chemie. 59 (2020) 4869-4872

G. De Gonzalo, **C. Martin**, Positive impact of natural deep eutectic solvents on the biocatalytic performance of 5-hydroxymethylfurfural oxidase, Catalysts, 10 (2020) 447.

M.G. Dal Farra, **C. Martin**, E. Bergantino, Y. Kandrashkin, A. van der Est, M. di Valentin, Electron spin polarization transfer induced by triplet-radical interactions in the weakly coupled regime, Phys. Chem. Chem. Phys, 22 (2020) 19982-19991.

C. Martin, C. Binda, M. Fraaije, A. Mattevi, The multipurpose family of flavoprotein oxidases, The Enzymes, 47 (2020) 63-86.

C. Martin, G. Tjallinks, M. Trajkovic, M.W. Fraaije, Facile stereoselective reduction of prochiral ketones using an F420-dependent alcohol dehydrogenase, ChemBioChem, (2020) DOI: 10.1002/cbic.202000651.

Acknowledgement

ACKNOWLEDGEMENT

First acknowledgment goes to **Marco**. You have been an excellent mentor, thanks for giving me this opportunity, for teaching me so much about science and academia, managing projects and people, and most of all for creating the best working environment a scientist can hope. Your ability to positively lead people is the reason why I managed to achieve many of the goals of the last four years. I hope to meet many other great people like you during the course of my life. Thank you for understanding me and for letting me develop in the way I wanted, and thank you for the patience that you had with me. **Marleen**, **Laura** and **Niek**, bedankt for making us feeling always so welcome in your home.

Thank to my second promotor **Prof. Dick Janssen** for the constructive advices, I admired your vast knowledge not only of chemistry, but of science in general.

Thanks to collaborators: **Prof. G. de Gonzalo**, to **Prof. Anton Glieder** and **Anna Haltz** from TU Graz and **Prof. Oscar Kuipers** for helping me learning how to handle *P. pastoris* and *B. subtilis*.

Thanks my paranyphms **Rudy** and **Misun** for supporting me in these last months and before. **Rudy,** thanks for being positive, and for the stability that you bring me, I feel like we have always been friends, I am so proud of what you have achieved and so happy to have you here, thank you for listening to me always. **Misun**, I am really honored of being your friend, you are truly strong and smart, thanks for your advices in and out of the lab and for the happiness and the jokes we shared together, you are a warrior.

Nikola I will never thank you enough for what you did for me you have been an important figure for these last four years. I am really proud of what you have achieved, seeing your successes was an inspiration for me.

Milos, apart from being a great friend you are a great scientist and a great Dad. Thanks for your great help with chemistry and for your patience with me. You are an example to follow, thanks also to your beautiful family: **Jasna** and **Sofija** for the moments we shared together.

I would like to thank the students who helped me with my projects: **Lucas**, **Amaury**, **Lester**, **Jorn**, **Fabrizio**, **Ronald**, **Julia**, **Andrea**, and in particular **Gwen**, thanks for being on my side these last months and for translating my summary**.** I really enjoyed teaching all of you, thanks for your patience and for following me around the lab.

Thanks for the constructive feedback during workdiscussion, for the nice lab environment and chats to **Henriette**, **Andy**, **Eduardo**, **Estela, Nyoman, Guang, Daniël** and in particular **Heijn** for the help with computational analysis.

Thank to **Christiaan** for being really nice helping to fix and explaining how to use instruments, always with patience and positive attitude. Bedankt to **Sandra** for being always so kind.

Thanks to previous lab members: **Hemant**, **Nina**, **Elisa, Dana**, **Antonija**, **Cyntia, Marzena**.

Thanks to past lab members **Hanna** and **Willem** for the advices.

Thanks to my two favorite Austrians: **Mathias**, I think we became friends almost instantly, you have being supportive at the beginning of my PhD, **Clemens** you are a great inspiration for young PhDs, thanks for being always available for discussions and for your advices.

Many the friends that left: **Ivana D.** you are an example of very strong and successful woman for me, **Sambi**, I missed having you around teasing people, but with me you always have been very sweet, you are a very joyful person. **Manu**, **Lili**, **Ilias** thank you for the nice moments together.

Mohamed I cannot wait to see your future successes, be strong. **Friso** I learned from you kindness and I appreciate how you always listened to me. For you both, it has been a great honor to stand next to you for your PhD defences. Thanks also to **Nina** for the nice chats.

Elvira R.: The Scientist, you are a great woman, I learned a lot from you, thank you.

Ale(jandro) thanks for the help with research and for the great time together, you are a very honest person and friend. Thanks also to **Mel**, guapa tu eres un fuegos artificiales, thanks to both of you for hosting us and for all the fun at your place.

Yapei, my dear **Yapapei**, you are a very true person, hard worker, I admire your strength, thank you for the amazing food you shared with me and how caring you have been. **Yiming**, I don't remember not seeing you smiling, your positiveness is amazing, you always know how to cheer up people around you. **Qinglong,** we shared this journey together, you have been always very calm, thank you for your patience with me. **Hugo**, we are a bit similar, both very practical and efficient, thank you for making me a bit more Dutch.

Andrea you can bring the Sun in the room, **Gautier** you are a beautiful person and **Jeroen** charming and smart, thank you for the circus spirit you created in lab 123, we made good science and good fun too.

Max. You are one of the most brilliant mind that I know, thank you for what you taught me in the lab. Thank you more for being such a good friend.

Cora. **Coretta**, you are one of the person that was most important for me during these four years. You listened to me and had the power of turning a bad day into a smile. Your energy is unique, like you.

Thank you **Lur** for being a very good friend and for teaching me to be a bit more patience in life. You are a very mature, cheerful and profound woman.

My Groningen friends, thanks for sharing so much fun with me: **Titia**, you are such a crystal clear person, **Reuben** and **Ginny** your humourism is special like the people you are. **Linda**, seeing you always made me happy, you are so good in sending positive vibes. **Ivana M.** you are always nice and kind. **Martin** I enjoyed a lot sharing the acting experience with you, thanks for the funny moments.

Italians of Groningen: **Elvira**, **Nikolas**, **Simone**, **Roxana**, **Ale(ssandro)**. **Elvira** we shared a lot of chats, you are a good accomplice and a true friend. **Nikolas**, thank you for the help with editing with the movies, thank you for making me laugh so much. **Simone**, you are a very deep person thank you for sharing your unique humor, **Roxana** we share the same energy thanks for the fun together. **Ale** you are young, positive, funny and truly smart I expect great things from you, as a friend and as a scientist. **Jacopo** and **Luca** thanks for the laughs and the jokes in the corridors.

Thank you **Joanna** for the help with the thesis, for the patience and for being always available.

Fermín gracias por compartir conmigo el tiempo, las palabras, las risas y la tristeza.

Grazie ai miei amici in Italia: ***Bobo***, ***Ste***, ***Giulia***, ***Valentina***, ***Cecilia***, ***Carlotta*** *e in particolare ad* ***Alberto*** *e* ***Ilenia*** *per il vostro supporto, riguardo molti degli aspetti di questi ultimi quattro anni.*

Grazie alla mia ***famiglia*** *matta e al* **Topo** *in Italia, per il vostro supporto incondizionato.*

The last, but most important acknowledgment is for **my parents**. Thank for how you educated me, for supporting me and for trusting me.

L'ultimo, ma piú importante ringraziamento, va ai ***miei genitori****. Grazie per come mi avete educato, per il vostro supporto e per fidarvi di me.*